Origin and fate of dissolved organic matter in the subsoil

Von der Naturwissenschaftlichen Fakultät der
Gottfried Wilhelm Leibniz Universität Hannover

zur Erlangung des Grades

Doktor der Naturwissenschaften

(Dr. rer. nat.)

genehmigte Dissertation von

Timo Leinemann, M. Sc.

Erscheinungsjahr: 2018

Referent: Prof. Dr. rer. nat. Georg Guggenberger

Korreferenten: Prof. Dr. rer. nat. Robert Mikutta, Prof. Dr. rer. nat. Karsten Kalbitz

Tag der Promotion: 23.03.2018

Abstract

Dissolved organic matter (DOM) is the most mobile fraction of organic matter in soil and thus is important for the dynamic of soil organic carbon (OC), which represents the largest terrestrial OC pool. DOM produced from plant litter in the forest floor is transported down into the mineral soil with the soil solution. During this transport interactions with soil minerals and microorganisms lead to a decreased DOC concentration in the subsoil and distinct DOM composition. To assess the changing characteristics of DOM from topsoil to subsoil three studies were conducted in a Dystric Cambisol in the Grinderwald beech forest, challenging the influence of different hydrological conditions on the DOM transport and the distribution of leaf litter derived DOC over the soil profile, as well as the importance of mineral sorption for the demobilization of DOC.

In *study I* a monitoring of the soil solution with segmented plate lysimeters was conducted. This enabled to investigate the spatial and temporal variability of water flux, DOC concentration and DOM composition in 10, 50 and 150 cm depth on the same spatial and temporal resolution over 15 month. The water flux was found to have an influence on the DOC concentration and DOM composition as a negative relationship between water flux and DOC concentration and a positive relationship between water flux and DOC flux was found. The aromaticity of the DOM, as assessed by specific UV absorbance at 280 nm, was positively correlated with the water flux in 50 cm and 150 cm depth indicating a bypassing of possible binding sites at higher water fluxes. In the topsoil the variability of the measured parameters was dominated by seasonal variations and in the subsoil for the most part by variations on the centimeter scale, highlighting the importance of hotspots for the OC dynamic.

In *study II* the leaf litter at the monitoring site of *study I* was replace by highly ^{13}C enriched beech leafs to follow the fate of litter derived DOC in the subsoil. Over 18 month after the label addition the overall contribution to DOC was found to be low (<3% in 10 cm depth and <0.3% in 50 and 150 cm depth). The transport to the subsoil was slow, as the ^{13}C enrichment in the subsoil DOC increased one year after the

label addition. A positive correlation of water flux and ^{13}C enrichment further indicates bypassing processes at high water fluxes.

In *study III* a column experiment was performed connecting undisturbed soil cores from three soil depths to a cascade. Each column included a patch of ^{13}C labelled OM-coated goethite to assess the interaction of soil solution and reactive mineral surfaces. The DOC concentration and DOM composition of the cascade percolates reassembled the known characteristics in a soil profile to a great extent. With the use of ^{13}C labelling it was possible to verify an intensive interaction of soil solution and goethite featuring a replacement of 18 – 31% of the OC sorbed to the goethite before the experiment by DOC from the percolate.

The data gained in this thesis highlights the importance of the water flux for the fate of DOM down the soil profile. The variability of all measured parameters was high and in the subsoil differences on the centimeter scale were constant to some part over the 15 month of observation, featuring drying and rewetting cycles. Sorption was found to play an important role for DOC cycling over the whole soil profile, but adsorption to reactive minerals was not only an irreversible process. Dissolved moieties are rather in constant interaction with the solid phase and thus evidence for a cascade like cycling of OM down the soil profile was found, featuring a preferential translocation of rather degraded moieties to the subsoil. This cascade can be influenced to some degree by high flow velocities that cause DOC to bypass possible sorption sites.

Zusammenfassung

Gelöste organische Substanz (DOM) stellt den mobilsten Anteil organischer Substanz in Böden dar und ist daher bedeutend für die Dynamik des größten terrestrischen Kohlenstoffspeichers. Aus Pflanzenstreu mobilisierter, gelöster organsicher Kohlenstoff (DOC) wird mit der Bodenlösung in den Mineralboden transportiert. Während dieses Transportes verringert sich die DOC Konzentration mit der Tiefe, als Folge von Sorption an Mineralen und mikrobiellem Abbau. Zudem verändert sich die Zusammensetzung der DOM von pflanzenbürtigen Stoffen zu Stoffen mikrobieller Herkunft. Um die sich verändernden Charakteristika der DOM vom Oberboden in den Unterboden zu untersuchen, wurden drei Studien im Grinderwald in einer schwach podsolierten Braunerde unter Buchenwald durchgeführt. Der Einfluss von unterschiedlichen hydrogeologischen Gegebenheiten auf den DOM Transport und die Verteilung von blattstreu-bürtigem DOC im Bodenprofil, sowie die Bedeutung von Sorption an Mineralen für die Retention von DOC wurde in diesen Studien untersucht.

In *Studie 1* wurde ein Monitoring der Bodenlösung mit segmentierten Saugplatten durchgeführt. Hierbei war es möglich, die räumliche und zeitliche Variabilität des Wasserflusses, der DOC Konzentration und der DOM Zusammensetzung in 10, 50 und 150 cm Tiefe mit der gleichen Auflösung über 15 Monate zu untersuchen. Eine negative Korrelation zwischen Wasserfluss und DOC Konzentration deutet auf Verdünnungseffekte hin. Die DOC Flüsse stiegen allerdings analog zum Wasserfluss an. Im Unterboden korreliert die Aromatizität der DOM positiv mit dem Wasserfluss. Dies ist ein Anzeichen für eine verringerte Sorption bei höheren Fließgeschwindigkeiten. Die Variabilität der gemessenen Parameter wurde im Oberboden von saisonalen Schwankungen dominiert. In 50 und 150 cm Tiefe waren die räumlichen Schwankungen zwischen den Segmenten der Saugplatten von größerer Bedeutung als die zeitlichen Schwankungen.

In *Studie II* wurde die Blattstreu oberhalb der Installationen aus *Studie I* durch mit ^{13}C angereicherter Buchenstreu ersetz, um den Anteil an streu-bürtigem Kohlenstoff im DOC in den Unterboden zu untersuchen. Der Anteil an streu-bürtigem Kohlenstoff war nach dem Austausch der Streu über die 18

untersuchten Monate gering (<3% in 10 cm Tiefe und <0.3% in 50 und 150 cm Tiefe). Die ^{13}C Anreicherung in der Bodenlösung stieg ein Jahr nach der Applikation der angereicherten Streu signifikant an. Dies ist ein Anzeichen für einen langsamen Transport in den Unterboden. Eine positive Beziehung zwischen Wasserfluss und ^{13}C Anreicherung deutet erneut auf eine geringere Intensität von Sorptionsprozessen bei hohen Fließgeschwindigkeiten hin.

In *Studie III* wurde ein Säulenexperiment durchgeführt. Hierfür wurden Säulen aus zwei ungestörten Stechzylindern und einem Päckchen mit ^{13}C angereichertem OC-belegtem Goethit dazwischen, zusammengesetzt. Drei Säulen ansteigender Tiefe wurden miteinander zu einer Kaskade verbunden und nacheinander perkoliert. Anhand des ^{13}C angereicherten OC auf dem Goethit konnten Austauschprozesse zwischen Bodenlösung und Mineralphase nachvollzogen werden. Mit dem Säulenaufbau konnte der Verlauf der DOC Konzentration und DOM Zusammensetzung, wie sie aus natürlichen Bodenprofil bekannt sind, in großem Maße nachgestellt werden. Durch den Einsatz von ^{13}C angereichertem OC konnten intensive Austauschprozesse zwischen DOC und mineral-assoziiertem OC festgestellt werden. 18 – 31% des vor dem Experiment am Goethit sorbiertem OC wurde durch OC aus der Bodenlösung ausgetauscht.

Die Ergebnisse dieser Arbeit stellen die Bedeutung des Wasserflusses auf den Verbleib von DOM im Bodenprofil heraus. Die Variabilität aller gemessenen Parameter war hoch. Trotz starken Schwankungen in der Bodenfeuchte waren die kleinräumigen Unterschiede im Unterboden über die 15 Monate des Monitorings partiell konstant. Sorption ist ein wichtiger aber nicht irreversibler Prozess der DOC Retention. DOC steht eher in konstanter Interaktion mit der Mineralphase. Dies ist ein Anzeichen für einen DOC Transport, der durch eine Kaskade von Sorptions- und Mobilisierungsprozessen dominiert wird. Hierbei werden degradierte Verbindungen präferentiell in den Unterboden verlagert. Diese Kaskade kann zu einem gewissen Grad von schellen Fließgeschwindigkeiten beeinflusst werden, da diese die Wahrscheinlichkeit einer Sorption an Mineraloberflächen herabsetzten.

Schlagwörter:

Subsoil

Dissolved organic matter

Mineral organic interactions

Table of content

List of tables and figures

Abbreviations

AL	aluminum
C	carbon
CG	OM-coated goethite
CO_2	carbon dioxide
DOC	dissolved organic carbon
$DO^{13}C$	$^{13}C/^{12}C$ ratio of dissolved organic matter
DOM	dissolved organic matter
Fe	iron
Fe_d	dithionite-citrate-extractable iron
GDC	goethite derived carbon
GL	goethite layer
H_2O	water
HCl	hydrochloric acid
ICP-OES	coupled plasma optical emission spectroscopy
IDC	intra date correlation
ISC	intra segment correlation
lmer	linear mixed-effect
log	logarithm
MC	mobilized carbon
n	number of samples

N	nitrogen
obs	observatory
OC	organic carbon
OM	organic matter
PG	pure goethite
qPCR	quantitative polymerase chain reaction
ROI	region of interest
SaCG	sandy soil with coated goethite
SaPG	sandy soil with pure goethite
SD	standard deviation
SDC	solution derived carbon
SEM	scanning electron microscope
SiCG	silty soil with OM-coated goethite
SiPG	silty soil with pure goethite
SSA	specific surface area
SUVA	specific UV absorbance
TPV	total pore volume
va	variance
ΔC	net carbon exchange

1. Introduction

1.1 Importance of soils for the terrestrial carbon cycle

Soils represent the largest terrestrial organic carbon (OC) pool, storing more OC than the phytomass and the atmosphere combined (Trumbore 2009). Scharlemann et al. (2014) recently reviewed 27 approaches for soil carbon stock estimation and ascertained a mean global OC pool of about 1500 Pg. Uncertainties about the most accurate method and the exact estimation are present, including possible overestimations by misuse of the parameters bulk density and stone content (Poeplau et al. 2017) and possible underestimations by overlooking circumpolar permafrost soils (Tarnocai et al. 2009). However, the importance of soil OC for the global carbon cycle, especially with focus on climate change and food security (Lal 2013) is broad consensus. The establishment of conservative agricultural methods, the reforestation of degraded ecosystems and a reduction of deforestation can increase global soil OC stocks. According to Lal (2004) this can possibly account for an offset of 5 to 15% of the global fossil-fuel emissions and lead to enhanced crop yields on a global scale. The highest soil OC concentrations are present in topsoils whereas subsoils are often depleted in OC concentration, but when soil OC stocks are considered, subsoils down to 2m depth account for more than half of the soil OC stored due to their great volume and bulk density (Jobbágy and Jackson 2000, Rumpel and Kögel-Knabner 2011).

1.2 Soil organic matter

On global scale the soil OC content in the top 20 cm is predominantly controlled by the climate, whereas below 20 cm soil depth the importance of texture increases, with positive correlation of clay content and soil OC content. In temperate climate the soil OC content down to 3 meter depth is highest in deciduous forest and declines from evergreen forest to grassland and cropland with a high degree of variability (Jobbágy and Jackson 2000). The following sections will focus on forest ecosystems in temperate climate as all experiments and investigations of this work were carried out in such environments, representing largely pristine vegetation in mid-latitude areas. Forest soils store high amounts of carbon, thus

understanding processes leading to changes in carbon stocks are of high importance (Grüneberg et al. 2017).

Sources of soil OC are litter fall, root growth, root exudation and bioturbation. In forest ecosystems plant litter accumulates on top of the mineral soil and forms organic horizons. Chemical and biological processes driven by precipitation and soil fauna lead to the breakdown and decomposition of plant debris. Water soluble compounds are mobilized and transported as dissolved organic matter (DOM) into the mineral soil (Anderson 1973). The growth and exudation of living roots and the decomposition of dead roots represent a direct input of OC to the mineral soil and affect the OC pools from topsoil to deep subsoil (Tefs and Gleixner 2011, Rasse et al. 2005). Furthermore roots supply easily degradable C rich substrates to the soil via exudation (Finzi et al. 2015, Lynch and Whipps 1990). Bioturbation by soil invertebrates is considered to have a positive effect on OC storage (Frouz et al. 2009, Lavelle et al. 1997) and e.g. earthworms dislocate OC from topsoil to deeper horizons (Don et al. 2008). The relative contribution of each of this sources to the OC content of soils is still controversial (Rumpel and Kögel-Knabner 2011). Studies were input from DOM and from root litter are quantified simultaneously are rare. Kleja et al. 2008 concluded that the transport of dissolved organic carbon (DOC) from the organic horizon and the input via roots are of equal importance for the soil OC content down to 50 cm depth of three Norway spruce stands in Sweden.

In the most soils together with a strongly decreasing OC concentration with depth the soil organic matter (OM) composition shifts from more plant derived compounds in the topsoil to highly processed rather microbial derived compounds in the subsoil. This is apparent in decreasing C:N ratios and increasing $\delta^{13}C$ values (Sandermann et al. 2008, Rumpel et al. 2012a, Brunn et al. 2014). Following kinetics, the ^{13}C content of microbial derived OC is increased, as microorganism rather incorporate heavier C and respire lighter C (Lerch et al. 2011). Studies on further fractionating processes like root exudation are reviewed by Werth and Kuzyakov (2010). Together with changing ^{13}C values soils show distinct ^{14}C profiles indicating an increasing age with depth (Trumbore et al. 2009, Rumpel et al. 2012). This leads to the

somewhat unreasonable finding that the youngest part of the soil contains the oldest OC. Ahrens et al. (2015) developed a process-oriented model to reproduce the development of ^{14}C depth distributions with the parameters OC sorption, DOC transport, microbial cycling and bioturbation.

Soil OM is present as particulate OM, mineral associated OM and DOM. Particulate soil OM consist of fragmented plant particles that spread through soil via bioturbation or root growth and decay. They exist separately as greater plant fragments or tend to aggregate with mineral particles when they are highly fragmented. The importance of particulate OM decreases with depth as the importance of mineral associated OM increases. In the subsoil 80-90% of the total soil OC are mineral associated (Rumpel et al. 2012). The mineral associated OM consist of degraded plant compounds or products of microbial cycling (Wagai et al. 2009). The most important sorbents in soil are metal (hydr)oxides and clay minerals due to their high specific surface area (SSA) and high abundance of reactive functional groups and surface charge (Kaiser and Guggenberger 2003). DOM is a small but important fraction of carbon in soil, due to its mobility and reactivity. The highest DOC concentrations are found under organic horizons and in the most ecosystems the concentration of DOC in the soil solution strongly declines with depth due to sorption to the mineral soil (Michalzik et al. 2001). The composition of DOM changes, concurrently with the solid soil OM, from plant derived compounds in the topsoil to rather degraded microbial derived compounds in the subsoil (Kaiser et al. 2002). This indicates a strong interaction and constant exchange of solid and dissolved organic moieties during the percolation of soil solution (Scott and Rothstein 2014).

Decomposition of soil OM by microorganisms is one essential driver of OM dynamics in soil from the organic layer to the subsoil. The most abundant organisms are bacteria and fungi (Veen and Kuikman 1990). The microbial abundance and diversity decreases with soil depth due to reduced carbon and nitrogen concentrations (Herold et al. 2014). Nevertheless, relative to the amount of microbial biomass the microbial activity is similar in topsoil and subsoil (Blume et al. 2002). The decomposition of OM starts with the course breakdown of the residues by detritivorous soil animals and microorganisms. Complex organic compounds are then broken down to simpler compounds. For example the decomposition of

cellulose over cellobiose to glucose under aerobic conditions leads to the end products CO_2 and H_2O. Whereas the decomposition of proteins over peptides to amino acids finally leads to the additional release of inorganic anions like nitrate and sulfate. The decomposability differs between substances from easily degradable sugars over cellulose to rather hardly decomposable substances like lignin (Osman 2013). However, the high diversity of microorganisms in soil provides a specialist for the decomposition of literally every compound and decomposition rates depend on the overall ecosystem conditions, like water supply and nutrient demands (Coleman et al. 2004).

Sorption to soil minerals is considered to be an important soil OC stabilization mechanism (Kalbitz et al. 2005). Sorption by ligand exchange reactions was found to provide the highest resistance against desorption and microbial mineralization. Thus in the common pH range in mid-latitude soils (3 – 7 pH) metal oxides like goethite protect sorbed soil OM stronger from degradation than phyllosilicates due to their pH variable charge (Mikutta et al. 2007). The concept of chemical recalcitrance of certain humic substances in soil OM against microbial metabolism is not anymore considered as an important process that leads to differences in turnover times between carbon pools. Recent studies rather showed that the relative spatial inaccessibility of OM for microbes and enzymes and interactions between OM and minerals control the stabilization of carbon (Dungait et al. 2012, Mikutta et al. 2006, von Lützow et al. 2006). The role of DOM as the most mobile fraction of carbon in soil is thus of high importance to understand soil OC cycling. Especially the spatial heterogeneity of DOC fluxes as one possible driver of microbial hotspots (Kuzyakov and Blagodatskaya 2015) and exchange processes between soil solution and reactive soil minerals are important to further understand the carbon cycling in soil (Lehmann and Kleber 2015).

1.3 Dissolved organic matter in soil

The highest production of DOM occurs underneath the organic horizon, which is fuelled by a steady input of plant litter (Don and Kalbitz 2005). In thicker organic horizons an intense cycling was detected by the use of ^{13}C labelling, as DOC mobilized and replaced OC from the Oi over the Oe and the Oa layer. The

authors suggest that the almost complete loss of the added labelled litter is generated by sorption and re-mobilisation as well as mineralisation to CO_2 in the Oe layer of a Haplic Podzol under a Norway spruce forest (Fröberg et al. 2007). Deciduous forest typically from thin mull-type organic layers. The DOC produced therein gets retained predominantly in the first centimetres of the mineral soil (Kammer and Hagedorn 2011). The source of DOC in the deeper mineral soil is thus only indirectly the litter layer as the most labile fractions of the leaf and root litter derived DOC get degraded to CO_2 by microbes or rapidly sorbed to reactive minerals in soil (Sanderman et al. 2008). This was resulted from the finding of an increasing relative abundance of microbial derived hexoses in comparison to plant derived phenolic DOM compounds due to selective retention of aromatic moieties (Kaiser et al. 2002). As the sorption of DOC is dominated by the clay sized mineral fraction, metal oxides and clay minerals are of utmost importance (Eusterhues et al. 2005). The content of poorly crystalline Fe and Al explains the variation in DOC adsorption behaviour to the greatest extent in samples of 52 mineral soils (Kothawala et al. 2009). The dominant sorption mechanism on goethite at low pH is ligand exchange due to the large number of functional groups. On clay minerals like pyrophyllite and vermiculite van der Waals forces and Ca^{2+} bridging are the dominating binding mechanism, as revealed by sorption experiments (Mikutta et al. 2007). The formation of secondary minerals like ferrihydrite under the presence of DOC leads to the coprecipitation of mineral-organic complexes and is another important OC demobilisation mechanism (Eusterhues et al. 2011, Mikutta et al. 2015).

The biodegradation of DOM is highly variable and related to its composition, as aromatic moieties are more stable than carbohydrates. The degradation of carbohydrate rich rather label DOM solutions leads to a relative increase of aromatic compounds and thus an increase of stability in the remaining DOM solution. The decay rates measured for DOM rich in aromatic moieties were comparable to these assumed for the stable soil OM pool in carbon models (Kalbitz et al. 2003). In soil solution a relative decrease of aromatic moieties with depth was observed by several studies (Kaiser et al. 2004, McCarthy et al. 1996). The reduction of DOC concentration with depth is thus rather a result of sorption to reactive soil minerals than biodegradation.

Across a variety of ecosystems the DOC flux in topsoils ranges from 10 to 85 g C m^{-2} y^{-1} and is reduced in the subsoil to 2 to 40 g C m^{-2} y^{-1}. The export of DOC from soils to streams amount to 1 to 10 g C m^{-2} y^{-1} (Neff and Anser 2001). The water flow as main driver of DOC transport in soil is highly variable on the temporal scale as induced by variations in precipitation and climate (Köhler et al. 2008) and on the spatial scale (Jarvis 2007). On the spatial scale the water flux is on the one hand controlled by matrix flow, a slow solute transport through small and medium scaled pores in homogeneous textured soil and on the other hand by preferential flow, a fast and unstable solute transport that occurs in macropores like root channels and animal burrows. This structures can persist over decades as their structure gets stabilized by microorganisms and fungal metabolite products like polysaccharides (Hagedorn and Bundt 2002). Preferential flow is also induced by heterogeneities in soil texture such as impeding layers or lenses that lead to flow interruption and consequent concentration of water flow, the so-called funnel flow. Unstable flow may also occur due to small scale differences in water repellency or air entrapments (Hendrickx and Flury 2001). Soil profiles always feature both, areas with matrix flow conditions and areas with preferential flow conditions, leading to a high heterogeneity of flow patterns on the centimetre scale. With increasing water flux a dilution of DOC concentrations was measured by Mertens et al. (2007) using suction plates in 120 cm depth. Nevertheless the total amount of transported DOC possibly increases as increased OM contents along preferential pathways of water flow were found compared to matrix flow conditions (Bogner et al. 2012). The flow velocity not only has an influence on the total amount of carbon transported but also on the DOM composition as at rapid flow conditions on storm events the selective retention of aromatic compounds is reduced in subsoil DOM (Kaiser and Guggenberger 2005). The impact of different flow regimes on the DOC transport is still not totally understood as field studies of percolating soil water with respect to spatial differences on the centimetre scale are very rare (Göttlein and Stanjek 1996).

Kaiser and Kalbitz (2012) published a conceptual model that declares the transport of DOC down the soil profile to be a sequence of sorption, microbial decomposition and remobilisation processes in numerous cascade steps down the soil profile. The process is powered by the steady input of young highly reactive

plant derived OC. Over the course of this cascade microbial degraded OC gets suppressed and remobilized by less degraded OM. This OM is transported further down with the percolating soil solution, accounting for the observed distinct OM composition and ^{14}C age profiles (Rumpel et al. 2012). The influence of different flow regimes is not incorporated in the concept but might lead to large variations of DOC transport on the spatial and temporal scale. The aim of this work was to verify this concept with field and laboratory experiments, focusing on the importance of litter input and solid-solution interactions under special consideration of variability induced by spatial and temporal variations in flow velocity, a process that was neglected by studies in the past (e.g. Michalzik et al. 2001, Kalbitz et al. 2005).

1.4 Hypotheses

H1: Water and DOC fluxes are dominated by small scale spatial variability caused by hydrological and physicochemical soil heterogeneities. This variability increases in the subsoil due to longer flow distances.

H2: At matric flow conditions the pronounced sorption of DOM compounds to minerals leads to strongly decreasing DOC concentrations and changing DOM compositions from topsoil to subsoil. Hence, the contribution of litter derived OC to DOC in the mineral soil is reduced with depth.

H3: At high water fluxes DOM bypasses sorption or microbial consumption sites so that DOC concentrations in the subsoil remain at a higher level. The preferential sorption of aromatic compounds is reduced and a higher proportion of young OC from the forest floor is transported to greater depth.

H4: Transported DOC is in intimate exchange with the mineral soil. The input of young highly reactive DOC to the mineral soil leads to a selective sorption and a consequent remobilisation of less binding affine OC compounds that are transported further down the soil profile.

H5: Mineral-organic complexes act as biogeochemical hotspots, especially in sandy subsoils. Hence, the sorption of OC to reactive minerals like goethite is to a large part not irreversible, as interaction with the soil solution lead to a mobilisation of OC, evoked by the exchange with reactive DOM compounds.

These hypotheses were addressed in the following three studies.

1.5 Studies

Study I: "Small scale variability of vertical water and dissolved organic matter fluxes in sandy Cambisol subsoils as revealed by segmented suction plates"

For the first study a high intensity monitoring of the DOC dynamics down to 150 cm depth was carried out in in an old growth forest stand (*Fagus sylvatica* L.) for 13 month. The vertical transported soil solution was sampled by segmented plate lysimeters, which were used in a field experiment for the first time, to evaluated differences in flow velocity on the centimetre scale. The weekly samples were analysed for DOC concentration and for DOM composition by UV-Vis absorbance. It was possible to calculate a water flow value for each DOM sample and statistically evaluate relationships between flow velocity and DOM characteristics under consideration of the spatial and temporal variability of all parameters. This study addressed parts of the hypotheses H1, H2 and H3.

Study II: "Transport of litter derived dissolved organic matter in the subsoil of a Dystric Cambisol: A 13C field labelling approach"

At the same field site of the first study a stable isotope labelling experiment was established by replacing the original leaf litter above the investigated soil profiles by ^{13}C enriched beach leaf litter. From February 2015 to June 2016 a total of 11 sets of samples of the above mentioned monitoring where measured for $DO^{13}C$ to follow the fade of litter derived DOC down the soil profile with regard to variations over time and on the centimetre scale. This study addressed parts of the hypotheses H2 and H3.

Study III: "Multiple exchange processes on mineral surfaces control the transport of dissolved organic matter through soil profiles"

In the third study a column experiment with undisturbed soil samples and ^{13}C labelled OM-coated goethite was conducted to investigate exchange processes between reactive minerals and DOC in a controlled environment. Three columns of samples of increasing depth were connected to a cascade and percolated

consecutively with the effluent of the above column. To start the cascade the 1th depth columns were percolated by DOM extracted from beech leaf litter. A patch of ^{13}C labelled OM-coated goethite was incorporated in each column to trace exchange processes between the reactive mineral and the liquid phase. By evaluating the changes of $\delta^{13}C$ values on the solid samples and in the soil solution before and after the experiment gross OC exchange was determined. With this approach it was possible to quantify the magnitude of exchange and mobilisation processes that would have been overlooked with the investigation of only net changes in OC content. This study focused on the hypotheses H4 and H5.

2. Study I

"Small scale variability of vertical water and dissolved organic matter fluxes in sandy Cambisol subsoils as revealed by segmented suction plates"

Contribution: I installed the monitoring equipment, performed the sampling, did parts of the laboratory work, collected and analyzed the data, compiled tables and graphs and wrote the manuscript. As the corresponding author I performed the review process of the paper.

Publication status: published in:

Biogeochemistry, Volume 131, pp 1-15, doi: 10.1007/s10533-016-0259-8

Small scale variability of vertical water and dissolved organic matter fluxes in sandy Cambisol subsoils as revealed by segmented suction plates

Leinemann, T.1; Mikutta, R.2; Kalbitz, K.3; Schaarschmidt, F.4, Guggenberger, G.1

1 Institute of Soil Science, Leibniz Universität Hannover, Herrenhäuser Straße 2, 30451 Hannover, Germany

2 Soil Science and Soil Protection, Martin Luther University Halle-Wittenberg, Von-Seckendorff-Platz 3, 06120 Halle (Saale), Germany

3 Institute of Soil Science and Site Ecology, Technische Universität Dresden, Pienner Strasse 19, 01737 Tharandt, Germany

4 Institute of Biostatistics, Leibniz Universität Hannover, Herrenhäuser Straße 2, Germany

Corresponding author:

Timo Leinemann, leinemann@ifbk.uni-hannover.de, +49-511-762-19250,

Acknowledgements

Funding of the research was provided by the Deutsche Forschungsgemeinschaft DFG within the research unit FOR 1806 "The Forgotten Part of Carbon Cycling: Organic Matter Storage and Turnover in Subsoils (SUBSOM)". We would like to thank Dr. Stefan Wessel-Bothe of Eco-Tech GmbH for help with establishing the soil observatories and Heike Steffen, Anne Kathrin Herwig and numerous student helpers for support in sample processing.

2.1 Abstract

Dissolved organic matter (DOM) is considered as a major carbon source in subsoils. As soil water fluxes are highly variable at small scale, and transport versus sorptive retention of DOM is related to water flux and associated contact time with minerals, knowledge of the small scale spatial variability of the dissolved organic carbon (DOC) concentrations and fluxes into the subsoil is decisive for a solid estimation of organic carbon (OC) translocation into the subsoil. Here, we made advantage of novel segmented suction plates (4 x 4 segments, each 36cm²) to analyze the small scale spatial and temporal variability of DOC transport at 10cm, 50cm and 150cm depth of three subsoil observatories (approximately 50 m apart) in a sandy Dystric Cambisol under beech in the Grinderwald, 40 km northwest from Hannover, Germany. Water fluxes, DOC concentrations and fluxes as well as the specific UV absorbance (SUVA) at 280 nm were determined in weekly samples from August 2014 to November 2015 for each individual segment. The DOC fluxes decreased with depth (19.6 g C m^{-2} year-1, 10 cm; 1.2 g C m^{-2} $year^{-1}$, 150 cm) and were strongly related to the water fluxes. The SUVA at 280 nm also decreased with depth (0.03 L mg C^{-1} cm^{-1}, 10cm; 0.01 L mg C^{-1} cm^{-1}, 150 cm), indicating a selective retention of aromatic moieties, that was eased with increasing water flux at least in the subsoil. The proportion of temporal fluctuations and small scale variability on the total variance of each parameter where determined by the calculation of intra class correlations. The seasonal heterogeneity and the small scale spatial heterogeneity were identified to be of major importance. The importance of the small scale spatial heterogeneity strongly increased with depth, pointing towards the stability of flow paths and suggesting that at a given substrate hydrological processes rather than physicochemical processes are decisive for the sorptive retention of DOM and the variability of OC accumulation in the subsoil. Our results clearly show the demand of small scale sampling for the identification of processes regarding carbon cycling in the subsoil.

Keywords: DOC flux, SUVA, segmented suction plates, small scale variability, beech forest

2.2 Introduction

Dissolved organic matter (DOM) is the most mobile fraction of carbon in soil and sediments. It contributes to the translocation of carbon, nitrogen, and phosphorus from the litter layer, where high concentrations of available carbon fuel microbial processes, in the often carbon limited mineral subsoil (Kalbitz and Kaiser 2008; Stevens et al. 1999). In the subsoil DOM gets immobilized by adsorption to reactive minerals, like metal oxides and clay minerals, or coprecipitation with metals, thereby forming mineral-associated organic matter (OM) (e.g. Guggenberger and Kaiser 2003; Scheel et al. 2007; Kleber et al. 2015). This mineral-associated OM undergoes microbial processing, and the resulting transformation-degradation products may be soluble or more easily desorbable than the originally sorbed compounds (Kaiser and Kalbitz 2012). According to these authors, a cascade of adsorption and desorption processes forces less degraded, highly sorptive, plant-derived DOM compounds like aromatic substances to be preferentially retained. Thereby weakly bound, partly microbial-derived OM, like polysaccharides, is released and transported further down into the deeper subsoil. This process of microbial driven competitive release of sorbed OM may be accentuated by limited availability of sorption sites together with a larger organic carbon (OC) loading of minerals in topsoil than in subsoil (Guggenberger and Kaiser 2003).

Formation and transport of dissolved OC (DOC) are directly linked to water flux in soil which is known to be highly variable over the soil profile (Jarvis et al. 2007). The content of organic compounds in the soil water can be quantified by the organic carbon content. The more water is moving through the pore space the higher is the total amount of transported carbon, even though at extreme water fluxes DOC concentrations are declining due to dilution effects (Mertens et al. 2007; Buckingham et al. 2008). In most studies DOC fluxes to subsoil are calculated from DOC concentrations in samples extracted by suction cups and water fluxes determined by numerical water budget models (McDowell and Likens 1988; Currie et al. 1996; Nielson et al. 1999; Fröberg et al. 2006; Rieckh et al. 2014). However, preferential flow processes are not necessarily detected using suction cups for soil water sampling, as shown by Hopp et al. (2005) by combination of dye tracing experiments and suction cup sampling. Preferential flow leads to

increased OM contents along the pathways compared to soil regions dominated by matric flow conditions (Bogner et al. 2012; Bundt et al. 2001). Such differences in the flow pattern of water may also have consequences for DOM composition. Under matric flow conditions, a selective retention of lignin-derived polyphenols rich in carboxylic groups takes place (McCarthy 1996; Kaiser et al. 2004). Consequently, Kaiser and Guggenberger (2005) reported a decrease in SUVA of DOM collected under matric flow conditions at 90 cm depth of a strongly aggregated loamy soil, indicating selective retention of aromatic compounds upon sorption. However, under rapid flow conditions induced by storm events, where the DOM bypassed mineral sorption sites, DOC concentration and DOM composition did not change much in 90 cm compared to surface organic horizons (Kaiser and Guggenberger 2005). While these results show that preferential water flux in case of extreme hydrological events can impact DOM composition in the subsoil, the general importance of preferential flow for the vertical transport and retention of DOM is not known.

Root channels and animal burrows are known as facilities for preferential flow processes at the centimeter scale (Jarvis et al. 2007). Since the structure of these features gets stabilized by microorganisms and fungal metabolites like polysaccharides, preferential flow paths might be persistent over decades (Hagedorn and Bundt 2002). After the decay of roots the next plant generations may continue using them for rooting (Murielle et al. 2011). In addition, heterogeneities in soil texture lead to so-called funnel flow, i.e., flow interruption and consequent higher DOC concentrations by impeding layers or lenses of different texture. Heterogeneous flow may also occur due to small scale differences in water repellency, air entrapments, or small scale textural layering (Hendrickx and Flury 2001). Despite this, very little information is currently available on the extent to which preferential flow paths modify the downward transport of DOM in the vadose zone at the centimeter scale, and the influence of preferential flow on DOC retention in the mineral subsoil has been neglected in the past (Michalzik et al. 2001; Kalbitz et al. 2005; Sawicka et al. 2016). Although some recent research has received the importance of preferential flow (Hagedorn et al. 2015), field studies are still rare.

In this study we investigated the spatial heterogeneity of vertical soil water fluxes and its impact on DOM translocation in the subsoil. For this we used segmented suction plates incorporated into soils of an old-growth forest stand (*Fagus sylvatica*) down to a depth of 150 cm at three locations in the stand. Over the course of 13 month, water fluxes and DOC concentrations in each of the segments as well as the DOM composition, assessed by UV absorption, were monitored on a weekly basis. This setup gives the unique possibility to compare the heterogeneities induced on the centimeter scale at given soil depth (”small scale spatial heterogeneity“) with those of different locations within the stand (“site heterogeneity”), under consideration of the heterogeneity induced by seasonal changes of meteorological conditions (“seasonal heterogeneity”). We hypothesize that there is a pronounced “small scale spatial heterogeneity” in water and DOC fluxes caused by hydrological and physicochemical soil heterogeneity as mentioned above. We expect that at matric flow conditions the pronounced sorption of DOM compounds to minerals leads to strongly decreasing DOC concentrations from topsoil to subsoil. In contrast, at higher water fluxes DOM may bypass sorption or microbial consumption sites so that DOC concentrations in the subsoil remain at a higher level, thus hydrological processes tend to have a higher importance on transport and processing of DOM than biochemical processes. In a given substrate we expect the “small scale spatial heterogeneity“ to be more pronounced than the “site heterogeneity”. Furthermore, we hypothesize that the “site heterogeneity” in water and DOC fluxes is also reflected in the “site heterogeneity” of DOM composition, as less pronounced DOM retention along preferential flow paths also result in limited selective retention of aromatic compounds. Finally, we hypothesize that there is a larger variability of water fluxes and DOC concentrations in the subsoil than in the surface soil due to longer flow distances that increase the magnitude of flow velocity effects.

2.3 Material and methods

Site description and establishment of the soil observatories

The experiment was carried out in the Grinderwald beech (*Fagus sylvatica*) forest, which was established in 1906 and is located approximately 40 km north-west of Hannover, Germany (52° 34’22.1 North,

9°18’49.7 East). The mean annual temperature is 9.7°C and the mean annual precipitation amounts to 762 mm (Deutscher Wetterdienst, Nienburg, period 1981-2010). Soils developed in Pleistocene fluvial and aeolian sandy deposits from the Saale glaciation and were dominated by Dystric Cambisols. They were relatively homogenous in their texture, pH, and OC contents (Supplement 1).

In July 2013 three subsoil observatories were installed by placing polyethylene shafts (1.5 m diameter) into the soil that provide the possibility to access the surrounding undisturbed soil down to 2 m depth. Among some other equipment not relevant for this study, in each of three soil observatories segmented suction plate lysimeters (25 x 25 cm) containing 16 squared segments (each 36 cm²), made from polyamide filter membrane (ecoTech Umwelt-Meßsysteme GmbH, Bonn, Germany), were installed horizontally in three depths (10 cm, 50 cm and 150 cm) to collect soil solution at high spatial resolution. In the following, samples from 10 cm depth will be referred to as topsoil samples and samples from 50 cm and 150 cm depth will be referred to as upper and deeper subsoil samples. At 10 cm the installation was realized by taking out a soil block of approximately plate size down to 10 cm depth, placing the plate beneath, and putting the soil block back into position. At 50 cm and 150 cm depth the plates were installed from inside the observatory. All plates were installed with a 1 mm x 1 mm polyethylene mesh on top to protect the surface from damage. Contact to the soil was achieved by a mixture of quartz silt and 2-mm sieved soil from the observatories, which was applied to ensure uniform, tight contact with the soil surface. Per observatory the suction plates where connected to a vacuum pump providing 50 mbar of suction to enable free percolation from each of the segments of the plate into separate sample bottles. Zsolany (1996) defined soil solution that is sampled with 50 mbar of pressure as free percolating water. To minimize effects of disturbance due to placement of the suction plates, particularly in the topsoil, the plates were equilibrated for seven months in the soil, confirming that all segments had contact to the soil. Additionally soil solution was sampled by glass suction cups (ecoTech Umwelt-Meßsysteme GmbH, Bonn, Germany), 6 per depth and observatory at 50 cm and 150 cm depth connected to a vacuum pump providing 150 mbar of suction, to compare the DOC in free moving water, sampled by the suction plates with water in stronger adhesion with the soil matrix of the subsoils. Throughfall was collected every week

with 15 precipitation collectors installed on the ground directly around the observatories. In addition, total precipitation was measured by a weather station at a pasture close to the forest.

Sampling and analyses

Soil solutions from the 16 segments per plate and the suction cups were collected from August 2014 to November 2015 on a weekly basis. In weeks with extreme water flux, the capacity of individual bottles (250 mL) per sampling date was reached (17 times at 10 cm depth, 1.6 %, 17 times at 50 cm, depth, 9.6 % and 57 times in 150 cm depth, 16.5 %). Thus, the mean and the variation of water flux for values of this magnitude will be underestimated in the data, whereas DOC concentrations should be valid because the concentration of a sample is not affected by the sampled volume in the first case. Dilution effects on the DOC concentration at high water flux rates, as described later in this study, have already taken place when the sample is collected in the bottle. Nevertheless an overestimation of DOC concentrations seems possible when high water fluxes occur after longer dry periods which possibly flush accumulated OM down the soil profile resulting in decreasing DOC fluxes at later phases of heavy rainfall events (Kalbitz et al. 2000). Following this assumption the magnitude of DOC flux underestimations is even smaller than the amount of water flux underestimations. Assuming an improbably high underestimation of the water flux of 20 %, would lead to an increase of DOC flux by less than 20 %. On the other hand, at many time points, there was no water flux at all in the majority of segments within suction plates. In consequence, observations for DOC, DOC flux and SUVA are then systematically missing. In total 1616 samples were taken, 1092 at 10 cm depth, 178 at 50 cm and 346 in 150 cm depth. Dry conditions prohibited sampling of 61 % of the theoretically possible number of samples at 10 cm depth, 93 % at 50 cm and 87 % in 150 cm depth.

As the bottles were placed within the observatory in the dark and at soil temperature ≤10°C, decomposition of DOM was considered minor (Peacock et al. 2015), and we refrained from toxifying the solutions. Collected solutions were brought to the laboratory, immediately weighed for volume determination and filtered to < 0.45 µm by polyethersulfon filters (VWR International; Radnor;

Pennsylvania). Samples were stored at 4°C for a maximum of 30 days until analyses. The concentrations of DOC were measured by high temperature combustion with a limit of quantification of 1 mg C L^{-1} (Vario TOC cube; Elementar, Hanau, Germany). The UV absorbance at 280 nm was determined at a Varian Cary 50 UV-Vis (Agilent Technologies, USA), and SUVA was calculated as the ratio of UV absorbance at 280 nm and DOC concentration (L mg^{-1} C cm^{-1}) (Chin et al. 1994; Scheel et al. 2007). Weekly water fluxes were calculated based on the sampled volume with regard to the area of the segments (36 cm^2) and given in mm, while weekly DOC fluxes were calculated by multiplying DOC concentrations with water fluxes and given in g C m^{-2}.

Statistics

In a preliminary analysis, we computed the means as well as the variances between the 16 segments within each suction plate, separately for each week, observatory and depth. In order to describe the extreme observed dependency of the variances on the means, we fitted linear mixed effect models for the log-transformed variances as dependent variable and the log-transformed means and the depth level (10 ,50, and 150 cm) as explanatory variables (fixed effects). To account for the nesting of observations within observatory and within plate over time, observatory and plate were included as random effects. If not stated otherwise, error values are given as standard deviation.

In a second series of linear mixed models, we analyzed the log-transformed original data (water flux, DOC concentration, DOC flux, SUVA), at the level of individual segments per suction plate, i.e. without computing means and variances at the level of suction plates. Applying the log-transformation to the data corrects for the very clear overall increase of variances with increasing means. On this transformed scale, we decomposed overall variance into three variance components. First, the differences between the three observatories (“site heterogeneity”), second, the mean differences between the segments of a particular suction plate (“small scale spatial heterogeneity“), and third, by temporal differences within each segment caused by seasonal changes of the hydrological conditions (“seasonal heterogeneity”). In order to discriminate between the contributions of variance imposed by all three factors, mixed effects models

(Bates et al. 2015) were applied. To determine the significance of differences between sites, the observatories were included as fixed effects in a mixed model, while changes within plate and between weeks were kept as random effects. Then, the means of observatories were compared by applying the Tukey method (Tukey 1949) on the fitted model using the R package "lsmeans" (Lenth 2016). Finally, in separate models for each observatory and depth, we used random effect models to estimate three variance components: the temporal variance between dates, the variance between segments (in average over time) and the residual variance. From these, the influences of the "small scale spatial heterogeneity" and of the "seasonal heterogeneity" were estimated by the calculation of intra-class correlations (Johnson and Koch 2011), showing the importance of the variance of one class of parameters in a dataset to the total variance of the dataset.

$$Intra\ date\ correlation\ (IDC) = \frac{va\ date}{va\ date + va\ segment + va\ residual} \quad \text{eq. 1}$$

$$Intra\ segment\ correlation\ (ISC) = \frac{va\ segment}{va\ segment + va\ residual} \quad \text{eq. 2}$$

The "intra-date correlation" (IDC) gives the ratio of the variance induced by the changes over time and the total variance (variance induced by temporal changes (va-date) + variance between the segments of one suction plate (va-segment) + residual variance (va-residual)). The "intra-segment correlation" (ISC) gives the ratio of the variance induced by the differences between the segments and the residual variance, excluding the variance induced by temporal changes. An "intra-date correlation" of unity would indicate that the observed variance between the segments of one suction plate is negligible and the differences are all induced by changes over time. In contrast, an "intra-segment correlation" of unity would support the assumption that the relative differences between the segments of one suction plate are totally constant over time. All statistical calculations were done with R software using the package "lme4" for calculation of mixed effects models (Bates et al. 2015), and the figures were created with the "ggplot2" package (Wickham 2009).

2.4 Results and discussion

Water fluxes

Precipitation occurred during 63 out of the 64 weeks of observation. In 31 weeks a throughfall of less than 5 mm were recorded, while more than 5 mm were measured in 32 weeks (Supplement 2). In total the throughfall amounted to 589 mm within the 63 weeks, which represents 52 % of the total precipitation. The water fluxes at 10 cm soil depth mirrored well the precipitation events, and even small events resulted in percolating water at all three observatories, ensuring continuous sampling (n = 1092). Total water flux at 10 cm soil depth during the observation period was 412 mm, representing 70 % of the throughfall. At 50 cm depth, soils were much drier, so that at a suction of 50 mbar percolating water could be collected only during wet periods (n = 178), amounting to a total water flux of 108 mm during the observation period. Interestingly, at a soil depth of 150 cm, water could be collected at more events (n = 346) and also the total flux was higher (233 mm during the observation period). Possibly the larger water fluxes through macropores (< 50 mbar) in the deeper subsoil as compared to the upper subsoil is caused by bypass processes due to heterogenic flow patterns (Flury et al. 1994). Strongly varying water fluxes are also obvious by the high standard deviation at all three depths (Table 1). In the subsoil different water fluxes between 0 mm and 70 mm during the same week can be explained by differences in texture. At loamy lenses in the C Horizons of the Grinderwald soils the silt contents increase were higher (Supplement 1), leading to a decrease of macropores, an increase of bulk density and thus a minor water movement.

We found that the three different observatories exhibited different total water fluxes (Table 1). At 10 cm depth observatory 2 showed the largest value (550 mm), while at 50 cm depth the largest water flux was observed at observatory 1 (168 mm), and in 150 cm depth at observatory 3 (467 mm). These fluctuations are most likely induced by differences in the substrate at the three observatories, with the coarsest texture in the subsoil of observatory 3 (Supplement 1). Unfortunately, the 150 cm depth suction plate in observatory 2 is installed inside a loamy lens and did not provide solution over the whole period. For that reason this plate was excluded from the analyses of variance. When comparing the mean values of the

water fluxes at the same soil depth under consideration of the temporal variations, only the differences between the topsoil suction plates were significant (p-value < 0.001). The suction plates in the subsoil gave no significantly different values (p-value > 0.01).

For all three observatories, the variance of the water flux within the suction plates increased with increasing average water flux (Fig. 1a). The variance of water fluxes during the observation period was seven to ten times higher in the subsoil than in the topsoil. This could be the result of longer flow paths to the subsoil. A flow path of 10 cm length seems to be too short for the development of distinct flow regimes (Flury et al. 1997) in the rather homogenous textured topsoil material with a high root density (Kirfel et al., in preparation). In the topsoils, the IDC was also noticeable larger (0.85) than the ISC (0.38), showing that in the topsoil the "seasonal heterogeneity" of the water flux is more important than the "small scale spatial heterogeneity" (Fig. 2a). Hence, in the topsoil different meteorological conditions have the strongest influence on the variance of water fluxes with the differences between the segments being less important. In the subsoil the ISC became more important (up to 0.72), pointing towards a higher impact of the "small scale spatial heterogeneity" and a declining influence of the meteorological conditions. This also reveals that in the subsoil relative differences between the segments of one suction plate appeared more stable over time than in the topsoil (Fig. 2a-c), including drying and wetting cycles, leading to large differences between the cumulative water fluxes per segment in the subsoil (Supplement 4). This finding corroborates the view that at least in the subsoil preferential flow paths in soil persist over months (Hagedorn and Bundt 2002). No significantly different variances of the water flux per suction plate were detected comparing the three observatories (p-value > 0.3), leading to the conclusion that in contrast to the "small scale spatial heterogeneity" the "site heterogeneity" is negligible when the variance of the water flux is analyzed.

DOC concentrations

The largest mean DOC concentrations for all three observatories were measured in the topsoil (64.2 ± 25.2 mg L^{-1}). Average concentrations declined with depth to 18.7 ± 19.0 mg L^{-1} at 50 cm and to 8.9 ± 14.7 mg

L^{-1} at 150 cm depth (Fig. 3a). The average DOC concentrations showed a high variability, though differences between the three observatories were not significant (p-value > 0.2).

The DOC concentrations in the topsoil varied during the season, with larger values in the dry and warm summer and autumn than in the winter with intermediate precipitation (Fig. 4). This corresponds to findings by Tipping et al. (1999), suggesting larger DOC concentrations at higher temperatures in field manipulation experiments due to an increase of microbial activity, which leads to a higher DOC production (Anderson and Ingvar Nilsson 2001). A positive correlation of DOC concentration and soil temperature at 10 cm depth were also observed by Clark et al. (2005) over the course of a 10 year time series. The DOC concentration in the soil water correlated negatively with the water flux (Fig. 5a). Hence, increasing water fluxes resulted in a dilution of the DOC concentration in soil solution as observed by Mertens et al. (2007), using plate lysimeters in a bare Luvisol down to 120 cm depth. In the topsoil the seasonal trends also contributed to the negative correlation. The slope of this relationship was steeper in the subsoil compared to the topsoil (Table 2), possibly due to the increased importance of stable flow paths (Fig. 2b) and higher variances in water flow (Fig. 1a).

The DOC concentrations in soil solutions collected by the suction plates were larger in the whole profile than those collected by suction cups. Mean DOC concentrations in suction cup solutions combined for all three observatories were 9.6 ± 7.9 mg L^{-1} at 50 cm depth and 5.9 ± 2.4 mg L^{-1} in 150 cm depth. Not only were the mean values nearly halved but also the standard deviations were greatly reduced. Rieckh et al. (2014) found almost the same DOC concentrations using suction cups (5.7 mg L^{-1} in 160 cm depth of a Luvisol), showing that the DOC concentrations in this study fit well to the possible range reported for other ecosystems (Supplement 3). Dosskey and Bertsch (1997) reported even smaller DOC concentrations and standard deviations of 1.8 ± 0.3 mg L^{-1} down to 99 cm depth in sandy forest soils using suction cups. This turns out to be four times smaller than the concentrations measured by the suction plates in 150 cm depth in this study and could be induced by the use of suction cups. These do not reproduce the high variability at centimeter scale and are subject to the limitation of gaining their small amount of subsoil

samples only at intense precipitation conditions. Free percolation water has a higher peak DOC concentration than pore water extracted by suction cups, the latter containing a DOC mixture from different pore sizes arising from longer exposure time of soil solution in fine pores with a higher water holding capacity (Hagedorn et al. 2000, Jardine et al. 1990). This enables more intimate reactions with the mineral matrix, thus leading to a more pronounced retention of DOM within finer pores (Kaiser and Guggenberger, 2005). These findings are supported by Mertens et al. (2007), who reported mean DOC concentrations of 9 mg L^{-1} in a bare Luvisol in 120 cm depth by using suction plate lysimeters. The relatively high DOC concentrations in the Grinderwald topsoils are favored by high input from the forest floor supported by moderate climate conditions (only 20 days with slightly negative temperatures and just two weeks with snow cover) and relatively little sorptive retention in the very sandy soil. The DOC concentrations in the subsoils are in the upper range of ecosystems in temperate climate conditions when compared to literature (Michalzik et al., 2001).

For all three observatories, the variance of the DOC concentration within the suction plates increased with increasing average DOC concentrations (Fig. 1b). Similarly to the water fluxes the variance of the DOC concentration was larger for the subsoil than for the topsoil for a given mean DOC concentration (p-value < 0.001). In the topsoil the variance of the DOC concentration increased by a factor of 4.8 when the mean DOC concentration doubled. In the subsoil the slope of this relationship steepened, with doubled mean DOC concentration leading to an increase of the variance by a factor of 6.1 and 9.9 at 50 cm and 150 cm depth, respectively (Fig. 1b). The increase in variance with depth can possibly be explained by the difference in flow path length. A 10 cm long soil column results in less possibility for variations than a 50 cm or even 150 cm long column. Hot spots of microbial activity like root channels, concentrations of reactive minerals, e.g. in loamy lenses, or combinations of both are interspersed with areas of bare sand with less reactive characteristics. The variance of the DOC concentrations was nearly equally influenced by seasonal fluctuations (IDC) and small scale fluctuations (ISC), with slightly larger values of IDC at all three depths (Fig. 2b). This shows that even with the high fluctuations from dry conditions to intense water flow, differences on the centimeter scale still contribute to the overall variance in the dataset.

Studies on small scale heterogeneity of soil solution are very rare. Göttlein and Stanjek (1996) also found highly variable solution chemistry parameters in a Podzol in soil solutes sampled by a grid of micro suction cups applied at a distance of 1.5 cm. Unfortunately, because of limited sample volumes no DOC concentrations could have been measured in their study.

DOC flux

The weekly DOC fluxes varied strongly during the observation period and were dependent on the weekly water fluxes (Fig. 5b). Even though the DOC concentrations declined with increasing water flux (Fig. 5a), the maximum absolute DOC transport occurs at the highest water flux. This is in accordance with Buckingham et al. (2008) who found a positive relation between annual DOC flux and annual water flux in three ecosystems using tension free collectors. This highlights the importance of precise water flux analysis on the small scale for correct analysis of the DOC input to the subsoil. The cumulative DOC flux in topsoils for all three observatories over the 63 weeks of observation (22.9 g m^{-2}) was much larger than in subsoils with 1.9 g m^{-2} at 50 cm and 1.4 g m^{-2} in 150 cm depth annual values for the hydrological year for each observatory are shown in Table 1). This represents a decline in transported DOC of more than 92 % in the first 50 cm of the soil profile and an additional 26 % from 50 cm to 150 cm depth. The total decline of the DOC flux within the 150 cm soil depth was 94 %. Similar strong reductions in carbon flux from topsoil to subsoil have been detected for many other forest ecosystems (Neff and Asner 2001). Nielson et al. (1999) found a DOC flux of 25.5 g m^{-2} $year^{-1}$ at 10 cm depth and 2.4 g m^{-2} $year^{-1}$ in 60 cm depth accounting for a total loss in DOC of 90 % in a oak forest on sandy soils in Denmark determined by horizontally installed funnel lysimeters. Kalbitz et al. (2004) reported a DOC flux of 16.1 ± 7.1 g m^{-2} $year^{-1}$ in 20 cm depth and 2.2 ± 0.8 g m^{-2} $year^{-1}$ in 90 cm depth, accounting for a total loss in DOC of 86 % in a coniferous forest stand in Germany determined by five replicates of ceramic suction cups. Both, adsorption to reactive minerals or co-precipitation (Moore 1989; Mikutta et al. 2006; Kleber et al. 2015) and consumption by microorganisms (Hur et al. 2011) have been discussed as potential processes that lead to the strong decline of the DOC fluxes over the soil profile. Biodegradation of DOM is considered to be

of less importance than sorption to reactive minerals (Qualls and Haines 1992). Consequently, Kalbitz and Kaiser (2008) estimated that 66 % of the subsoil OC stocks are DOM-derived. However, mineralization of OM and loss to CO_2 must happen, otherwise the OC content of the soil would not be as low as observed (Kalbitz et al. 2005) (Supplement 1). We think that this is to a large part stemming from sorbed OM. According to Don et al. (in preparation), there is quite a large pool of mineral-associated OM in the Grinderwald subsoil, which is turning over quite fast, even though root biomass and adsorbed DOC both account as possible sources.

This study benefits from the fact that data necessary for DOC flux calculations (water flux and DOC concentrations) were determined for each individual soil solution sample (maximal 16 per soil depths, observatory and sampling point), in contrast to the common practice to use one modeled water flux value per depth and DOC concentrations mostly gained from suction cups (Neff and Asner 2001). This gave the unique possibility to investigate the small scale heterogeneity of DOC fluxes to the subsoil. In the subsoil the segments of one suction plate exhibit highly different total DOC flux values resulting in differences of about 90 % comparing the segments with the highest DOC flux to those with the lowest one (Fig. 6). These differences among segments largely persisted throughout the entire observation period, supporting our hypothesis that in subsoil the spatial differences are constant over time and possibly contribute to hotspots of soil OC (Chabbi et al 2009) and microbial activity (Niebuhr et al., submitted).

Due to the large variations of the input variables for the DOC flux calculation (water flux and DOC concentration) the differences between the three observatories were not significant (p-value > 0.5). Further, in all three observatories and depths the variance of the DOC flux increased with increasing mean DOC flux (p-values < 0.001), whereas differences between the variances of the different observatories and depths were not significant (p-values > 0.09; Fig. 1c). Calculation of intra-class correlations reveals that in the topsoil the “seasonal heterogeneity” was of utmost importance for the DOC fluxes (IDC >> ISC; Fig. 2c). In the subsoil the influence of the “small scale spatial heterogeneity” on the total variance in the DOC flux dataset increased (IDC = ISC) (Fig. 2c). This underlines the importance of the variance of the water

flux for the determination of DOC fluxes, which showed comparable patterns in the intra-class correlations. The constancy of flow paths over time (Fig. 2a) and the positive correlation of water flux and DOC flux (Fig. 5b) supported the hypothesis that small scale differences in the DOC transport are stable over time and possibly contribute to the development of heterogenic OC distributions in small spatial scales. This fits also to the study of Don et al. (2012), who showed a higher variance of OC stocks on small spatial scale than for samples of greater spatial distance in forest ecosystems, and is consistent with the result of no significant differences between the three observatories in this study. The clustered distribution of microorganisms (Kuzyakov and Blagodatskaya 2015) and the pore structure of soils act as main source for this heterogeneity, both might be affecting the DOC flux in soil too.

Specific UV absorbance

The absorbance at 280 nm was used as an indicator for the aromaticity of DOM (Kalbitz et al. 2003). According to Fig. 3, the average SUVA at 280 nm decreased significantly from topsoil (0.03 L mg C^{-1} cm^{-1} ± 0.01) to subsoil (0.01 L mg C^{-1} cm^{-1} ± 0.01) at all three observatories (Fig. 3b). as the SUVA at 280 nm is correlated to aromatic C and H in soil solution (Kalbitz et al. 2003, Scheel et al. 2007), this supports the assumption of a selective change in DOM composition passing the soil profile, due to the preferential retention of aromatic moieties by Al and Fe (hydr)oxides and a selective enrichment of carbohydrate-derived moieties in solution (Kaiser et al. 2004). This also underlines the larger importance of retention processes over microbial processes because mineralization by microorganisms preferentially alters non-aromatic compounds like sugars (Kalbitz et al. 2003). The differences between observatory 1 and observatory 3 were not significant (p-value > 0.05). For observatory 2 the differences to the other observatories were significant (p-value < 0.001), but this was only due to higher values at 10 cm depth (mean difference of 12 %) and was not apparent in the subsoil.

In the subsoil we observed a significant positive correlation of SUVA and water flux, which was not observed in the topsoil (Fig. 5c). This indicates that under larger water fluxes, i.e., higher flow rates, aromatic compounds were relatively less retained or microbial processed during their transport down the

profile. The positive relation of water flux and SUVA was detectable even at small water fluxes. This shows that the water flux does not only have an influence on the composition of DOM transport under extreme hydrological conditions as was reported by Kaiser and Guggenberger (2005) and Hagedorn et al. (2015), but also under normal flow conditions. The change in SUVA confirms that plant-derived aromatic components are preferentially retained in the upper soil. Between 50 and 150 cm, constant SUVA values, however, indicate a proportional retention of UV-active and non UV-active DOM components. Together, with the insignificant changes in DOC concentrations (p-value > 0.1) and DOC fluxes (p-value > 0.1) this indicates that in the deeper subsoil the interactions of DOM with the solid soil phase are small and/or not detectable by the used analytical approach.

In contrast to the small "site heterogeneity" between the observatories, the variance induced by "seasonal heterogeneity" (IDC) and „small scale spatial heterogeneity" (ISC) was of major importance for the whole variance of the dataset (Fig. 2d). In the topsoil, like with the water flux and the DOC concentration, the IDC was distinctly higher than the ISC, pointing again towards the major importance of seasonal changes for the SUVA in the first 10 cm (Fig. 2d). In the subsoil the differences between the segments became more important showing that the change of DOM composition was sensitive to small scale sampling, which is likewise consistent to concentrations and fluxes of DOC.

2.5 Conclusions

The soil observatories were well suited to follow the temporal behaviour of DOC concentrations and fluxes in different soil depths down to 150 cm. A negative correlation of DOC concentration and water flux suggests dilution effects of DOM in the topsoil, which was also mirrored at greater soil depth. In the subsoil the SUVA was positively correlated to the water fluxes even at small water fluxes, thus indicating a kinetic control on the preferential sorption of aromatic DOM compounds. Hence our results show that small scale differences in flow regimes decisively affect processes of carbon transport in the subsoil. This also implies that in a given substrate hydrological processes rather than physicochemical processes are crucial for the sorptive retention of DOM. The higher heterogeneity in substrate and the longer exposure

time of water in the subsoil compared to the topsoil increases the decoupling of water flow and liquid solid interaction processes from meteorological conditions. Consequently, capturing the large "small scale spatial variability" of DOM transport and water flux at the same high resolution will decrease the uncertainty of DOC flux estimation. Furthermore, a strong contribution of DOC for "small scale spatial variability" of soil OM distribution in the subsoil can be concluded. The large "small scale spatial variability" of DOC fluxes hints to an important role of DOC for the formation of biogeochemical hotspots in the subsoil.

2.6 References

Anderson S and Ingvar Nilsson S (2001) Influence of pH and temperature on microbial activity, substrate availability of soil-solution bacteria and leaching of dissolved organic carbon in a mor humus. Soil Biol Biochem 33:1181-1191, doi:10.1016/S0038-0717(01)00022-0

Bates D, Maechler M, Bolker B, Walker S (2015). Fitting Linear Mixed-Effects Models Using lme4. J Statt Softw of Statistical Software. 67:1-48. doi:10.18637/jss.v067.i01

Bogner C, Borken W, Huwe B (2012) Impact of preferential flow on soil chemistry of a podzol. Geoderma 175-176:37-46. doi:10.1016/j.geoderma.2012.01.019

Bruelheide H, Udelhoven P (2005) Correspondence of fine-scale spatial variation in soil chemistry and the herb layer vegetation in beech forests. Forest Ecol and Manag 210:205-223. doi:10.1111/j.1365-2389.1996.tb01861.x

Buckingham S, Tipping E, Hamilton-Taylor J (2008) Concentrations and fluxes of dissolved organic carbon in OK topsoil. Sci total Environ 407:460-470. doi:10.1016/j.scitotenv.2008.08.020

Bundt M, Jäggi M, Blaser P, Siegwolf R, Hagedorn F (2001) Carbon and nitrogen dynamics in preferential flow paths and matrix of a forest soil. Soil Sci Soc Am J 65:1529-1538. doi:10.2136/sssaj2001.6551529x

Chabbi A, Kögel-Knabner I, Rumpel C (2009) Stabilized carbon in subsoil horizons is located in spatially distinct parts of the soil profile. Soil Biol and Biochem 41:256-261. doi:10.1016/j.soilbio.2008.10.033

Chin Y-P, Alken G, O´Loughlin E (1994) Molecular Wright, Polydispersity, and Sprectroscopic Properties of Aquatic Humic Substances. Environ Sci Technol 28:1853-1858. doi: 10.1021/es00060a015

Clark H M, Chapmann P J, Adamson J K, Lane S N (2005) Influence of draught-induced acidification on the mobility of dissolved organic carbon in peat soils. Global Change Biology 11:791-809. doi:10.1111/j.1365-2486.2005.00937.x

Don A., Bärwolff M., Kalbitz K., Andruschkewitsch R., Jungkunst H F, Schulze E D (2012) No rapid soil carbon loss after a windthrow event in the High Tatra. Forest Ecol and Manag 276:239-246. doi:10.1016/j.foreco.2012.04.010

Dosskey M G, Bertsch P M (1997) Transport of dissolved organic matter through a sandy forest soil. Soil Sci Soc. Am J 61:920-927. doi:10.2136/sssaj1997.03615995006100030030x

Flury M, Flühler H, Jury W A, Leuenberger J (1994) Susceptibility of soils to preferential flow of water: A field study. Water Resour Res 30:1945-1954. doi:10.1029/94WR00871

Fröberg M, Berggren D, Bergkvist B, Bryant C, Mulder J (2006) Concentration and fluxes of dissolved organic carbon (DOC) in three Norway spruce stands along a climatic gradient in Sweden. Biogeochemistry 77:1-23. doi:10.1007/s10533-004-0564-5

Göttlein A and Stanjek H (1996) Mico-scale variation of solid-phase properties and soil solution chemistry in a forest podzol and its relation to soil horizons. Eur J of Soil Sci 47:627-636. doi:10.1111/j.1365-2389.1996.tb01861.x

Guggenberger G, Kaiser K (2003) Dissolved organic matter in soil: challenging the paradigm of sorptive preservation. Geoderma 113:293-310. doi:10.1016/S0016-7061(02)00366-X

Hagedorn F, Bundt M (2002) The age of preferential flow paths. Geoderma 108:119-132. doi:10.1016/S0016-7061(02)00129-5

Hagedorn F, Kaiser K, Feyen H, Schleppi P (2000) Effects of redox conditions and flow processes on the mobility of dissolved organic carbon and nitrogen in a forest soil. J Environ Qual 29:288-297. doi:10.2134/jeq2000.00472425002900010036x

Hagedorn F, Bruderhofer N, Ferrari A, Nklaus P A (2015) Tracking litter-derived dissolved organic matter along a soil chronosequence using ^{14}C imaging: Biodegradation, physico-chemical retention or preferential flow. Soil Biol Biochem 88:333-343. doi:10.1016/j.soilbio.2015.06.014

Hendrickx J, Flury M (2001) Uniform and preferential flow mechanisms in the vadose zone. In: Council N R (ed) Conceptual Models of Flow and Transport in the Fractured Vadose Zone, National Academy Press, Washington, DC, pp 149-187 doi:10.17226/10102

Hopp L, Pfeiffer S, Durner W (2006) Spatial variability of arsenic and chromium in the soil water at a former wood preserving site. J Contam Hydrol 85:159-178. doi:10.1016/j.jconhyd.2006.01.005

Hur J, Lee B M, Shin H-S (2011) Microbial degradation of dissolved organic matter (DOM) and its influence on phenanthrene–DOM interactions. Chemosphere 85:1360-1367. doi:10.1016/j.chemosphere.2011.08.001

Jardine P M, Wilson G V, McCarthy J F, Luxmoore R J, Taylor D L, Zelazny L W (1990) Hydrogeochemical processes controlling the transport of dissolved organic carbon through a forested hillslope. J Contam Hydrol 6:3-19. doi:10.1016/0169-7722(90)90008-5

Jarvis N J (2007) A review of non-equilibrium water flow and solute transport in soil macropores: principles, controlling factors and consequences for water quality. Eur J Soil Sci 58:523-546. doi:10.1111/j.1365-2389.2007.00915.x

Johnson W D, Koch G G (2011) Intraclass Correlation Coefficient. In: Lovric M, (ed) International Encyclopedia of statistical science, Springer, Berlin Heidelberg, pp: 685-687. doi:10.1007/978-3-642-04898-2_309

Kalbitz K, Solinger S, Parker J-H, Michalzik B, Matzner E (2000) Controls on the dynamics of dissolved organic matter in soil: A review. Soil Sci 165:277-304. doi:10.1097/00010694-200004000-00001

Kalbitz K, Schmerwitz J, Schwesig D, Matzner E (2003) Biodegradation of soil-derived dissolved organic matter as related to its properties. Geoderma 113:273-291. doi:10.1016/S0016-7061(02)00365-8

Kalbitz K, Zuber T, Park J-H, Matzner E (2004) Environmental controls on concentrations and fluxes of dissolved organic matter in the forest floor and in soil solution. In: Matzner E (ed) Ecological Sudies Vol, 172, Biogeochemistry of forested catchments in a changing environment, Springer Berlin Heidelberg. doi:10.1007/978-3-662-06073-5_19

Kalbitz K, Schwesig D, Rethemeyer J, Matzner E (2005) Stabilization of dissolved organic matter by sorption to the mineral soil. Soil Biol Biochem 37:1319-1331. doi:10.1016/j.soilbio.2004.11.028

Kalbitz K, Kaiser K (2008) Contribution of dissolved organic matter to carbon storage in forest mineral soils. J Plant Nutr Soil Sci 171:52-60. doi:10.1002/jpln.200700043

Kaiser K, Kalbitz K (2012) Cycling downwards - dissolved organic matter in soil. Soil Biol Biochem 52:29-32. doi:10.1016/j.soilbio.2012.04.002

Kaiser K, Guggenberger G (2005) Storm flow flushing in a structured soil changes the composition of dissolved organic matter leached into the subsoil. Geoderma 127:177-187. doi:10.1016/j.geoderma.2004.12.009

Kaiser K, Guggenberger G, Haumaier L, Zech W (2002) The composition of dissolved organic matter in forest soil solutions: changes induced by seasons and passage through the mineral soil. Org Geochem 33:307-318. doi:10.1016/S0146-6380(01)00162-0

Kuzyakov Y, Blagodatskaya E (2015) Microbial hotspots and hot moments in soil: Concept & review. Soil Biol Biochem 83:184-199. doi:10,1016/j.soilbio.2015,01,025

Lenth V L (2016) Least-Squares Means: The R Package lsmeans. J Stat Softw 69: doi:10.18637/jss.v069.i01

Malik A, Gleixner G (2013) Importance of microbial soil organic matter processing in dissolved organic carbon production. FEMS Microbial Ecology 86:139-148. doi:10.1111/1574-6941.12182

Mattsson T, Kortelainen P, Laubel A, Evans D, Pujo-Pay M, Räike A, Conan P (2009) Export of dissolved organic matter in relation to land use along a European climatic gradient. sci total environ 407: 1967-1976. doi:10.1016/j.scitotenv.2008.11.014

McCarthy J F, Gu B, Liang L, Mas-Pla J, Williams T M, Yeh T-C J (1996) Field tracer tests on the mobility of natural organic matter in a sandy aquifer. Water Resour Res 32:1223-1238. doi:10.1029/96WR00285

McDowell W H, Likens G E (1988) Origin, composition, and flux of dissolved organic carbon in the hubbard brook valley. Ecol Monogr 58:177-195. doi:10.2307/2937024

Mertens J, Vanderborght J, Kasteel R, Pütz T, Merckx R, Feyen J, Smolders E (2007) Dissolved Organic Carbon Fluxes under Bare Soil. J Environ Qual 36:597-606. doi:10.2134/jeq2006.0368

Michalzik B, Kalbitz K, Park J-H, Solinger S, Matzner E (2001) Fluxes and concentrations of dissolved organic carbon and nitrogen – a synthesis for temperate forests. Biogeochemistry 52:173-205. doi:10.1023/A:1006441620810

Mikutta R, Kleber M, Torn M S, Jahn R (2006) Stabilization of soil organic matter: association with minerals or chemical recalcitrance? Biogeochemistry 77:25-56. doi:10.1007/s10533-005-0712-6

Moore T R (1989) Dynamics of dissolved organic carbon in forested and disturbed catchments, Westland, New Zealland 1. Maimai. Water resour res 25:1321-1330. doi:10.1029/WR025i006p01321

Neff J C, Asner G P (2001) Dissolved organic carbon in terrestrial ecosystems: Synthesis and a model. Ecosystems 4:29-48. doi:10.1007/s100210000058

Peacock M, Freeman C, Gauci V, Lebron I, Evans E D (2015) Investigations of freezing and cold storage for the analysis of peatland dissolved organic carbon (DOC) and absorbance properties, Environmental Science Processes & Impacts 17: 1290-1301, doi: 10.1039/c5em00126a

Qualles R G and Haines B L (1992) Biodegradability of dissolved organic matter in forest throughfall, Soil Solution, and Stream Water. Soil Sci Soc Am J 56: 578-586. doi:10.2136/sssaj1992.03615995005600020038x

Rieckh H, Gerke H H, Siemens J, Sommer M (2014) Water and dissolved carbon fluxes in an eroding soil landscape depending on terrain position. Vadose Zone J 13. doi:10.2136/vzj2013.10.0173

Sawicka K, Monteith D T, Vaguelova E I, Wade A J, Clark J M (2016) Fine-scale temporal characterization of trends in soil water dissolved organic carbon and potential drivers. Ecological Indic In press. doi:10.1016/j.ecolind.2015.12.028

Scheel T, Dörfler C, Kalbitz K (2007) Precipitation of dissolved organic matter by aluminum stabilizes carbon in acidic forest soils. Soil Sci soc Am J 71: 64-74. doi:10.2136/sssaj2006.0111

Stevens D P, Cox J W, Chittleborough D J (1999) Pathways of phosphorus, nitrogen, and carbon movement over and through texturally differentiated soils, South Australia. Aust J Soil Res 37, 679-693.

Tipping E, Rigg E, Harrison A F, Ineson P, Taylor K, Benham D, Poskitt J, Rowland A P, Bol R, Harkness D D, Woof C (1999) Climatic influences on the leaching of dissolved organic matter from upland UK moorland soils, investigated by a field manipulation experiment. Environ Int 25:83-95. doi:10.1016/S0160-4120(98)00098-1

Tukey J W (1949) Comparing individual means in the analysis of variance. Biometrics 5:99-114. doi:10.2307/3001913

Wickham H (2009) ggplot2. Elegant graphics for data analysis. Springer, Dordrecht Heidelberg London New York. doi:10.1007/978-0-387-98141-3

Zsolnay A (1996) Dissolved humus in soil waters. In: Piccolo, A. (Ed.), Humic Substances in Terrestrial Ecosystems. Elsevier, Amsterdam, pp. 171– 224. doi:10.1016/B978-044481516-3/50005-0

2.7 Tables

Table 1: Annual water flux, mean annual dissolved organic carbon (DOC) concentration and flux in the three depths per observatory. Data were obtained by the individual segments of the suction plates, values ± standard deviation are given. Annual values are calculated as the sum of 53 weekly samplings from October 2014 to October 2015.

	Observatory 1		
Depth (cm)	Water flux (mm $year^{-1}$)	DOC (mg L^{-1})	DOC flux (g m^{-2} $year^{-1}$)
10	240 ± 58	72.0 ± 26.4	13.0± 3.8
50	164 ± 87	20.9 ± 23.8	3.7 ± 2.4
150	211 ± 223	12.46 ± 23.0	1.5 ± 1.3
	Observatory 2		
Depth (cm)	Water flux (mm $year^{-1}$)	DOC (mg L^{-1})	DOC flux (g m^{-2} $year^{-1}$)
10	481 ± 128	66.7 ± 25.4	27.6 ± 5.6
50	33 ± 40	30.0 ± 16.4	0.7 ± 0.7
150	-	-	-
	Observatory 3		
Depth (cm)	Water flux (mm $year^{-1}$)	DOC (mg L^{-1})	DOC flux (g m^{-2} $year^{-1}$)
10	305 ± 65	51.8 ± 18.0	14.9 ± 2.9
50	112 ± 96	13.4 ± 10.1	1.4 ± 1.6
150	407 ± 301	6.9 ± 6.2	2.1 ± 1.3

Table 2: Results of the regression models (Fig. 5) using water flux and DOC concentration, DOC flux, and SUVA. Equations are in the form of: y=b+mx

depth (cm)	equation	sample size (n)	standard error of m[a]	p-value
10	log(DOC) = 6.2 - 0.10 x log(Flux)	1092	0.03	< 0.001
50	log(DOC) = 5.4 - 0.31 x log(Flux)	178	0.04	< 0.001
150	log(DOC) = 4.3 - 0.26 x log(Flux)	346	0.03	< 0.001
10	log(DOC flux) = - 3.9 + 0.93 x log(Flux)	1092	0.04	< 0.001
50	log(DOC flux) = - 4.5 + 0.77 x log(Flux)	178	0.05	< 0.001
150	log(DOC flux) = - 5.9 + 0.79 x log(Flux)	346	0.05	< 0.001
10	log(SUVA) = - 5.3+ 0.08 x log(Flux)	1083	0.03	< 0.01
50	log(SUVA) = - 8.8 + 0.34 x log(Flux)	178	0.05	< 0.001
150	log(SUVA) = - 8.6 + 0.27 x log(Flux)	320	0.04	< 0.001

[a] denotes the standard error of the slope parameter m, derived from the model fit

2.8 Figures

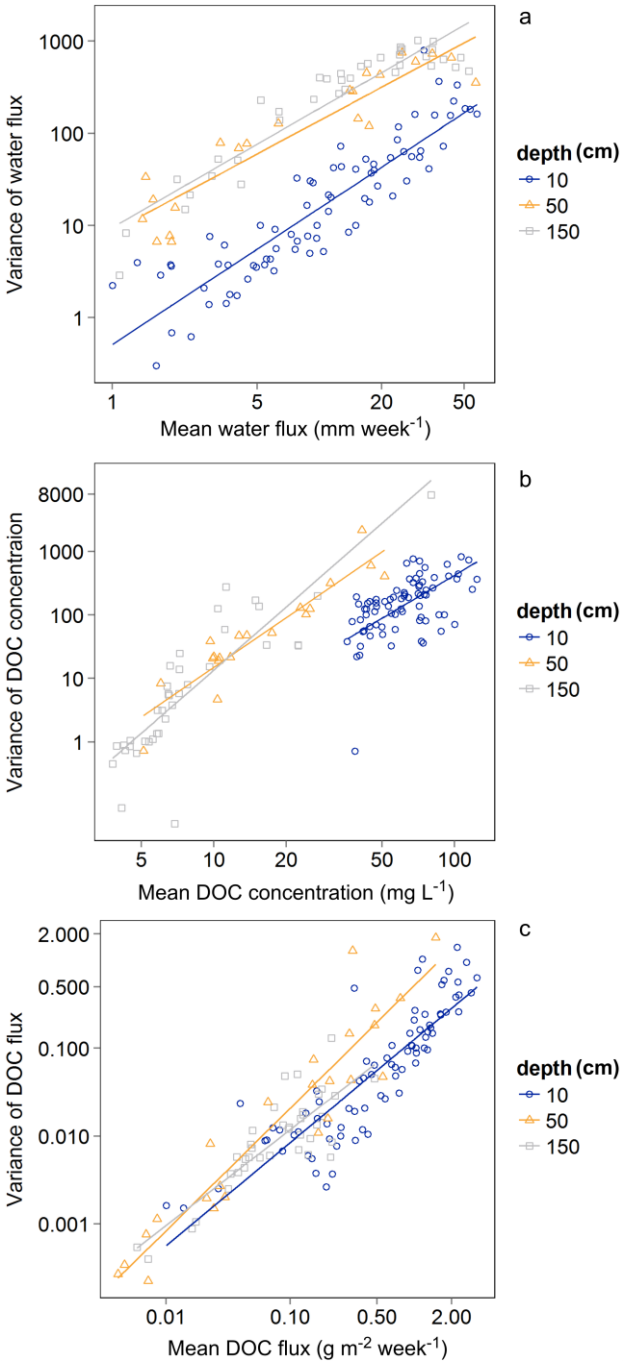

Fig. 1: Relationship of (a) the mean water flux and the variance of the water flux, (b) the mean dissolved organic carbon (DOC) concentration and the variance of the DOC concentration, and (c) the mean DOC flux and the variance of the DOC flux, calculated for the sixteen different values from each segmented plate at each sampling time.

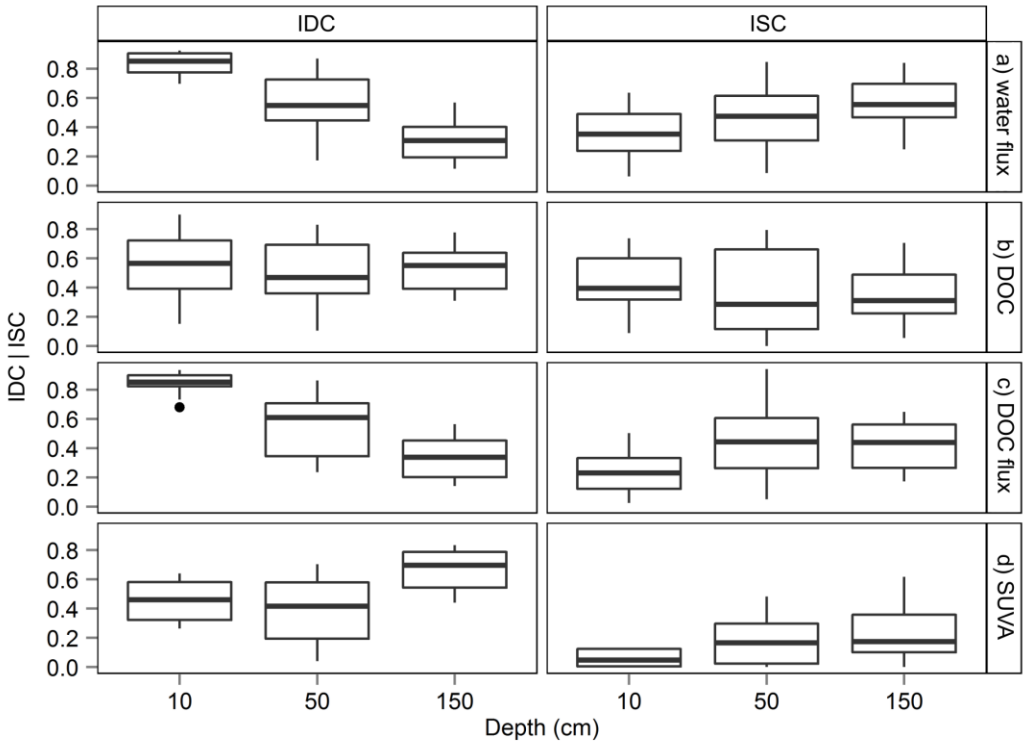

Fig. 2: Intra-date correlation (IDC) and intra-segment correlation (ISC) of (a) the water flux, (b) dissolved organic carbon (DOC) concentration, (c) DOC flux, and (d) specific UV absorbance (SUVA) at 280 nm at all three depths of the three observatories. The median is shown as the solid line. The 25 % quartile is shown by the bottom of the box while the 75 % quartile is represented by the top of the box. The lower limit of the whisker represents the 25 % quartile minus 1.5 times the difference between the 75 % quartile and the 25 % quartile. The upper limit of the whisker represents the 75 % quartile plus the difference of 1.5 times the difference between the 75 % quartile and the 25 % quartile.

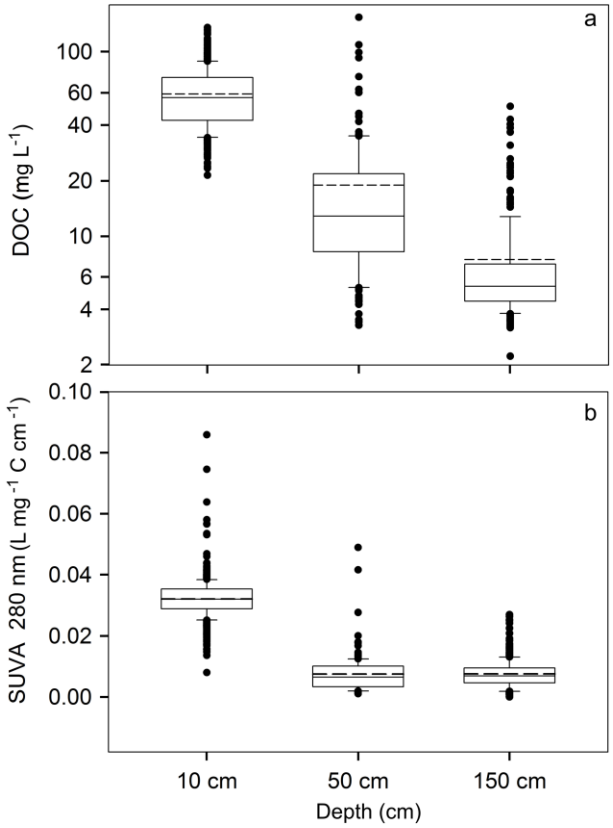

Fig. 3: Box plot of the (a) average dissolved organic carbon (DOC) concentrations with logarithmic scale of the y-axis due to the high range in the data set and (b) specific UV absorbance (SUVA) at 280 nm at the tree depths. The median and mean value are shown as solid line and dashed line, respectively. The 25 % quartile is shown by the bottom of the box. The 75 % quartile is shown by the top of the box. The lower limit of the whisker represents the 25 % quartile minus 1.5 times the difference between the 75 % quartile and the 25 % quartile. The upper limit of the whisker represents the 75 % quartile plus the difference of 1.5 times the difference between the 75 % quartile and the 25 % quartile.

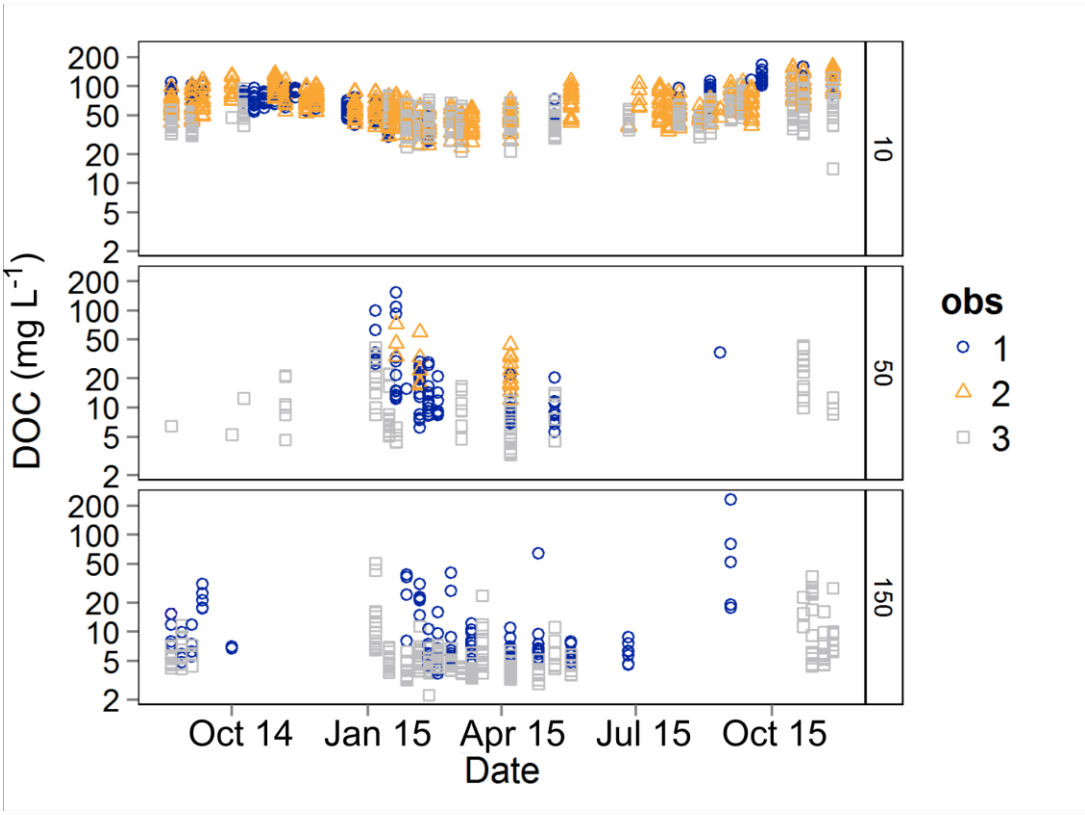

Fig. 4: Fluctuations of the dissolved organic carbon (DOC) concentrations per depth (cm) and observatory (obs) over the observation period.

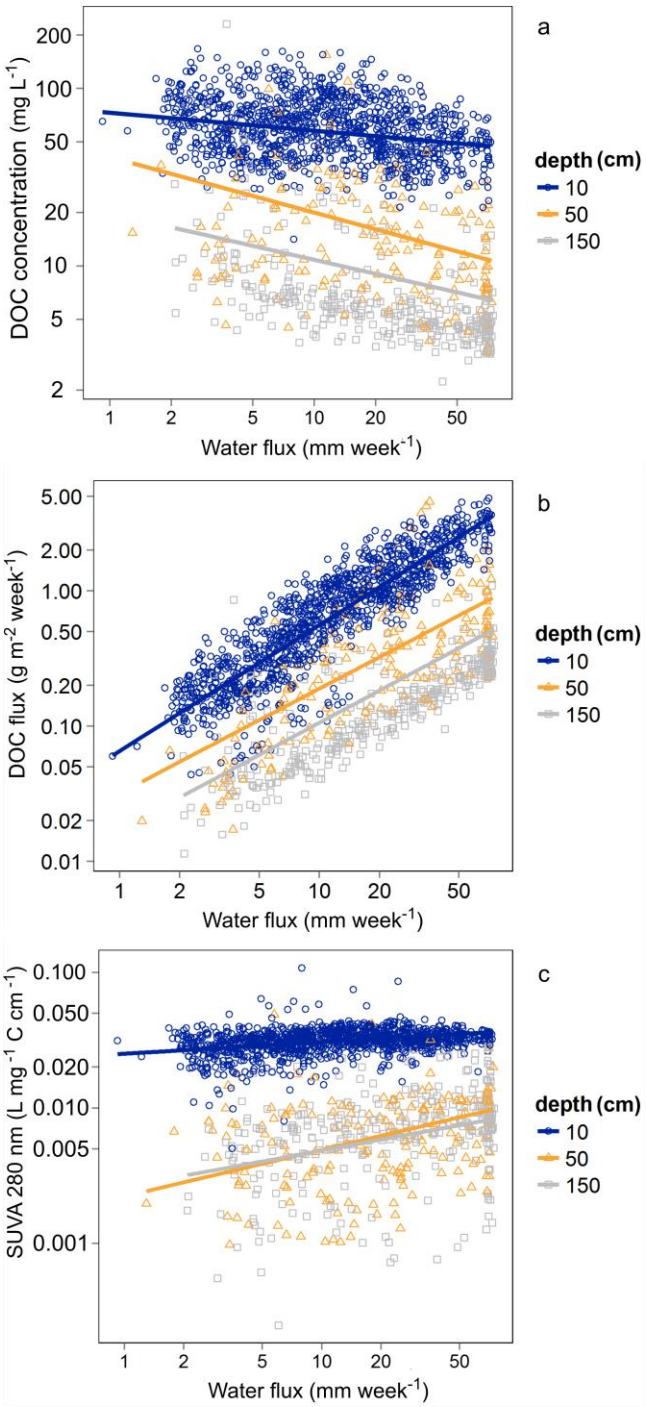

Fig. 5: Relationship between water flux and (a) dissolved organic carbon (DOC) concentration, (b) DOC flux, and (c) specific UV absorbance (SUVA) at 280 nm. Both axes are logarithmical. The correlations are calculated with linear mixed effects models using the R package lme4. For equations, standard error and p-values see Table 2.

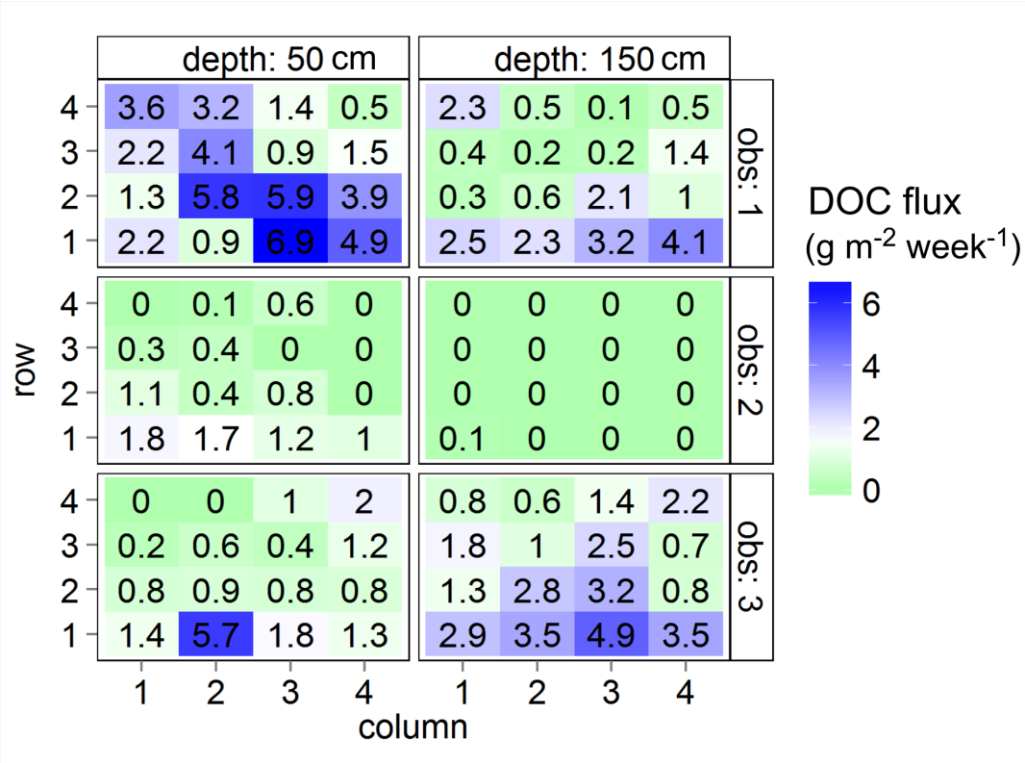

Fig. 6: Total dissolved organic carbon (DOC) flux (g m^{-2} $year^{-1}$) of the individual segments in the subsoil of the three observatories (obs). Green colored segments show values lower than the overall mean value, white colored segments show values near the overall mean value and blue colored segments show vales higher than the overall mean value. Depth is given in cm.

2.9 Supplement

Supplement 1: Soil horizons and general soil parameters at the three observatories**.**

Horizon	Depth (cm)	N (%)	OC (%)	pH ($CaCl_2$)	Clay (%)	Silt (%)	Sand (%)
Observatory 1							
EA	0-9	0.07	1.49	3.03	1.94	33.07	64.99
Bsw	9-15	0.05	1.13	3.33	1.77	32.63	65.60
Bw	15-74	0.03	0.44	3.98	2.99	35.52	61.49
C	74-117	0.01	0.06	4.01	4.85	36.21	58.94
2C	117-165	0.00	0.02	4.09	1.67	7.77	90.57
3C	117-165	0.00	0.04	4.04	1.32	6.73	91.95
4C	190+	0.00	0.02	4.03	2.47	15.55	81.98
Observatory 2							
EA	0-9	0.06	1.70	3.09	1.71	27.82	70.47
Bsw	9-20	0.04	1.08	3.29	2.74	30.86	66.40
Bw	20-58	0.03	0.67	3.95	2.35	33.77	63.88
C	58-81	0.01	0.12	3.97	1.93	22.50	75.57
2C	81-110	0.00	0.03	4.01	1.74	10.21	88.05
3C	110-140	0.02	0.26	3.63	6.32	47.56	46.12
4C	140-188	0.00	0.02	3.71	1.93	5.17	92.90
5C	188+	0.00	0.01	4.14	9.65	27.41	62.94
Observatory 3							
EA	0-12	0.05	1.36	3.45	2.73	32.21	65.06
Bsw	12-35	0.03	0.67	3.94	3.84	34.64	61.52
Bw	35-70	0.02	0.28	3.87	3.03	36.11	60.87
C	70-100	0.01	0.15	3.58	4.92	41.14	53.94
2C	100-140	0.02	0.05	4.09	3.64	16.65	79.71
3C	140-195	0.01	0.01	4.19	1.53	3.61	94.85
4C	195+	0.01	0.05	4.08	2.46	14.55	82.99

Supplement 2: Throughfall (mm) and mean water flux per sampling for the three observatories at the three depths (mm) over the sampling period of 63 weeks.

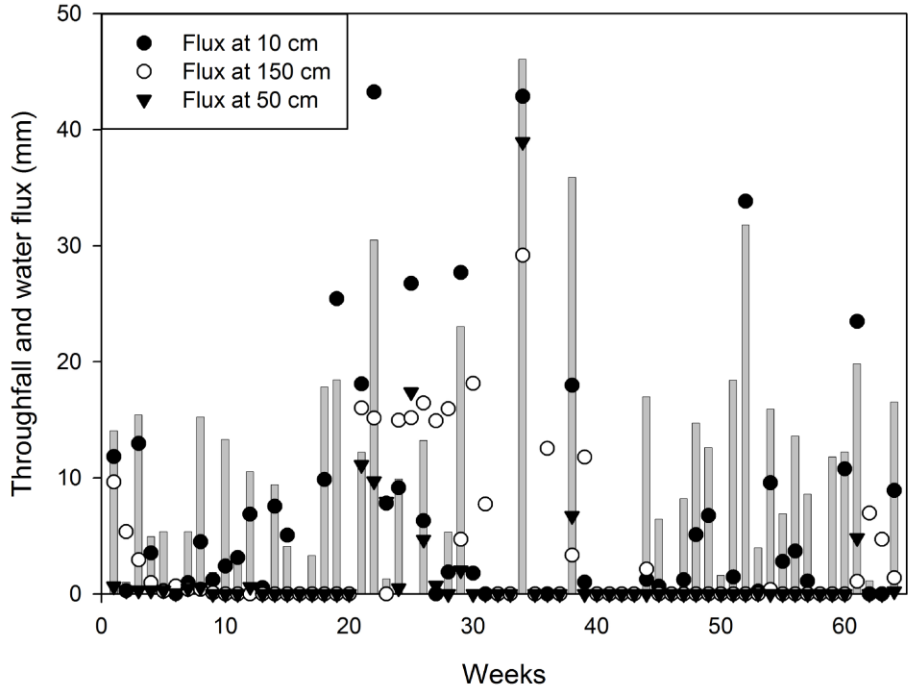

Supplement 3: Results of different studies on DOC concentrations and DOC fluxes in the subsoil

depth (cm)	DOC (mg L^{-1})	DOC Flux (g m^{-2} $week^{-1}$)	reference
10	59.2 ± 21.2	0.41 ± 0.71	this study
50	18.9 ± 20.1	0.05 ± 0.27	this study
150	7.5 ± 6.7	0.03 ± 0.1	this study
9 - 15	28.5	0.5	Mc Dowell and Likens (1988)
18	5.9	0.1	Mc Dowell and Likens (1988)
30	3	0.04	Mc Dowell and Likens (1988)
10	25.5 ± 7.1	0.24	Dosskey and Bertsch (1997)
30	13.7 ± 6.1	0.1	Dosskey and Bertsch (1997)
76 - 99	1.8 ± 0.3	0.01	Dosskey and Bertsch (1997)
0	49.3	0.5	Fröberg et al. (2006)
40 - 50	5.9	0.02	Fröberg et al. (2006)
40	30.2	0.1	Rieckh et al. (2014)
70	10.8	0.03	Rieckh et al. (2014)
160	5.7	0.02	Rieckh et al. (2014)

References

Dosskey M G, Bertsch P M (1997) Transport of dissolved organic matter through a sandy forest soil. Soil Sci So. Am J 61:920-927. doi:10.2136/sssaj1997.03615995006100030030x

Fröberg M, Berggren D, Bergkvist B, Bryant C, Mulder J (2006) Concentration and fluxes of dissolved organic carbon (DOC) in three Norway spruce stands along a climatic gradient in Sweden. Biogeochemistry 77:1-23. doi:10.1007/s10533-004-0564-5

McDowell W H, Likens G E (1988) Origin, composition, and flux of dissolved organic carbon in the hubbard brook valley. Ecol Monogr 58:177-195. doi:10.2307/2937024

Rieckh H, Gerke H H, Siemens J, Sommer M (2014) Water and dissolved carbon fluxes in an eroding soil landscape depending on terrain position. Vadose Zone J 13:1-14. doi:10.2136/vzj2013.10.0173

Supplement 4: Total water flux (mm year^{-1}) of the individual segments of the three observatories (obs). Green colored segments show values lower than the overall mean value, white colored segments show values near the overall mean value and blue colored segments show vales higher than the overall mean value.

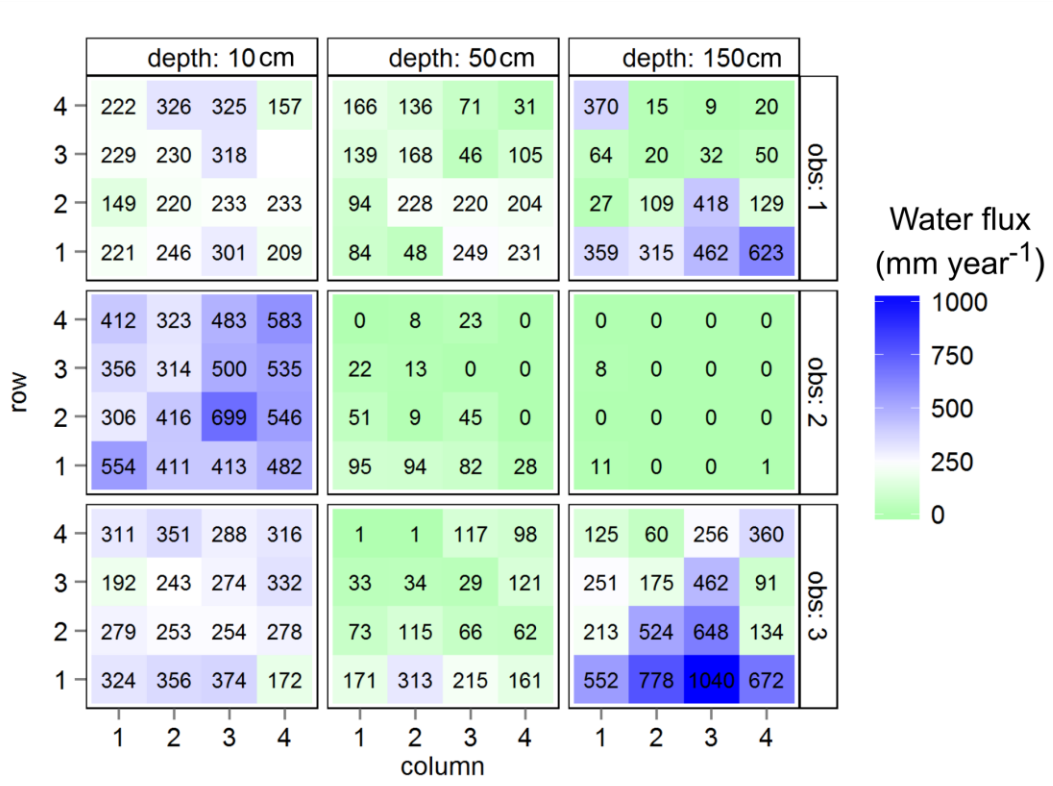

3. Study II

"Transport of litter derived dissolved organic carbon in the subsoil of a Dystric Cambisol: A ^{13}C field labelling approach"

Contribution: I collected the samples in the field, analyzed the data, compiled tables and graphs and wrote the manuscript. This study incorporates results acquired within the master thesis of Carsten Beyer carried out at the University of Halle-Wittenberg.

Publication status: Not yet submitted Manuscript

Transport of litter derived dissolved organic matter in the subsoil of a Dystric Cambisol: A ^{13}C field labelling approach

3.1 Abstract

The input of dissolved organic matter (DOM) is an important source of carbon to the subsoil. The concentration of dissolved organic carbon (DOC) declines with depth and in this regard the composition of DOM changes. Therefore, the origin of dissolved organic carbon in subsoils is arguable. In this study a field labelling experiment was carried out, to investigate the contribution of litter derived carbon to DOC with increasing soil depth. For this reason the leaf litter on top of a dystric cambisol under beech was replaced by a highly ^{13}C labelled beech leaf litter (1241 $\delta‰^{13}C$ VPDB) in January 2015. To follow the fate of litter derived DOC the soil solution was monitored by a high resolution sampling approach using segmented plate lysimeters consisting of 16 segments, each 4x4cm wide, installed in 10, 50 and 150 cm depth. Monthly samples were analyzed for DOC concentration and $\delta‰^{13}C$ ratio from January 2015 to June 2016. The mean % labelled C in DOC in 10 cm depth was nearly constant over time with only minor exceptions over the observation period (1.1 ± 0.8 % in Observatory 1; 2.8 ± 1.9 % in Observatory 2; 2.8 ± 1.5 % in Observatory 3). In 50 and 150 cm depth ten times lower proportions of labelled C in DOC were found (0.2 ± 0.2 % for all observatories combined). The mean values increased one year after the label addition in all three observatories indicating slow transport processes. These findings point towards the reliability of the "cascade model" proposed by Kaiser and Kalbitz 2012 as the DOM found in the subsoil is rather highly processed microbial derived than directly litter derived. Never the less it was possible to detect litter derived C in deep subsoil DOC for the first time.

3.2 Introduction

The transport of dissolved organic matter (DOM) through soil links topsoils rich in organic matter (OM) with the often carbon depleted subsoils. In forest ecosystems the deposition of leaf litter on the soil surface is a steady source for easy degradable OM, which can be transferred in dissolved form by leaching from the forest floor to the subsoil (Don and Kalbitz 2005). Kalbitz and Kaiser (2008) estimated that 25 – 66 % of the OC in the subsoil of a Haplic Podzol is DOM derived. In soils with

thick organic layers DOC derived from "young" litter can be retained in Oa horizons and thereby (re-)mobilizes older OM (Fröberg et al. 2007a; Müller et al. 2009). In soils with thin mull-type organic layers DOC derived from fresh litter can be strongly retained in the first centimetres of the mineral soil (Kammer and Hagedorn 2011, Müller et al. 2009) by binding to reactive fine-sized minerals like clay minerals and Fe and Al oxides and/or (co-)precipitation with Al and Fe (Kalbitz et al. 2000).

The transport of DOM through the soil profile leads to a fractionation of different molecular species observed in DOM. Commonly a selective retention of aromatic moieties and an increasing abundance of microbial derived hexoses in comparison to plant derived phenolic DOM compounds is observed (Kaiser et al. 2002). In addition the increased ^{14}C age of OM in the subsoil compared to the topsoil (Rumpel et al. 2012) may be induced by the remobilisation of previously bound "old" OM by competitive adsorption of "young" litter derived DOM in numerous cascade steps down the soil profile as postulated by Kaiser and Kalbitz (2012). Experimental evidence for the stepwise adsorption and desorption of OM during infiltration in the mineral soil is given in the column experiment described in *study III*.

The described characteristics of young and old OM exchange are affect by preferential flow conditions, where bypassing of adsorption sites on mineral surfaces is possible (Kaiser and Guggenberger 2005, Leinemann et al. 2016) and less degraded litter derived DOM can reach relatively fast into deeper horizons in the mineral soil. This issue was observed by Hagedorn et al. (2015) in an undisturbed column experiment down to 10 cm soil depth, using ^{14}C enriched DOM. However 90 % of the added litter derived DOM were retained in the first 3 cm of the soil columns.

The contribution of root litter was recently highlighted for carbon sequestration in subsoils by comparing the incorporation rate of different litter forms into the OC of a sandy soil in a 270 days incubation experiments (Hu et al. 2016). Despite the fact that fine root litter was incorporated to a greater extent into the OC stock than leaf litter, the authors concluded that the laboratory experiments did not account for vertical transport processes and that field experiments are needed to gain further insights on the carbon sources in the subsoil.

Even though the importance of deep subsoils (>30 cm) for the terrestrial C cycling is known (Rumpel and Kögel-Knabner 2011), field studies on the fate of litter derived carbon in the subsoil are rare. This is due to analytical difficulties that arise from low DOC concentrations, adsorptive retention to mineral surfaces, dilution of tracer DOM molecules by older OM compounds with depth and the impact of preferential flow.

To overcome such experimental difficulties, an in situ litter manipulation experiment was performed. A litter strongly enriched in ^{13}C was used in the Grinderwald beech forest at three soil observatories that were equipped with segmented plate lysimeters (4 x 4 segments, each 36 cm^2) in 10, 50 and 150 cm depth. Here the variability of the water and DOC flux on the centimetre scale can be monitored (Leinemann et al. 2016, *study I*). Soil solution was sampled monthly from January 2015 to June 2016 and measured for $DO^{13}C$. For the determination of DOM composition four sets of samples from January 2015 to April 2015 were analysed by spectroscopic methods. With the described setup it was investigated how large and how fast the input of litter derived DOC to the deep mineral subsoil is and if spatial differences in flow velocity influence the transport of litter derived DOC.

3.3 Material and methods

Site description

The litter manipulation experiment was carried out in a beech (*Fagus sylvatica* L.) forest called Grinderwald, planted in 1906, which is located approximately 40 km NW of Hannover, Germany (52° 34’22.1 North, 9°18’49.7 East). The mean annual temperature is 9.7°C and the mean annual precipitation amounts to 762 mm (Deutscher Wetterdienst, Nienburg, period 1981-2010). Soils developed in Pleistocene fluvial and aeolian sandy deposits from the Saale glaciation are typically Dystric Cambisols. The three different sites under investigation were relatively homogenous in the thickness of the soil horizons, their texture, pH, and OC contents. Details on the soil characteristics at the study site are given in *study I.*

Sampling

In July 2013 three soil observatories were installed. They were equipped with segmented suction plate lysimeters at 10, 50, and 150 cm depth. The plates were designed to sample vertically moving water by each 16 separate, squared, 36 cm^2 wide segments, with a polyamide filter membrane (0.45 µm pore size), (ecotech Umwelt-Meßsysteme GmbH, Bonn, Germany), with a low vacuum of 50 mbar. As defined by Zsolany (1996) this is suitable to sample free percolating water. Additionally 6 glass suction cups were installed per depth and observatory (25, 50, and 150 cm). For details on the installation and the sampling procedure see Leinemann et al. (2016). The sampling started in August 2014 on a weekly basis and will be continued until 2019. In this study the results from monthly samplings from January 2015 to August 2016 are reported. In January 2015 the original leaf litter was removed on a 1.5 m radius ring around the observatory shaft (14.8 m^2 surface area). On one half ring the litter was replaced by $\delta^{13}C$ enriched beech leaf litter obtained from IsoLive bv, Wageningen, Netherlands. To obtain a total amount of 250 g litter m^{-2} according to Phillipson et al. (1975) 273 g labelled beech leafs were mixed with 1575 g of beech litter from trees of almost the same age, resulting in a $\delta^{13}C$ of 1241‰ VPDB. On the other half of the ring with 7.4 m² the original litter was replaced by the same almost fresh beech leaf litter used for mixing to ensure comparable chemical composition of litter on the two sites. The two half rings were separated by a sheet pile wall already in 2013 to disable the exchange of soil solution from the labelled to the unlabelled site. The segmented plate lysimeters and three suction cups per depth were installed in the half ring with labelled litter on top. Three suction cups per depth were used as control as they were installed in the unlabelled half ring.

Analyses

The collected solutions were immediately weighed for volume determination and filtered to < 0.45 µm by polyethersulfon filters (VWR International; Radnor; Pennsylvania) in the laboratory. Samples were stored at 4°C in the dark for a maximum of 30 days until analyses. The concentrations of DOC were measured by high temperature combustion with a limit of quantification of 1 mg C L^{-1} (Vario TOC cube; Elementar, Langenselbold, Germany). The UV absorbance at 280 nm was determined at a Varian Cary 50 UV-Vis (Agilent Technologies, USA), and the specific UV absorbance (SUVA) was calculated as the ratio of UV absorbance at 280 nm and DOC concentration given in L mg C^{-1} cm^{-1} (Chin et al. 1994; Scheel et al. 2008). Weekly water fluxes were calculated based on the sampled volume with regard to the area of the segments (36 cm^2) and given in mm, while weekly DOC fluxes were calculated by multiplying DOC concentrations with water fluxes and given in g C m^{-2}. An aliquot of each sample of one weekly set of samples per month was frozen in liquid nitrogen and stored at -18 °C for measurement of the $\delta^{13}C$ ratio of DOM ($DO^{13}C$). The $DO^{13}C$ was analysed directly in solution using a high-temperature combustion system for direct ^{13}C measurement from liquid samples (Federherr et al., 2014; Kirkels et al., 2014). For that an isoTOC cube (Elementar group, Langenselbold, Germany) total organic carbon analyser was coupled with a continuous flow isotope ratio mass spectrometer (Isoprime100, Isoprime Ltd, Cheadle Hulme, UK). The proportion of OC in DOC derived from the labelled litter (%-labelled C in DOC) was calculated relative to the $\delta^{13}C$ of the solution sampled in the control site (eq.1), were $\delta^{13}C_{sample}$ and $\delta^{13}C_{control}$ represent the $\delta^{13}C$ ratio of the solution sampled from the labelled half and the solution sampled in the same depth of the unlabelled half and $\delta^{13}C_{litter}$ represents the $\delta^{13}C$ ratio of the applied labelled litter. Samples with %-labelled C in DOC below 0.05 were set to zero with regard to the detection limit of the measurements.

$$Labelled\ C\ in\ DOC\ \ (\%) = \frac{(\delta^{13}C_{sample} - \delta^{13}C_{control})}{(\delta^{13}C_{litter} - \delta^{13}C_{control})} x\ 100 \qquad \text{(eq.1)}$$

Four sets of samples taken at 06.Jan.2015, 05.Feb.2015, 05.March.2015 and 07.April.2015 were analysed for the concentration of hexoses, pentoses, amino acids, proteins and phenols using spectrophotometric methods described in Chantigny et al. (2008). For hexose determination 2 ml anthrone sulfuric acid was mixed with 1 ml sample and absorbance was measured at 625 nm.

Concentrations were calculated from a glucose standard curve. Pentoses were determined by mixing each 1 ml of sample with iron and orcinol reagent. After heating and subsequent cooling of this mixture 2 ml of ethanol (95 %) were added and absorbance was measured at 660 nm. Concentrations were calculated from a ribose standard curve. Amino acids were determined by mixing 2 ml of sample with 1.25 ml of ninhydrin reagent and heated for 5 to 7 minutes at 100 °C. Subsequent to cooling the absorbance were measured at 570 nm. Concentrations were calculated using a glycin standard curve. Proteins were determined by using 0.5 ml of sample and 0.5 ml of Bradford protein reagent. Absorbance was measured at 620 nm and concentrations were calculated using an albumin standard curve. Phenols were determined by using 0.7 ml sample and 50 µl of folin-ciocalteu reagent and 100 µl saturated potassium carbonate solution. Absorbance was measured at 725 nm and concentrations were calculated from a 4-hydroxybenzoic acid standard curve. The relative concentration of the DOM compounds was calculated as the ratio of the component concentration (mg L^{-1}) and the DOC concentration (mg L^{-1}) of the respective sample.

Statistics

At first mean values of the data obtained were calculated for each observatory depth and sampling date. The significance of differences between the mean values of the same plate lysimeter was tested for $p < 0.05$ by applying the Tukey method (Tukey, 1949). For the determination of the relationship between %-labelled C in DOC and water flux, mixed effect models were run, with water flux and sampling depth as exploratory variables (fixed effects). Observatory, plate lysimeter and segment were included as random effects, to account for the nesting of observations within observatory and within plate lysimeter over time. Preliminarily samples with zero %-labelled C in DOC were removed from the data set to enable the needed log-transformation to approximate to a uniform distribution. If not stated otherwise, error values are given as standard deviation. All statistical analyses were carried out with R statistics version 3.2.1 (R Core Team, 2015) using the "lme4" (Bates et al., 2015) and the "lsmeans" package (Lenth, 2016). Figures were created with the ''ggplot2'' package (Wickham 2009).

3.4 Results and discussion

Absolute concentration of DOM compounds

In general, the concentration of the five analysed DOM components declined from topsoil to subsoil in the three observatories in accordance with the DOC concentration (Table 1). The standard deviation of all measured parameters was high and increased with depth, which is in accordance with the high variability of DOC concentrations in soil solution sampled with segmented plate lysimeters (Leinemann et al. 2016, *study I*).

A strong decline from 10 to 50 cm sampling depth and comparable values in 50 and 150 cm sampling depth were determined for amino acids, proteins and phenols. The reduction of the N rich amino acids and proteins should be induced by biodegradation. The reduction of phenols with depth is rather caused by preferential sorption processes (Kalbitz et al. 2003).

At the first and second observatory the hexose concentrations showed like the other components a comparable decline with depth. At the third observatory an increase in 150 cm depth was recorded. Here the mean hexose concentration nearly doubled the mean DOC concentration, which is an indication for a possible hexose overestimation in this samples (Chantingy et al. 2008).

The pentose concentrations declined only slightly from 10 to 50 cm depth and decreased distinctly in 150 cm depth. These changes were comparable in all three observatories and indicate a reduced importance of plant derived compounds in DOM with depth, as pentoses are mainly derived from plant polysaccharides (Oates 1984).

Relative concentration of DOM compounds

The three observatories showed different depth trends when the component concentration was examined relative to the DOC concentration (Fig. 1), to omit the impact of the differing DOC concentrations with depth. The relative amino acid concentration showed an increase with depth in all observatories. The relative protein concentration was rather stable with depth, but showed larger differences between the three observatories. The relative phenol concentration declined with depth in all three observatories (Fig. 1). This was comparable to the absolute concentrations and highlights the

importance of the previously described preferential retention of aromatic compounds by sorption to reactive minerals (Kalbitz et al. 2003). The relative pentose concentration increased with depth in all three observatories, which was contradictory to the absolute concentrations but matches the finding of a relative increase of aliphatic compounds in DOM with depth (Kaiser et al. 2002).

Likewise to the absolute concentrations the relative hexose concentrations were characterised by large differences between the observatories, with comparable results in the first and second observatory and extremely high values in the third observatory (Fig. 1). In the first and second observatory the relative and absolute hexose concentrations are in accordance with the reported up to seven-fold decline in microbial biomass with depth at the study site (Preusser et al. 2017), as hexoses are predominantly of microbial origin (Cheshire 1977).

Functional ratios of DOM compounds

The ratio of hexoses and pentoses gives a relative indication for the contribution of microbial compounds and plant compounds on the DOM composition (Cheshire 1977). A ten-fold decline of the ratio from 10 to 50 cm depth and comparable ratios around unity in 50 and 150 cm depth were observed for the second and first observatory, respectively. This again is in agreement with the decline in microbial biomass mentioned above. However, the third observatory again largely differed from the other two with increasing ratios with depth (Fig. 2).

During the degradation of organic residues proteins are fragmented into amino acids (Martin and Thimann 1972). With increasing degradation of OM compounds the ratio of amino acids to proteins increases. In accordance with this finding the ratio increased with depth at the second and third observatory indicating that subsoil DOM is derived from microbial processed OM (Fig. 2). At the first observatory the ratio decreased with depth highlighting the possible high variability of the DOM composition. However the reliability of the 150 cm data of the first observatory is decreased due to a low number of samples (n = 14) in comparison to the third observatory (n = 44).

Contribution of litter derived labelled carbon to DOC in the topsoil

In 10 cm depth the mean contribution of litter derived DOC to the total DOC content was below 3 % in all observatories (Table 2). One month after addition of the litter only small amounts of labelled carbon were measured in 10 cm depth and in 13 of the 23 samples no ^{13}C enrichment was found (Table 2). At the first observatory over the time period of 18 month the range of labelled carbon in the samples increased from 0.08 to 4.5 %, but the mean values were not significantly different with 1.07 % ± 0.81 (Fig. 3). At the second observatory the mean % of labelled carbon in DOC increased after two month and remained relatively stable for the next 10 month. Likewise to the first observatory the range of the values increased one year after the label addition. In February and April 2016 also significantly higher mean values compared to February 2015 were observed. At the last sampling date after 18 month the mean value was comparable to March 2015 again, which was 3 month after the label addition. At the third observatory the mean % of labelled carbon in DOC remained nearly constant with mean % of total DOC of 2.83 % ± 1.47 over the whole sampling period and did not show an increase of range one year after addition of the labelled litter like observed in observatory 1 and 2. The results from 10 cm depth indicate that the soil solution in the topsoil equilibrates with the components deriving from the labelled litter layer in a period of about two month. The low mean contribution of litter derived DOC to the total DOC is in agreement with recent results from Hagedorn et al. (2015) who observed a strong retention of litter derived carbon already in the first centimetres of mineral soil using undisturbed soil columns percolated with ^{14}C enriched litter derived DOC. This could be induced by the primarily production of soluble slightly negatively charged proteins during the decomposition of litter (Martin and Thimann 1973), that are prone to sorption on positively charged soil minerals like goethite or clay minerals. Furthermore an intense combustion to CO_2 by microorganisms is supposable, as the biodegradability of DOC produced from fresh litter was observed to be high (30 to 95 %, Don and Kalbitz 2005).

Contribution of litter derived labelled carbon to DOC in the subsoil

The contribution of litter derived C to DOC in the subsoil is distinctly lower than in the topsoil, with mean values under 0.4 % in all observatories. In both 50 and 150 cm depth, after one month, the %-

labelled C in DOC was above the level of quantification (<0.05) in only 3 of 34 samples of all three observatories. Four month after the label addition still half of the samples from depth 50 and 150 cm showed no enrichment in ^{13}C (Table 2). One year after the label addition the majority of samples were enriched in ^{13}C leading to values up to 1.4 % and 0.5 % of total DOC in 50 and 150 cm depth, respectively. At the last three sampling dates from February 2016 to June 2016 at 150 cm depth significantly higher mean %-labelled C in DOC compared to the first year after the label addition were reached (Fig. 3). The second observatory was distinguished from the other observatories, as sampling was only possible at the last three sampling dates. The comparability with the other two observatories is thus reduced, as before and after this dates no water reached to the 150 cm depth lysimeter (Fig. 5), which was installed into a loamy lens.

In recent studies on the fate of litter derived DOC solution was sampled only down to 15 cm depth (Egli et al. 2016, Guelland et al. 2013, Hagedorn et al. 2003). The enrichment of the ^{13}C tracer was highest in the study of Guelland et al. (2013) with a $\delta^{13}C$ ratio of 88‰ and thus tracing litter derived DOC down the deep subsoil was impossible. In this experiment the high ^{13}C enrichment (1241‰) together with the long monitoring period enables the quantification of small proportions of litter derived DOC in the subsoil.

Even though the proportion of litter derived C to DOC in the subsoil was above the limit of quantification it was approximately ten times smaller than in the topsoil. This highlights the importance of sorptive retention of DOC in the mineral soil <50 cm depth (e.g. Kaiser and Kalbitz 2008). The increase of labelled DOC in the subsoil one year after the litter addition (Fig. 3) suggests that the transport of litter derived DOC is to a large part slower than the movement of water. Over the sampling period a mean water flux of 200 to 400 mm per year was recorded in 150 cm depth (Fig. 4), which represented a prominent part of the throughfall at the study site (approx. 500 mm $year^{-1}$, *study I*) and thus indicates high percolation rates, as expected in sandy soils.

The slow transport of litter derived DOC supports the idea of the cascade like DOC transport throughout the soil profile (Kaiser and Kalbitz 2012; s*tudy III*). For the next years of continued DOC monitoring it is thus likely that the proportions of labelled C in subsoil DOC (50 and 150 cm depth)

will increase, until new unlabelled litter input at the forest floor dilutes the signal too much. As it is assumed in the "cascade model" that the high ^{14}C ages of subsoil OC (Rumpel et al. 2012) are provoked by slow DOC cycling, featuring numerous sorption and desorption events for the same C-atom, like included in a process model by Ahrens et al. 2015.

Variability of litter derived C in DOC on the centimetre scale

High ranges of the %-labelled C in DOC at certain sampling dates suggest that the transport of litter derived DOC is variable in rate, which might be induced by differences in flow velocity on temporal and on spatial scale. Hagedorn et al. (2015) found higher enrichment of the used ^{14}C tracer in macropores and increasing heterogeneity in label distribution with depth after percolation of undisturbed soil cores. These results highlight the importance of heterogeneities induced by different flow paths on the centimetre scale, which were not investigated in the field thus far.

The content of labelled C in DOC in mg L^{-1} was summated for each segment of the plate lysimeters over time to show if the differences between the segments of one lysimeter were constant (Fig. 5). The difference between the individual segments increased in the most plates as the lines are further away from each other over time. The fact that most lines in figure 4 do not cross indicates stability of soil solution transport passageways. This is especially the case in 150 cm depth were some segments received nearly no labelled carbon over time and others received a sum of more than 0.1 mg L^{-1} labelled carbon until the last sampling date (Fig. 5). In 10 cm depth the maximum difference between two segments of one lysimeter amounted to 80 % (segment 4:4 and segment 2:1, observatory 3, Fig. 6). In 150 cm depth the maximum difference between two segments amounted to 90 % (segment 4:1 and segment 1:2, observatory 3, Fig. 7). This corresponds to the finding that the spatial variability of the DOC flux is more important in the subsoil than in the topsoil due to longer flow paths and a thus higher possibility of the occurrence of heterogeneous flow patterns (Leinemann et al. 2016, *Study I*).

Relationship between water flux and litter derived C in DOC

In 10 cm depth and in 150 cm depth for all three observatories a significant positive linear relationship between the water flux and the %-labelled C in DOC was found using linear mixed effect models (Fig.

8). In 50 cm depth such a relationship was not observed. High water fluxes during heavy rain storm events were considered to affect the DOM composition in subsoils, leading to increased aromaticity (Kaiser and Guggenberger 2005). With higher flow velocity the sorption of DOC to reactive minerals seemed to be reduced, thus in the topsoil and the deep subsoil (150 cm) more litter derived carbon was found in the lysimeter segments, sampling in areas with higher flow velocity. The missing trend in 50 cm depth could be induced by up to three times higher amounts of oxalate-extractable Fe in the *Bw*-horizon (1.6 mg g^{-1}) compared to the C-horizon (0.3 mg g^{-1}) and the A-horizon (0.8 mg g^{-1}) , as found by a grid sampling at the study site (Heinze et al. 2017). With more available adsorption sites for DOM components the possibility of bypassing could be reduced even at higher flow velocities. A higher number of samplings gained from a longer period would strengthen the reliability of the results as due to dry conditions and the variability between the three observatories the availability of samples was limited at 50 cm depth. When including the samples with 0 %-labelled C in DOC in the models no significant relationship would have been recognised, as at all flow velocities zero values occurred. In the topsoil this is limited to the first sampling date only and in the subsoil to single lysimeter segments.

3.5 Conclusion

The direct contribution of litter derived OC to DOC is low in the whole mineral soil but with the use of highly enriched ^{13}C labelled leaf litter it was possible to determine even small amounts down to 150 cm depth. In 10 cm soil depth in about one to two month nearly constant values were reached. In the deep subsoil the proportions of litter derived DOC slightly increased one year after the addition of labelled litter. This indicates that the transport of DOC from the organic layer to the subsoil proceeds slowly. Due to the intense retention of litter derived DOM components in the topsoil and the delayed increase of ^{13}C in the subsoil a stepwise DOC transport as assumed in the “cascade model” is most likely. The flow regime had an influence on the transport of litter derived DOC, thus at high water fluxes the transport of litter derived DOC is considerably higher than at matrix flow conditions, most like due to less intimate interactions with adsorption sites of the solid phase and the DOC. It can be concluded, that litter derived OC in soil gets not entirely immobilized by sorption and not entirely

consumed and transformed to CO_2 by microorganisms, but participates to a certain degree to the DOC even in the deep subsoil.

3.6 References

Ahrens, B., Braakhekke, M., C., Guggenerger, G., Schrumpf, M., Reichstein, M., 2015. Contribution of sorption, DOC transport and microbial interactions to the ^{14}C age of a soil organic carbon profile: Insights from a calibrated process model. Soil Biology & Biochemistry 88, 390-402.

Chantigny, M.H., Angers, D.A., Kaiser, K., Kalbitz, K. 2008. Extraction and characterization of dissolved organic matter (p. 617–635). In: Carter, M.R., Gregorich, E.G. (Ed.) Soil Sampling and Methods of Analysis. 2nd ed. Canadian Soil Science Society – Taylor & Francis, Boca Raton, FL.

Cheshire, M.V. 1977. Origins and stability of soil polysaccharide. European Journal of Soil Science 28:1-10.

Chin, Y-P., Alken, G., O´Loughlin, E. 1994. Molecular weight, polydispersity, and spectroscopic properties of aquatic humic substances. Environmental Science Technology 28:1853-1858

Don, A., Kalbitz, K. 2005. Amounts and degradability of dissolved organic carbon from foliar litter at different decomposition stages. Soil Biology & Biochemistry 37:2171-2179.

Fedeher, E., Cerli, C., Kirkels, F.M.S.A., Kalbitz, K., Kupka, H.J., Dunbach, R., Lange, L., Schmidt, T.C. 2014. A novel high-temperature combustion based system for stable isotope analyses of dissolved organic carbon in aqueous samples. I: development and validation. Rapid Communication in Mass Spectroscopy 28:2559-2573.

Fröberg, M., Breggren Kleija, D., Hagedorn, F. 2007. The contribution of fresh litter to dissolved organic carbon leached from a coniferous forest floor. European Journal of Soil Science 58:108-114.

Heize, S., Ludwig, B., Piepo, H.-P., Mikutta, R., Don, A., Wordell-Dietrich, P., Helfrich, M., Hertel, D., Leuschner, C., Kirfel, K., Kandeler, E., Preusser, S., Guggenberger, G., Leinemann, T., Marschner, B., 2017. Factors controlling the variability of organic matter in the top- and subsoil of a sandy Dystric Cambisol under beech forest. Geoderma 311, 37-44.

Hu, Ya-Lin., Zeng, De-Hui., Ma, Xiang-Qing., Chang, S.X. 2016. Root rather than leaf litter input drives soil carbon sequestration after afforestation on a marginal cropland. Forest Ecology and Management 362:38-45.

Kammer, A., Hagedorn, F. 2011. Mineralisation, leaching and stabilization of ^{13}C-labelled leaf and twig litter in a beech forest soil. Biogeosciences 8:2195-2208.

Kalbitz, K., Kaiser, K. 2008. Contribution of dissolved organic matter to carbon storage in forest mineral soils. Journal of Plant Nutrition and Soil Science 171:52-60.

Kalbitz, K., Schmerwitz, J., Schwesing, D., Matzner, E., 2003. Biodegradation of soil-derived dissolved organic matter as related to its properties. Geoderma 113, 273-291.

Kaiser K., Guggenberger G. 2005. Storm flow flushing in a structured soil changes the composition of dissolved organic matter leached into the subsoil. Geoderma 127:177-187.

Kaiser, K., Guggenberger, G., Haumeier, L., Zech, W. 2002. The composition of dissolved organic matter in forest soil solutions: changes induced by season and passage through the mineral soil. Organic Geochemistry 33:307-318.

Kaiser, K., Kalbitz, K. 2012. Cycling downwards – dissolved organic matter in soils. Soil Biology and Biochemistry 52:29-32

Kirkels, F.M.S.A., Cerli, C., Fedeherr, E, Gao, J., Kalbitz, K. 2014. A novel high-temperature combustion based system for stable isotope analysis of dissolved organic carbon in aqueous samples. II: optimization and assessment of analytical performance. Rapid Communication in Mass Spectroscopy 28:2574-2586.

Leinemann, T., Mikutta, R., Kalbitz, K., Schaarschmidt, F., Guggenberger, G. 2016. Small scale variability of vertical water and dissolved organic matter fluxes in sandy Cambisol subsoil as revealed by segmented suction plates. Biogeochemistry 131:1-15.

Martin, C., Thimann, K.V., 1972a. The role of protein synthesis in the senescence of leaves. I. The formation of protease. Plant Physiology 49:64-71.

Müller, M., Alewell, C., Hagedorn, F. 2009. Effective retention of litter-derived dissolved organic carbon in organic layers. Soil Biology and Biochemistry 41:1066-1074.

Oades, J., M., 1984. Soil organic matter and structural stability: mechanisms and implications for management. Plant and Soil 76, 319-337.

Phillipson, J., Putman, R.J., Steel, J., Woodell, S.R.J. 1975. Litter input, litter decomposition and evolution of carbon dioxide in a Beech woodland – Wytham Woods, Oxford. Oecologia 20:203-217.

Rumpel, C., Chabbi, A., Marschner, B., 2012. Carbon storage and sequestration in subsoil horizons: knowledge, gaps and potentials. In: Lal, R., Lorenz, K., Hüttl, R.F., Schneider, B.U., von Braun, J. (Eds.), Recarbonization of the Biosphere. Springer, Netherlands, pp. 445e464.

Rumpel, C., Kögel-Knabner, I. 2011. Deep soil organic matter – a key but poorly understood component of terrestrial C cycle. Plant Soil 228:142-158.

Scheel, T., Haumeier, L., Ellerbrock, R.H., Rühlmann, J., Kalbitz, K. 2008. Properties of organic matter precipitated from acidic forest soil solution. Organic Geochemistry 39:1439-1453.

Zsolnay, A. 1996. Dissolved humus in soil waters. (p 171–223) In: Piccolo, A. (ed) Humic substances in terrestrial ecosystems. Elsevier, Amsterdam.

3.7 Tables

Table 1: Mean concentration of DOC, hexoses, pentoses, amino acids, proteins and phenols in the soil solutions sampled with segmented plate lysimeters at the three observatories in 10, 50 and 150 cm depth ± standard deviation. The samples were collected once per month from January 2015 to April 2015.

Depth (cm)	DOC (mg L^{-1})	Hexose (mg L^{-1})	Pentose (mg L^{-1})	Amino acid (mg L^{-1})	Protein (mg L^{-1})	Phenol (mg L^{-1})	Sample size (n)
			Observatory 1				
10	45.3 ± 10.2	11.0 ± 4.4	2.3 ± 3.7	1.3 ± 0.4	2.2 ± 1.6	6.9 ± 1.8	30
50	17.1 ± 9.8	0.6 ± 0.8	2.5 ± 4.2	0.8 ± 0.7	0.6 ± 0.7	0.6 ± 0.2	34
150	11.2 ± 9.3	0.9 ± 1.1	0.9 ± 1.2	0.7 ± 0.6	0.9 ± 1.4	0.4 ± 0.4	14
			Observatory 2				
10	44.9 ± 24.5	12.4 ± 3.3	4.9 ± 4.5	1.5 ± 0.6	3.3 ± 2.2	8.9 ± 3.3	61
50	22.2 ± 7.8	1.6 ± 2.0	2.7 ± 4.2	0.8 ± 0.5	0.6 ± 0.9	0.8 ± 0.2	12
150	-	-	-	-	-	-	-
			Observatory 3				
10	40.7 ± 11.9	11.2 ± 3.6	3.4 ± 4.7	1.3 ± 0.5	2.7 ± 2.4	6.2 ± 2.1	42
50	9.4 ± 6.6	8.3 ± 3.3	2.6 ± 5.0	0.8 ± 0.4	0.8 ± 1.0	0.3 ± 0.1	23
150	6.3 ± 3.5	11.6 ± 5.1	1.1 ± 1.8	0.6 ± 0.3	1.0 ± 1.0	0.3 ± 0.4	44

Table 2: Mean $\delta DO^{13}C$ and mean %-labelled C in DOC ± standard deviation for the total number of samples (n) and the number of samples with 0 %-labelled DOC per depth (cm) and observatory.

Observatory	Depth (cm)	Mean δ $DO^{13}C$	Mean %-labelled C in DOC	n	Number of samples with 0 %-labelled C in DOC
1	10	-15.06 ± 10.41	1.07 ± 0.81	97	7
1	50	-24.63 ± 4.09	0.23 ± 0.31	69	20
1	150	-24.6 ± 2.63	0.26 ± 0.19	60	15
2	10	23.93 ± 37.09	2.75 ± 1.94	123	6
2	50	-21.12 ± 6.18	0.35 ± 0.30	28	3
2	150	-26 ± 0.65	0.08 ± 0.04	22	0
3	10	25.46 ± 28.09	2.83 ± 1.47	111	0
3	50	-22.13 ± 4.82	0.28 ± 0.24	62	12
3	150	-25.91 ± 6.23	0.16 ± 0.20	89	39

Table 3: Results of the regression models shown in Fig. 7 using water flux and %-labelled C in DOC.

Depth (cm)	Equation	Standard error of m[a]	p value
10	log(%-label) = -0.3 + 0.2 x log(Flux)	0.1	< 0.05
50	log(%-label) = -2.4 + 0.006 x log(Flux)	0.1	< 1
150	log(%-label) = -4.6 + 0.4 x log(Flux)	0.1	< 0.001

[a] denotes the standard error of the slope parameter m, derived from the model fit. Equations are in the form of: y = b + mx.

3.8 Figures

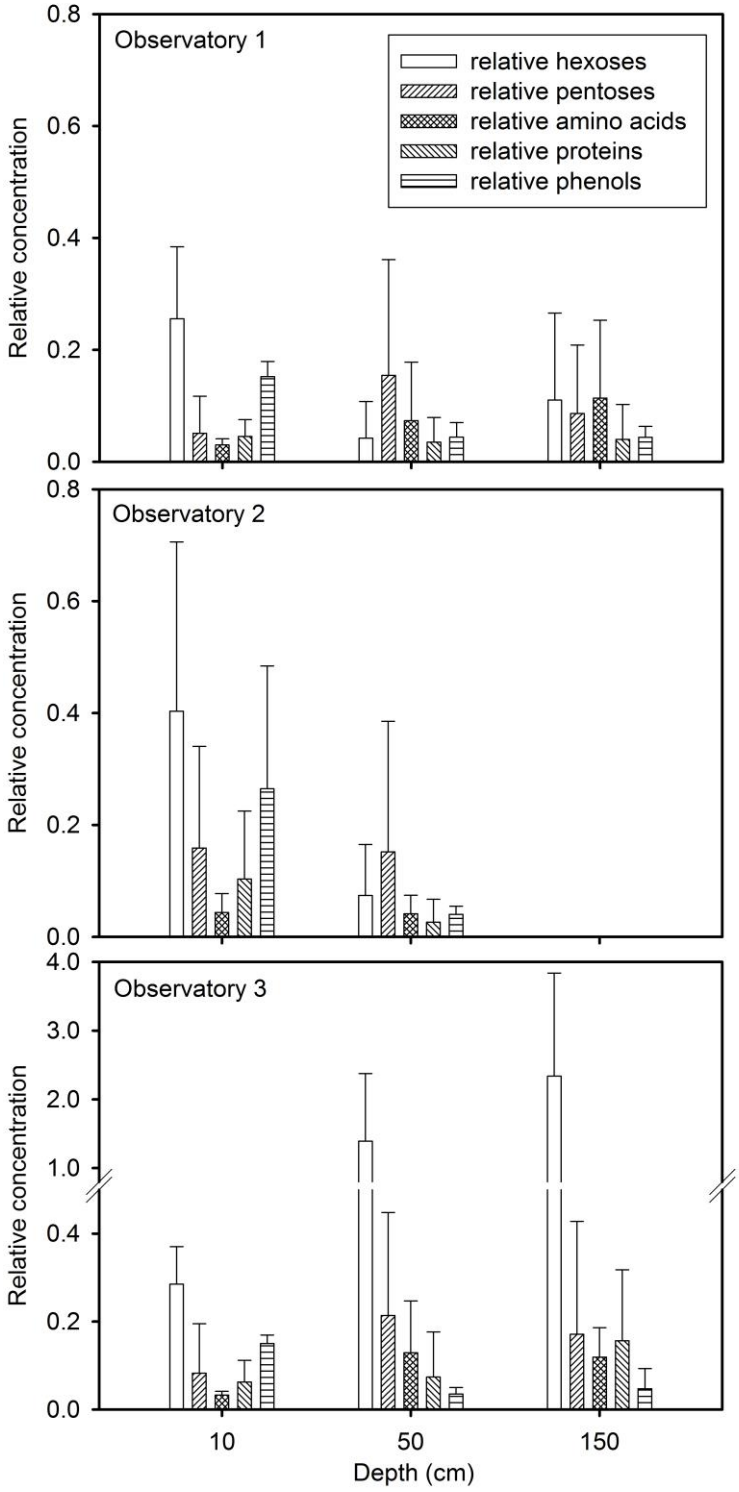

Fig. 1: Mean relative concentration ± standard deviation of hexoses, pentoses, amino acids, proteins and phenols of the three depths sampled at 10, 50 and 150 cm shown separately for the three observatories.

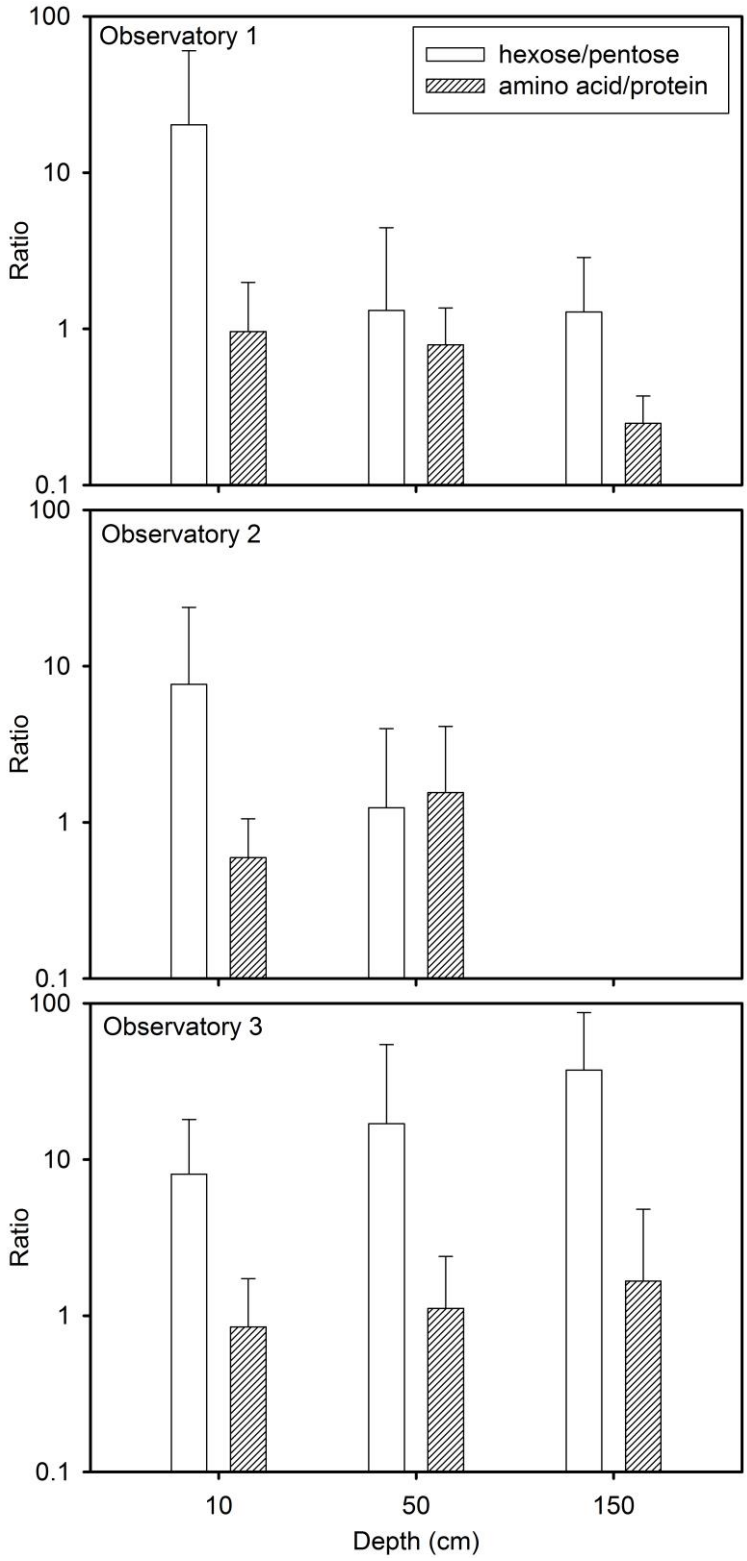

Fig. 2: Mean hexose to pentose and mean amino acid to protein ratio at the three depths shown separately for each observatory. Ratios are shown in logarithmical scale with standard deviation.

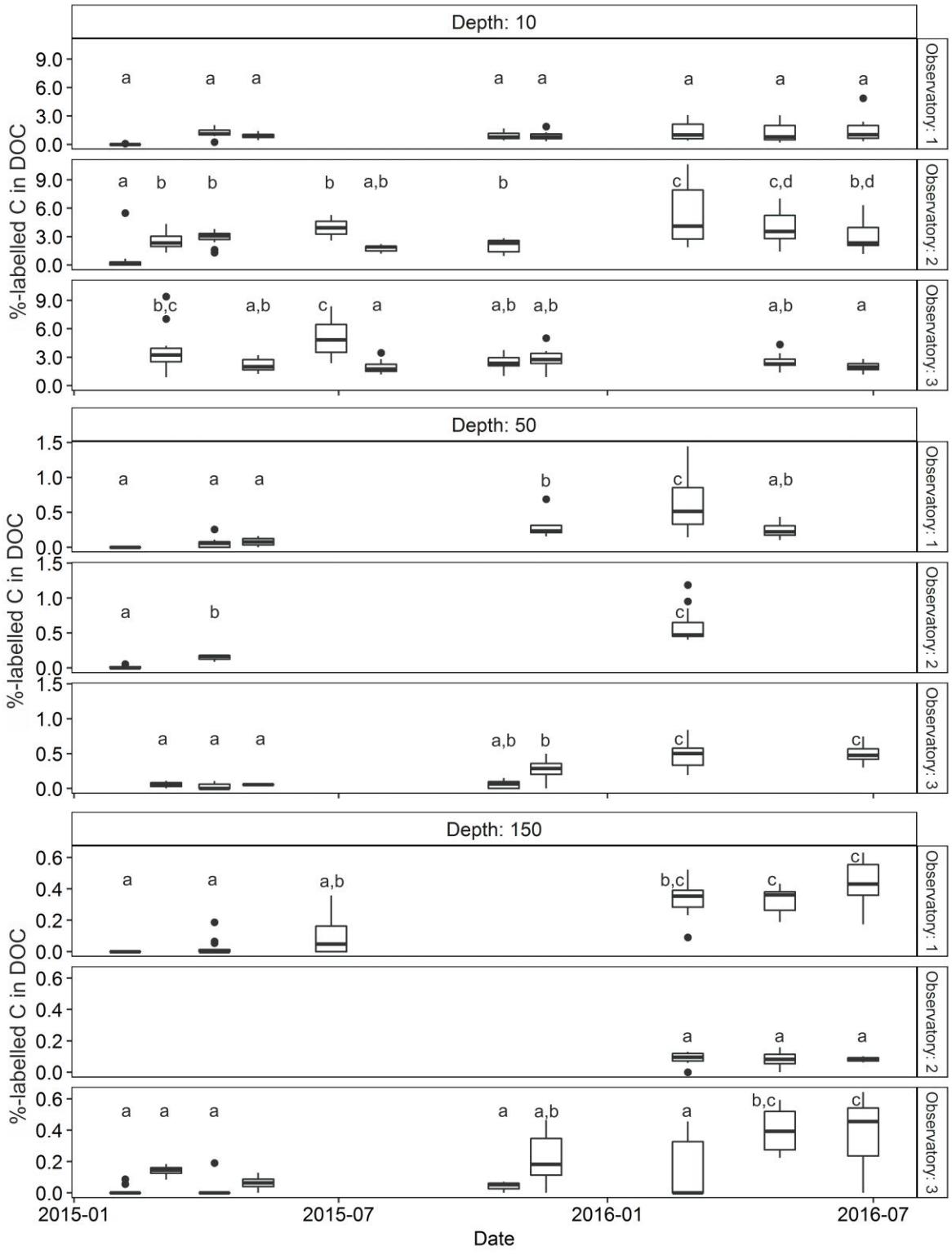

Fig. 3: Boxplot of %-labelled C in DOC of each sampling date per depth (cm) and observatory. Different letters above the boxplots display significantly different mean values per depth and observatory ($p < 0.05$).

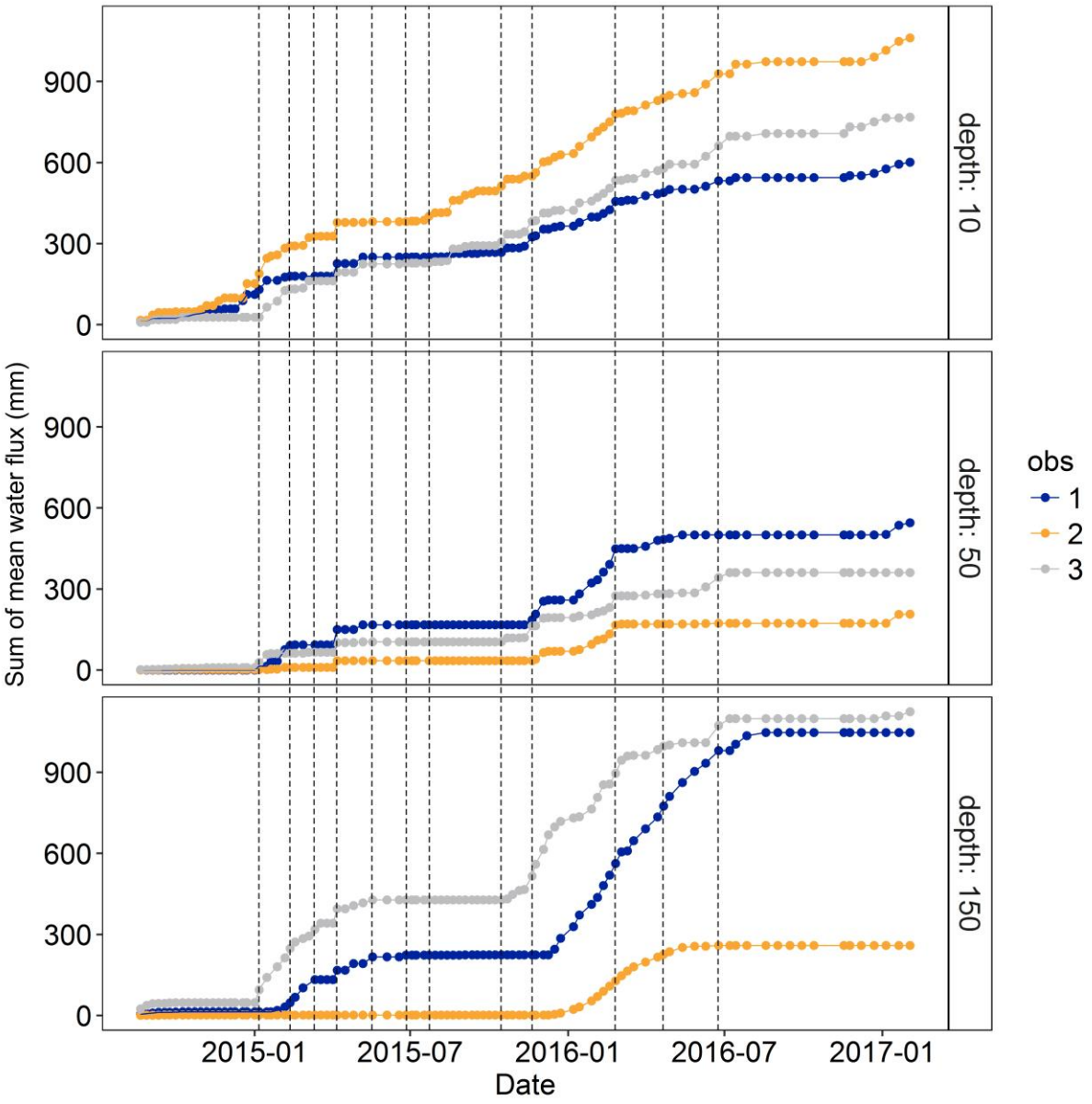

Fig. 4: Sum of the mean water flux per segmented plate lysimeter over the whole sampling period. The sampling dates were $DO^{13}C$ was determined are indicated by dotted lines.

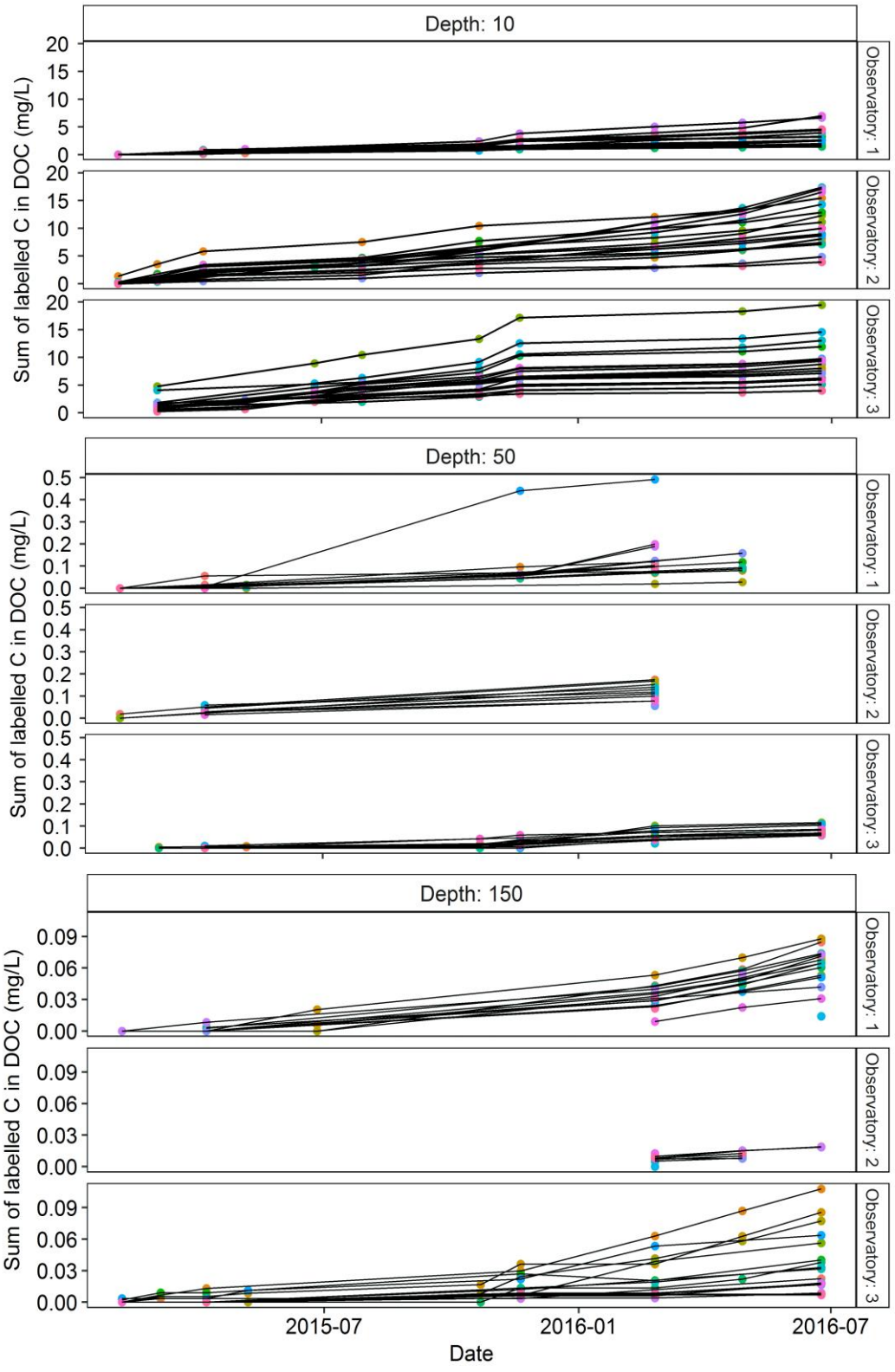

Fig. 5: Cumulative curves of labelled C in DOC (mg L^{-1}) over time per individual segment and depth (cm). Samples from the same segment are summated and connected by lines.

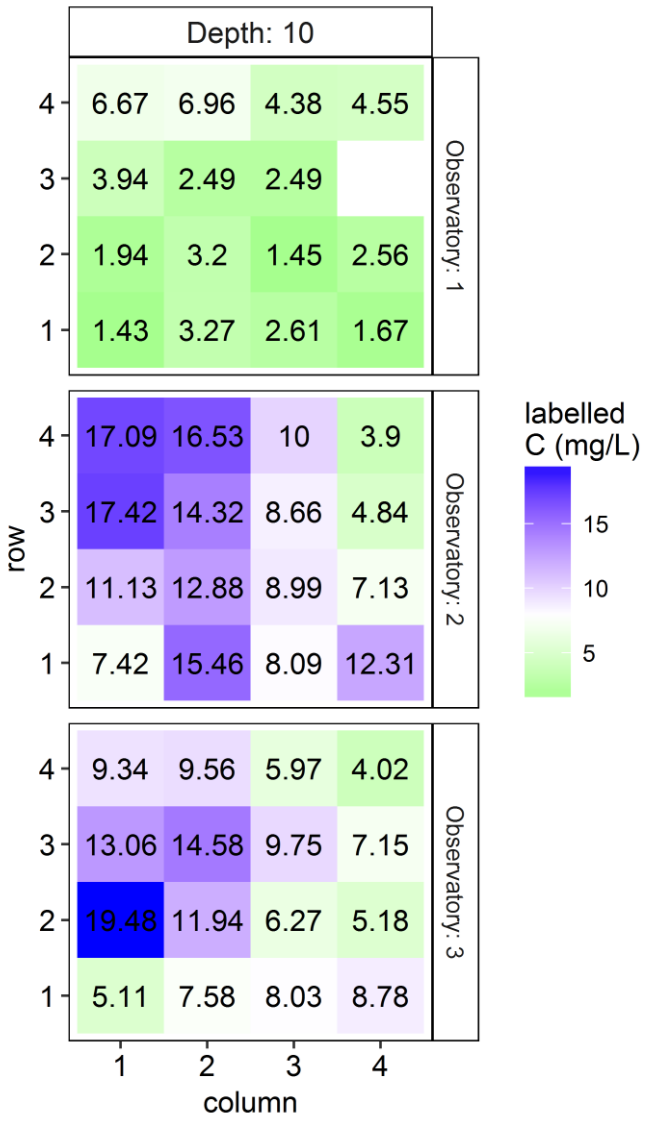

Fig. 6: Sum of labelled C in DOC (mg L^{-1}) over all samplings per each plate lysimeter segment in 10 cm depth at the last sampling date (24.06.2016), corresponding to the respective data points in Figure 5. *Green* colored segments show values lower than the overall mean value, *white* colored segments show values near the overall mean value and *blue* colored segments show values higher than the overall mean value.

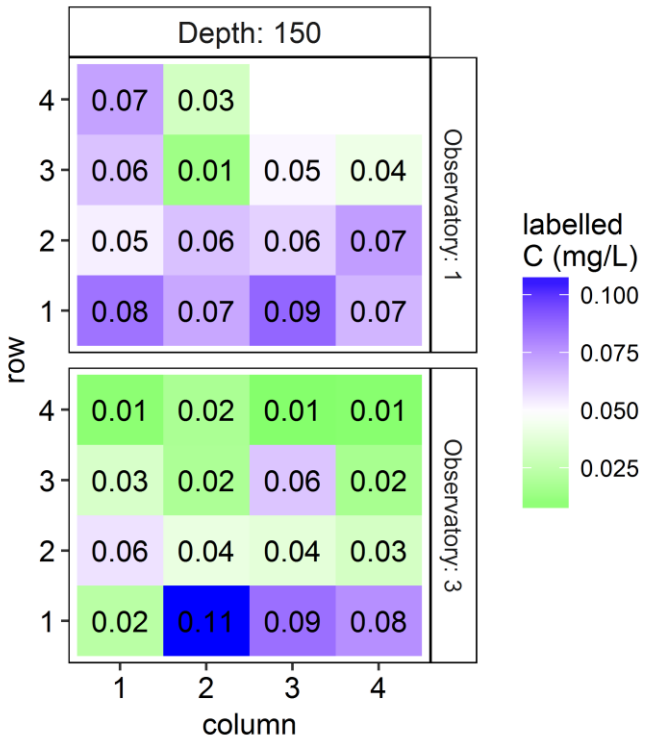

Fig. 7: : Sum of labelled C in DOC (mg L^{-1}) over all samplings per each plate lysimeter segment in 150 cm depth at the last sampling date (24.06.2016), corresponding to the respective data points in Figure 5. Data for observatory 2 not displayed because of the limited number of available samples. *Green* colored segments show values lower than the overall mean value, *white* colored segments show values near the overall mean value and *blue* colored segments show values higher than the overall mean value.

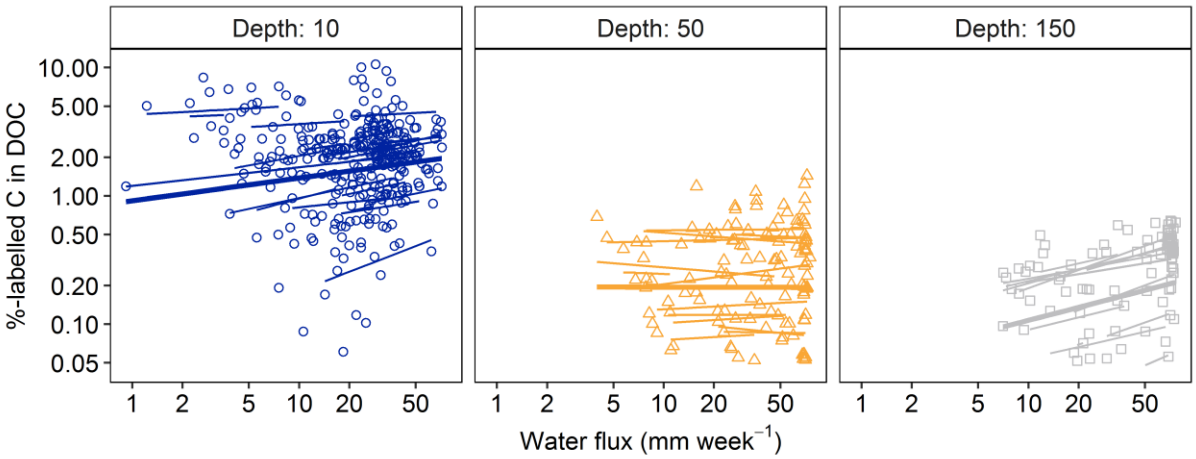

Fig. 8: Relationship between water flux and %-labelled C in DOC per depth (cm). The thin lines represent the relationship within the samples from one plate lysimeter at one sampling date and the bolt lines represent the corresponding mean relationships. Both axes are logarithmical. The correlations are calculated with linear mixed effects models using the R package lme4. For equations, standard errors of the slopes and p-values of the mean relationships see Table 3.

4. Study III

"Multiple exchange processes on mineral surfaces control the transport of dissolved organic matter through soil profiles"

Contribution: I designed the experiment, conducted about two-thirds of the laboratory analyses, collected and analysed the data, compiled tables and graphs and wrote the manuscript. The microbial data of this manuscript was collected and analysed by Sebastian Preußer of the Universität Hohenheim. As the corresponding author I performed the review process of the paper.

Publication status: published in:

Soil Biology and Biochemistry, Volume 118, March 2018, Pages 79-90, doi: 10.1016/j.soilbio.2017.12.006

Multiple exchange processes on mineral surfaces control the transport of dissolved organic matter through soil profiles

Leinemann, T.[1]; Preusser, S.[2], Mikutta, R.[3]; Kalbitz, K.[4]; Höschen, C [5]; Mueller, C.W.[5]; Kandeler, E.[2]; Cerli, C. [6]; Guggenberger, G.[1]

[1]Institute of Soil Science, Leibniz Universität Hannover, Herrenhäuser Straße 2, 30451 Hannover, Germany

[2]Institute of Soil Science and Land Evaluation, Soil Biology Department, University of Hohenheim, Emil-Wolff Str. 27, 70599 Stuttgart, Germany

[3]Soil Science and Soil Protection, Martin Luther University Halle-Wittenberg, Von-Seckendorff-Platz 3, 06120 Halle (Saale), Germany

[4]Institute of Soil Science and Site Ecology, Technische Universität Dresden, Pienner Strasse 19, 01737 Tharandt, Germany

[5]Chair of Soil Science, Department Ecology and Ecosystem Management, Center of Life and Food Sciences Weihenstephan, Technische Universität München, Emil-Ramann-Straße 2, 85354 Freising, Germany

[6]Institute for Biodiversity and Ecosystem Dynamics, Earth Surface Sciences Research Group, Universiteit van Amsterdam, Sciencepark 904, 1098 XH Amsterdam, Netherlands.

4.1 Abstract

Organic topsoil layers are important sources of dissolved organic matter (DOM) transported to deeper soil layers. During passage through the mineral soil, both organic matter (OM) quality and quantity change markedly. Whether these alterations are due to sorption processes alone or to additional stepwise exchange processes of OM on mineral surfaces ("cascade model") is not fully understood. To test the "cascade model", we conducted a laboratory flow cascade experiment with undisturbed soil columns from three depths of two different soil profiles (Dystric and Eutric Cambisol) using carbon (C) isotope labelling. Each of the connected topsoil and subsoil columns contained a goethite (α-

FeOOH) layer either with or without sorbed ^{13}C-labelled OM to assess the importance of OM immobilization / mobilization reactions with reactive soil minerals. By using a multiple method approach including ^{13}C analysis in the solid and solution phases, nanometer scale secondary ion mass spectrometry (NanoSIMS), and quantitative polymerase chain reaction (*q*PCR), we quantified organic carbon (OC) adsorption and desorption and net OC exchange at goethite surfaces as well as the associated microbial community patterns at every depth step of the column experiment. The gross OC exchange between OM-coated goethite and the soil solution was in the range of 15-32%. This indicates that a considerable proportion of the mineral associated OM was mobilized and replaced by percolating DOM. We showed that specific groups of bacteria play an important role in processing organic carbon compounds in the mineral micro-environment. Whereas bulk soils were dominated by oligotrophic bacteria such as *Acidobacteria*, the goethite layers were specifically enriched with copiotrophic bacteria such as *Betaproteobacteria*. This group of microorganisms made use of labile carbon derived either from direct DOM transport or from OM exchange processes at goethite surfaces. Specific microorganisms appear to contribute to the cascade process of OM transport within soils. Our study confirms the validity of the postulated "cascade model", featuring the stepwise transport of OM within the soil profile.

Keywords

Cascade model; DOM; reactive minerals; ^{13}C; NanoSIMS; microbial community composition

4.2 Introduction

Dissolved organic matter (DOM) mobilized in topsoil and transported to subsoil horizons is an important source of carbon (C) throughout the soil profile. In most soils the concentration of dissolved organic carbon (DOC) declines strongly with soil depth, with up to 90% net loss in the first meter of the soil profile (Michalzik et al., 2001). This is likely due to its adsorption to reactive minerals such as iron (Fe) oxides (Kaiser and Guggenberger, 2000) and clay minerals (Saidy et al. 2013), or to co-precipitation with aluminum (Al) and Fe (Scheel et al., 2008; Mikutta et al., 2014). According to

Kalbitz and Kaiser (2008), as much as 19-50% of the organic matter (OM) in the subsoil of a sandy Podzol can be derived from DOM.

Positive correlations between the content of pedogenic Al and Fe with the content of soil organic carbon (OC) (Kaiser and Guggenberger, 2000) and of OC resistant to chemical degradation (Mikutta et al., 2006) suggest that the association of OM with Fe and Al oxides is an important stabilisation mechanism for OM. Especially in acidic soil environments, such as in Dystric Cambisol subsoils, Fe oxides with high specific surface area (SSA) provide reactive surfaces that are important for the binding of OM (Eusterhues et al., 2005). Gu et al. (1994) and Kaiser et al. (1997) concluded that the adsorption of DOM to Fe oxides is dominated by ligand exchange involving carboxyl and hydroxyl functional groups, promoting oxidized aromatic moieties (i.e., lignin-degradation compounds) over carbohydrates in the sorption process (Chorover and Amistadi, 2001; Kaiser, 2003). Thus not only does the concentration of DOC decrease with soil depth but the composition of DOM also changes. A relative enrichment in carbohydrates and sugars along with the selective removal of carboxylated aromatic moieties from soil solution has been observed in batch experiments (Kaiser et al., 1997), saturated soil column experiments (Guo and Chorover, 2003), and in field experiments (Kaiser et al., 2004; McCarthy et al., 1996). Binding of DOM to Fe oxides such as goethite is not only selective for specific compounds, but can also lead to a strong reduction in SSA due to clogging of micropores by selective sorption at the mouths of pores (Kaiser and Guggenberger, 2007). At higher OM loadings, multiple layers of OM are possibly formed on the mineral surfaces, suggesting stronger binding and stabilization of OM that is in direct contact with the mineral surface (Kaiser and Guggenberger, 2003) and enhanced exposure of the outermost OM layer to desorption and exchange processes.

A major source of DOM in temperate forest soils is leaching from the forest floor, leading to highest DOC concentrations directly below the soil organic layer (Michalzik et al., 2001). Most of this DOM is either retained or consumed in the upper centimeters of the mineral soil (Fröberg et al., 2007), whereas DOM at greater soil depths is not directly derived from the organic layer (Hagedorn et al., 2004). Based on such observations, Kaiser and Kalbitz (2012) proposed a stepwise cascade of adsorption to reactive minerals, microbial transformation, and re-release into the soil solution during

the transport of DOM down the soil profile. This cascade assumes that previously bound, more degraded OM moieties get remobilized by the input of fresh highly surface-reactive plant-derived DOM and are transported further down the soil profile where they replace and consequently remobilize even older OM. This conceptual view, therefore, could link the chemical fractionation of DOM during passage down the soil column with the increasing ^{14}C age of DOM and OM as soil depth increases (Sanderman et al., 2008), but experimental data is lacking.

The microbial community adapts to the quantity of bioavailable OM; thus microbial community composition indicates co-evolution with concurrently changing OM properties as soil depth increases (Heckman et al., 2013). In deeper soil, the magnitude of OM processing differs considerably between different soil compartments. Microbial densities are mostly low and heterogeneously distributed depending on OM availability and chemical composition (Preusser et al., 2017; Angst et al., 2016). In contrast to the generally slow process rates in subsoil, reactive minerals such as goethite are known as hotspots of biogeochemical interactions (Eusterhues et al., 2005) and may therefore be of major importance for OM processing in deeper soil layers. Nevertheless, several physicochemical characteristics of water-extractable OM (apparent molar mass, pH, and electrical conductivity) may modify responses of the bacterial and fungal communities in the presence of Fe and Al oxide phases (Heckman et al., 2013).

The objective of this study, therefore, was to test the "cascade model" of Kaiser and Kalbitz (2012) by elucidating whether changes in amounts and composition of DOM within soil profiles are due to sorption processes alone or to additional stepwise exchange of OM on mineral surfaces, processes which may be driven in part by microbial activity. We hypothesize that (i) the input of plant-derived DOM to mineral topsoils leads to selective adsorption of plant-derived compounds to reactive surfaces; (ii) fresh DOM input partially replaces older mineral-associated OM, which subsequently gets remobilized and further transported to deeper soil; and (iii) these mineral-organic associations act as biogeochemical hotspots of high resource availability leading to changes in microbial abundance and community composition. These hypotheses were tested by a column experiment using three connected undisturbed soil horizons from two soils (Dystric and Eutric Cambisol), each horizon

containing a thin interspersed layer of goethite coated with ^{13}C-labelled OM. Incorporation of the labelled OC made it possible to quantify net OC retention and DOM-induced exchange of goethite-associated OM. For selected samples, nanoscale secondary ion mass spectrometry (NanoSIMS) was used to study the microscale (im)mobilization of OM at the goethite surfaces. Concomitant shifts in microbial community composition in the bulk soil and the goethite layers were analyzed by domain- and taxa-specific quantitative polymerase chain reaction (*q*PCR) assays.

4.3 Material and methods

Soil sampling

Undisturbed soil cores of 100 cm^3 (ø 5.7 cm, h 4.0 cm) were taken from two sites in Lower Saxony, Germany; a sandy Dystric Cambisol (IUSS Working Group WRB, 2014) developed from Pleistocene fluvial and aeolian sandy deposits at the Grinderwald (52° 34’22.12" N, 9° 18’ 49.76" E), and a silty Eutric Cambisol (IUSS Working Group WRB, 2014) developed from basalt near Dransfeld (51° 28' 35.60" N, 09° 45' 32.46" E). Both sites were covered with evenly aged (~100 years) European beech (*Fagus sylvatica* L.) forest. Soil cores were taken from three depths: 4 cm, 30 cm and 100 cm at the sandy site, and 4 cm, 12 cm and 26 cm at the silty site, because core sampling in deeper soil layers at the silty site was impossible due to high stone content near the solid bedrock (Table1).

Preparation of goethite coated with ^{13}C-labelled organic matter

Goethite was produced by increasing the pH of a 0.5 M $FeCl_3$ solution to 12 with 5 M NaOH and subsequent aging of the precipitate to goethite at 55°C for 48 hours (Schwertmann and Cornell, 2000). The suspension was dialyzed against double deionized water until the conductivity was <10 µS cm^{-1} and subsequently frozen in liquid nitrogen, freeze-dried, and sieved <200 µm. For the organic matter coating, ^{13}C-labeled DOM was prepared by extraction of a mixture of 10 g labelled beech leaves (12.3 atom% ^{13}C) (IsoLife BV, Wageningen, Netherlands) and 240 g of naturally grown beech leaves in 2500 mL double deionized water (1:10, w/v), to limit the need for expensive ^{13}C-labelled plant litter. The litter material was ground to a maximum size of approximately 3 cm with a stick blender, mixed with the water, and then extracted after being held at room temperature for 16 h. The litter material was removed by a coarse sieve and the remaining solution was pre-filtered by pressure filtration

through glass fibre filters (GF 92, Whatman, Chicago, USA) and finally pressure filtered through 0.45-µm cellulose nitrate filters (Sartorius, Göttingen, Germany). The bulk solution had a concentration of 1519.5 ± 15.3 mg C L^{-1} and 119.6 ± 1.6 mg N L^{-1}. The solution was diluted to 500 mg C L^{-1} with double deionized water for further handling. Ten g of goethite were shaken in 1000 ml of this DOM solution for 24 hours in the dark on an overhead shaker and subsequently centrifuged for 20 min at 2000 *g*. The supernatant was decanted and the residual goethite was washed two times for 10 minutes with ultrapure water und each time centrifuged for 10 minutes at 2000 *g* and decanted. The residual OM-coated goethite was freeze dried and stored in the dark until use. The OM-coated goethite had an OC concentration of 19.4 mg g^{-1} and 0.19 mg m^{-2}. SSA decreased considerably as a result of the OM loading (Table 2), even though the sorption capacity of the mineral was not reached as compared to investigations by Kaiser and Guggenberger (2007). The OM coating on the goethite had a $\delta^{13}C$ ratio of 1298.9‰ VBDP.

Column experiment

Two soil cores of one depth were assembled into one soil column, with 2.8 g of goethite embedded in a 200-µm polyester mesh (Franz Eckerd GmbH, Waldkirch, Germany) placed tightly in between the cores (Fig. 1). For both soil types two variations of the experiment were performed, one using pure goethite (PG) and one using OM-coated goethite (CG). This resulted in four treatments: pure goethite between sandy soil cores (Sa_{PG}), OM-coated goethite between sandy soil cores (Sa_{CG}), pure goethite between silty soil cores (Si_{PG}), and OM-coated goethite between silty soil cores (Si_{CG}). Each column was equipped with an inlet and outlet and sealed with a solvent free sealing compound (water stop, MEM Bauchemie GmbH, Leer, Germany). Dissolved OM used in the column experiment was extracted from air dried, ground beech leaves sampled in autumn 2014 from the Grinderwald forest floor in double deionized water at room temperature for 16 h (1:10, w/v) and subsequently filtered through 0.45-µm cellulose nitrate filters (Sartorius AG, Göttingen, Germany). The resulting concentration of 1246.7 ± 25.7 mg C L^{-1} was diluted to approximately 30 mg C L^{-1} with double deionized water. The $\delta^{13}C$ ratio of the beech litter extract was -28.9‰ VPDB.

Three columns, representing soil from the different soil depths, were combined into one cascade with three replicates (Fig. 1). The experiments were carried out in a temperature controlled cabinet at a constant temperature of 8°C, closely approximating the mean annual temperature at the sampling sites. The prepared solution was pumped at a flux rate of 5.5 ml h^{-1} (3 mm h^{-1}) for 32 days into the first column inlet and the efflux from the first depth compartment was sequentially pumped into the second and third depth compartments. A volume of 100 ml of the outflow solution from each column and the inflow solution from the first depth column was sampled after 1, 2, 4, 8, and 16 days, and at the end of the experiment (first depth 32 days, second depth 27 days and third depth 22 days). The second and third columns had to be started after a 5 day delay with respect to their upper column because ca. 300 ml of percolation solution had to accumulate to enable secure solution supply. In total 4224 ml (2346 mm) solution were pumped through the first depth compartment, 3564 ml (1969 mm) through the second depth compartment, and 2904 ml (1604 mm) through the third depth increment, simulating the cumulative mean water flux of three years' mean precipitation. The volume reduction over depth was due to the cascade design of the experiment, as the available solution for the second and third columns declined by the withdrawn sample volume (100 ml per sampling). However, such a decrease in water flux with soil depth occurs also in the natural environment, as was recorded for the sampling site Grinderwald (Leinemann et al., 2016). After the experiment, the soil was removed from the cores, air dried, and stored for further measurements.

Measurements

DOC concentration was measured by high temperature combustion (Vario TOC cube; Elementar, Langenselbold, Germany), and the UV absorbance of DOM was determined at 280 nm on a Varian Cary 50 UV-Vis spectrophotometer (Agilent Technologies, Santa Clara, CA, USA). The $\delta^{13}C$ value of DOM ($DO^{13}C$) was analysed directly in solution using a high-temperature combustion system for direct ^{13}C measurement from liquid (Federherr et al., 2014 and Kirkels et al., 2014). For this, an isoTOC cube (Elementar group, Langenselbold, Germany) total organic carbon analyzer was coupled with a continuous flow isotope ratio mass spectrometer (IsoPrime100, Isoprime Ltd, Cheadle Hulme, UK).

All samples were manually acidified to pH ~2 by HCl (37%) in order to remove dissolved inorganic C and/or prevent (re)dissolution of atmospheric CO_2. Samples were injected 4 times and only the last three injections were used for data analyses. Injection volume ranged between 0.2 and 1 ml depending on the TOC content. Both at the beginning and at the end of each sequence a set of international standards (Caffeine IAEA-600 Sucrose IAEA-CH6; Coplen et al., 2006) dissolved in the blank water at a TOC concentration similar to the one expected for the samples were run as samples, allowing for 2 point normalisation. To be able to use a two point normalisation for labelled samples also, artificial standards were prepared by thoroughly mixing non-labelled and 99%-labelled glucose in proportions to obtain the desired label. The mixtures were then normalised vs international standard as solid using an Elemental Analyzer (vario ISOTOPE cube, Elementar group, Hanau, Germany) coupled to IRMS (IsoPrime100, Isoprime Ltd., Cheadle Hulme, UK) and then used to prepare the standard solutions as described above. The artificial solid mixtures were checked several times during the entire period of analyses to ensure the consistency of the obtained values. Blanks samples of the same water used for the preparation of the normalising standards were analysed before, after, and between samples. All calculations for corrections and normalisation were done according to those described in Kirkels et al. (2014).

After the experiment, soil columns were opened and the soil core above and below the goethite as well as the goethite layer were sampled separately, freeze dried and stored in the dark until analyses. C and N content and $\delta^{13}C$ ratios of solid samples were measured using an Elementar IsoPrime100 IRMS (IsoPrime Ltd, Cheadle Hulme, UK) coupled to an Elementar vario MICRO cube EA CN analyzer (Elementar Analysensysteme GmbH, Langenselbold, Germany). Total pedogenic Fe (dithionite-citrate-extractable Fe, Fe_d) of the soil samples before the experiment were determined according to Blakemore et al. (1987), in which 1.00 g air-dried soil in the presence of 1 g sodium dithionite was extracted with 20 ml 22% sodium citrate. After 16 hours of shaking and addition of 5 ml of 5 mM $MgSO_4$, samples were centrifuged for 20 min at 500 g and filtered. The filtrate was analyzed for Fe by inductively coupled plasma optical emission spectroscopy (ICP-OES; Varian 725-ES, Varian Australia Pty Ltd., Mulgrave, Australia). The specific surface area (SSA) and pore volumes of solid samples were analysed by N_2 adsorption-desorption at 77 K, after outgassing the samples at 232 K for

24 hours until the pressure remained constant below 9.0×10^{-4} Torr (Autosorb MP1, Quantachrome, Boynton Beach, FL, USA). SSA was determined by the multipoint BET method using 11 points in the 0.05-0.3 P/P_0 range (Brunauer et al., 1938). Total pore volume (TPV) of pores with a radius <1839.6 Å was taken at a partial pressure of 0.99. Average pore radius was calculated as $r_p = 2V_{liq}/SSA$, where V_{liq} is the volume of liquid N_2 contained in the pores.

To map the distribution of sorbed OC to the goethite surface, an aliquot of the OM-coated goethite before the experiment (G0) and an aliquot of the OM-coated goethite after the experiment from each of the three depths of the columns with the sandy soil (4 cm = G1, 30 cm = G2, 100 cm = G3) were analysed with a NanoSIMS 50L (Cameca, Gennevilliers, France). In order to facilitate adhesion to a thin layer of goethite, a small quantity of dried sample was spread on a silica wafer and placed at -20°C in a freezer for one minute. Afterwards, the sample was placed at room temperature for another minute, generating condensation water that served to adhere the samples to the wafer, which was then dried in a desiccator overnight. Loose material was removed with compressed air and the remaining sticking sample was subsequently coated with gold to avoid possible charging effects (Sputter Coater S150A, Edwards, Crawley, UK) during subsequent scanning electron microscope (SEM) imaging. Using SEM on each sample, four regions with representative single layered goethite aggregates were chosen for subsequent NanoSIMS analyses. A Cs^+ ion beam with 16 keV impact energy, ~4 pA, primary current was used and $^{12}C^-$, $^{13}C^-$, $^{16}O^-$ and $^{56}Fe^{16}O^-$ secondary ions were recorded using electron multipliers on a raster area of 30 µm × 30 µm (256 × 256 pixels) by collecting 100 planes per spot with a dwell time of 1 ms $pixel^{-1}$. Appropriate slits were used to ensure a mass resolution to solve mass interferences present between $^{13}C^-$ and $^{12}C^1H^-$. Prior to analysis the region was sputtered using a high primary beam current between 500 and 600 pA to remove contaminants, the Au layer, and to implant primary ions in the surface to enhance secondary ion emission. The images were corrected for electron multiplier dead time (44 ns) and further processed using the look@nanoSIMS software (Polerecky et al., 2012) operated with Matlab 2013b (The MathWorks Inc., Natick, MA, USA). Regions of interest (ROIs) were selected by the interactive threshold function on the basis of the $^{12}C^-$ counts of the accumulated measurements, as they represented areas of sorbed OM containing moieties rich in $^{13}C^-$ abundance as well. The areas corresponding to goethite were selected similarly on

the basis of $^{56}Fe^{16}O^-$ counts. The distribution of sorbed OM to the goethite was quantified by calculating the percentage of area covered by OM on the goethite surface. The $^{13}C^-$ / $^{12}C^-$ was calculated for the OM ROIs to evaluate OC dynamics on the goethite surface over the course of the experiment. The ratio numbers were multiplied by 100 to better visualise small differences. The numbers then were in the range of atom% ^{13}C. To compare with NanoSIMS atom% ^{13}C the bulk EA-IRMS measurements were converted from the δ‰ notation to atom% ^{13}C values by taking the $^{13}C^-$ / $^{12}C^-$ ratio of the EA-IRMS standard (0.0111802) into account (Frey, 2007). For further discussion of the results the ROIs with an atom% ^{13}C of <1.40 were considered to consist mainly of newly sorbed OC as they occurred on the samples only after the column experiment (Supplement 6) and are referred to as low enriched. The ROIs with an atom%^{13}C of >1.4 and <2.4 are referred to as intermediate enriched and to possibly consist of a mixture of old and new sorbed OC. The ROIs with an atom%^{13}C of >2.40 are referred to as high enriched and were considered to consist of mainly old OC, as the they were similar to or higher than bulk EA-IRMS measurements of the OM-coated goethite before the experiment.

For *q*PCR analysis, DNA was extracted from 0.3 g sample of the experimental run with pure goethite (Supplement 2) using a FastDNA SPIN Kit for soil (BIO101, MP Biomedicals, Santa Ana, CA, USA) and quantified with a Nanodrop ND-2000 spectrophotometer (Thermo Scientific, Waltham, MA, USA), followed by dilution of the samples with ultra-pure water to a target concentration of 5 ng DNA μl^{-1}. The quantification of the abundances of total bacteria, fungi, and archaea and the abundances of the bacterial taxa *Betaproteobacteria*, *Actinobacteria*, *Acidobacteria*, *Bacteroidetes*, *Firmicutes*, *Verrucomicrobia* and *Gemmatimonadetes* via *q*PCR was carried out with an ABI prism 7500 Fast System (Applied Biosystems, Foster City, CA, USA). For each *q*PCR assay a cocktail of 0.75 µl of each forward and reverse primer, 0.375 µl T4gp32, 7.5 µl SYBR Green, 4.125 µl ultra-pure water, and 1.5 µl DNA template (for total bacteria and archaea only 1.0 µl) was mixed. Standard curves were generated in triplicate with serial dilutions of a known quantity of the respective isolated plasmid DNA. Each *q*PCR run included two no-template controls showing no or negligible values. Supplement 1 lists the selected primers, thermal cycling conditions, and PCR efficiencies. Sampling strategy as

well as sample storage made it possible to measure the *q*PCR derived from samples of the sandy Dystric Cambisol only. *Calculations*

The total amount of DOC transported at each sampling point was calculated by multiplying the measured DOC concentration with the volume of percolate passing the column over the period represented by the sample (eq. 1).

$$total\ transported\ DOC\ (\ mg\ ) = DOC\ concentration\ (\ mg\ L^{-1}\ )\ \times flux\ (\ L\ h^{-1}\ ) \times period\ (\ h\ ) \quad \text{(eq. 1)}$$

DOC exchange in the 1st depth increment was calculated by subtracting the cumulative DOC in the inflow solution (DOC_{in1}) from the cumulative outflow solution (DOC_{out1}) (eq. 2). Because of the delayed start for the second depth increment, the cumulative DOC of the 4th to the 6th samples of the outflow from the first depth compartment (DOC_{out1}) was subtracted from the sum of cumulative DOC from the second depth compartment (DOC_{out2}) (eq. 3). For the third depth compartment the cumulative DOC of the 4th to the 6th samples of the second depth compartment (DOC_{out2}) was subtracted from the sum of the cumulative DOC of the third depth compartment (DOC_{out3}) (eq. 4).

$$DOC\ exchange\ 1.depth = \sum_{i=1}^{6} DOC_{out1} - \sum_{i=1}^{6} DOC_{in1} \quad \text{(eq. 2)}$$

$$DOC\ exchange\ 2.depth = \sum_{i=1}^{6} DOC_{out2} - \sum_{i=4}^{6} DOC_{out1} \quad \text{(eq. 3)}$$

$$DOC\ exchange\ 3.depth = \sum_{i=1}^{6} DOC_{out3} - \sum_{i=4}^{6} DOC_{out2} \quad \text{(eq. 4)}$$

The specific UV absorbance (SUVA) at 280 nm was calculated as the ratio of UV absorbance of the solutes and DOC concentration (L mg C^{-1} cm^{-1}). Mean values for inflow and outflow solutions were calculated for the six sampling times. For the net SUVA change in the first depth the mean SUVA of the inflow solution ($SUVA_{in1}$) was subtracted from the mean SUVA of the outflow solution from the first depth compartment ($SUVA_{out1}$) (eq. 5). For the SUVA change in the second depth compartment, the mean SUVA of the outflow solution from the first depth compartment ($SUVA_{out1}$) was subtracted from the mean SUVA of the outflow solution from the second depth compartment ($SUVA_{out2}$) (eq. 6). For the SUVA change in the third depth compartment the mean SUVA of the outflow solution from

the second depth compartment ($SUVA_{out2}$) was subtracted from the mean SUVA of the outflow solution from the third depth compartment ($SUVA_{out3}$) (eq. 7).

$$SUVA\ change\ 1.depth = SUVA_{out1} - SUVA_{in1} \quad \text{(eq. 5)}$$

$$SUVA\ change\ 2.depth = SUVA_{out2} - SUVA_{out1} \quad \text{(eq. 6)}$$

$$SUVA\ change\ 3.depth = SUVA_{out3} - SUVA_{out2} \quad \text{(eq. 7)}$$

The proportion of C derived from the OM-coated goethite in the outflow solution (goethite-derived OC, GDC_{DOM}) of each column was calculated relative to the $\delta^{13}C$ ratio of the respective inflow solution (eq. 8), where $\delta^{13}C_{out}$ and $\delta^{13}C_{in}$ represent the $\delta^{13}C$ ratio of the outflow and the inflow solutions and $\delta^{13}C_{CG}$ represents the $\delta^{13}C$ ratio of the OM-coated goethite. The $\delta^{13}C$ ratios were averaged over the six sampling times.

$$GDC_{DOM}\ (\%) = \frac{(\delta 13C_{out} - \delta 13C_{in})}{(\delta 13C_{CG} - \delta 13C_{in})} x\ 100 \quad \text{(eq. 8)}$$

The proportion of C on the OM-coated goethite-derived from the solution after the experiment (solution-derived OC, $SDC_{goethite}$) was calculated relative to the $\delta^{13}C$ ratio of the inflow solution ($\delta^{13}C_{in}$), where $\delta^{13}C_{CGA}$ represents the $\delta^{13}C$ ratio of the goethite after the experiment and $\delta^{13}C_{CG}$ represents the $\delta^{13}C$ ratio of the OM-coated goethite before the experiment (eq. 9). Hence, the remaining proportion of OC on the goethite after the experiment was still derived from the OM-coating applied before the experiment.

$$SDC_{goethite}\ (\%) = \frac{(\delta 13C_{CGA} - \delta 13C_{CG})}{(\delta 13C_{in} - \delta 13C_{CG})} x\ 100 \quad \text{(eq. 9)}$$

The relative change in OC concentration (ΔC) of the OM-coated goethite before (C_{before}) and after the experiment (C_{after}) was calculated by equation 10.

$$\Delta C\ (\%) = \frac{(C_{after} - C_{before})}{C_{before}} x\ 100 \quad \text{(eq. 10)}$$

The previously goethite-bound OC that was mobilized during the experiment (MC) was calculated by the difference in the absolute amount of SDC and the net change in OC content of the mineral before (C_{before}) and after the experiment (C_{after}) relative to the OC content before the experiment.

$$MC\ (\%) = \frac{\left(\frac{SDC(\%) \times C_{after}}{100} - \left(C_{after} - C_{before}\right)\right)}{C_{before}} x\ 100 \qquad \text{(eq. 11)}$$

The magnitude of change in the $\delta^{13}C$ ratios of the soil samples before and after the experiment was too small to calculate the respective GDC in the soil samples. Thus the total amount of OC retained in the soil cores that was mobilized from the OM-coated goethite (Retained MC) was calculated as the difference between the total amount of MC and the total amount of GDC in the outflow solution (eq. 12). The total amount of MC (mg) was the product of C_{before} (mg g^{-1}) and MC (%) times the weight of the goethite between the soil cores (2.8 g), divided by 100. The total amount of GDC (mg) was the product of the total DOC_{output} (mg) and the GDC (%), divided by 100.

$$Retained\ MC\ (mg) = \frac{C_{before} \times MC(\%) \times 2.8}{100} - \frac{total\ DOC_{output} \times GDC(\%)}{100} \qquad \text{(eq. 12)}$$

Statistical analysis

Effects of soil type (soil), depth (depth), position inside the column above the goethite or below the goethite (pos), OM-coating of the goethite (goethite), and interactions of these factors were analysed with linear mixed-effect (lmer) models. Due to the design with three experimental repetitions of the three–step cascade system, the soil columns were set as random factor. Comparison of means was conducted for all factors and interactions. Significance was tested at $p < 0.05$ in all cases. Homogeneity of variance was tested for all parameters by Levene's test. All statistical analyses were carried out with R statistics version 3.2.1 (R Core Team, 2015) using the "lme4" (Bates et al., 2015) and the "lsmeans" package (Lenth, 2016).

4.4. Results

DOC transport

Mean DOC concentration in the column outflow solution decreased with increasing depth, and the columns with OM-coated goethite had higher DOC concentrations than the columns with pure goethite (Fig. 2). Both results were more pronounced for the soil developed from sand than for the silty soil developed from basalt (Table 1). Concurrent with the DOC concentration, cumulative DOC

transport also decreased with depth, and more DOC was found in the effluent of columns with OM-coated goethite than in the effluent of columns with pure goethite (Fig. 2). With respect to cumulative DOC flux, the differences with depth were more pronounced for the sandy soil than for the silty soil (Fig. 3). The net OC exchange was calculated to evaluate whether, over the course of the experiment, OC was retained or released in the columns. Samples from the first depth showed a higher cumulative DOC flux in the outflow than in the inflow indicating that DOC was released over the course of the experiment (values above the 1:1 line in Fig. 3). The samples from the first depth compartments with silty soil and pure goethite were an exception as OC was retained. In contrast, all columns from the second and third depths retained OC, and under all experimental conditions less OC was retained for the experiments with OM-coated goethite than for those with pure goethite ($F_{1,10}$ = 11.98, p <0.01; Supplement 4).

Aromaticity of DOM

The outflow solution of the first depth of the sandy soil had a higher mean SUVA than the inflow solution (Fig. 4). But with increasing depth the mean SUVA of the column outflow decreased (depth: $F_{2,133}$ = 100.06, p <0.01). The effect of OM-coated or pure goethite on SUVA was less pronounced than on the DOC concentration (Fig. 3 and 4). The silty soil showed smaller differences in SUVA between the three depths than the sandy soil. A depth trend was only apparent in the columns with OM-coated goethite (significant difference between first and third depths, p <0.01; Fig. 4; Supplement 5). The sandy soil had a higher mean SUVA in the outflow of the first depth compartments than the silty soil. The mean SUVA of the outflow of the second depth compartments with sandy soil was in the same range as in case of the silty columns, while for the third depth compartments it was lower for the sandy soil than for the silty soil.

Exchange of OC between goethite, soil and solution

Along with the sorptive exchange of unlabelled DOM from the percolation solution with the labelled goethite-bound OM, the $\delta^{13}C$ ratio of the outflow DOM solution significantly increased with soil depth (depth: $F_{2,72}$ = 76.7, p <0.01). This increase was less pronounced in the effluent of the silty soil columns than of the sandy soil columns (Fig. 5A). In the sandy soil, the proportion of labelled OM

desorbed from the goethite to total DOM increased from the first to the second depth and then remained constant (Fig. 5B). In the silty soil, the contribution of labelled OM desorbed from the goethite to the DOM output of the columns did not change significantly with depth (Fig. 5B).

Percolation of the DOM solution through all first depth compartments increased the OC content of the goethite. In the second and third depths, the OC content was in the range of the OM-coated goethite before the experiment (19.4 mg g^{-1}) or slightly decreased (Table 2). As an unlabelled DOM solution ($\delta^{13}C$ of –28.9‰) was used, the $\delta^{13}C$ of the goethite-associated OM decreased during the experiment (Table 2). In the first depth compartments of both soils the proportion of OM adsorbed to the goethite after the experiment was evenly distributed between new OM derived from the percolation solution and OM that had already been adsorbed before the experiment (Fig. 6). With increasing depth, the proportion of unlabelled OM newly sorbed to the goethite decreased. In the columns derived from silty soil, the goethite from the second and third depth compartments had similar percentages of goethite- and solution-derived OC (Fig. 6). A replacement of pre-experimentally bound OC, calculated according to equations 8-11, was evident in all columns, even where the net OC exchange (ΔC) of the goethite was negative. More OC was replaced in the columns of the silty soil than in those of the sandy soil ($F_{1,9} = 35.1$, $p < 0.01$), but the depth patterns were similar (Fig. 6).

In the first and second depth compartments of the sandy soil, the OC adsorbed to goethite from the percolation solution (SDC) exceeded the overall increase in OC content (ΔC) over the course of the experiment. Hence, for both soil depths, around 20% of the goethite-derived OM was exchanged by OM from the percolation solution (MC), while the rest of the OC was sorbed additionally. In the third depth, both the OC content and the $\delta^{13}C$ ratio of the goethite decreased, leading to a calculated proportion of 12% of OM derived from the percolation solution and 18% of the OM adsorbed to the goethite before the experiment was mobilized. In the first depth compartments with silty soil, 31% of the OM adsorbed to the goethite before the experiment was exchanged over the course of the experiment. In the second and third depths, an overall decrease in OC concentration of the goethite as compared to the concentrations before the experiment corresponded to an adsorption of 20% OC from the solution, and about 25% of the previously bound OC was replaced (Fig. 6, Table 2).

The $\delta^{13}C$ ratio of the original soil increased with increasing depth (Table 1). After the percolation experiment, in the first and second depth compartments the $\delta^{13}C$ ratio of the soil either above or below the goethite showed major changes compared to the $\delta^{13}C$ ratio of the original soil. In the third depth the $\delta^{13}C$ ratios of the soil above and below the goethite increased by 10.4‰ and 11.7‰, respectively (Supplement 5). Based on the difference between the amount of mobilized OC from the goethite and the measured goethite-derived OC in the DOM solutions, we were able to determine the amount of OC mobilized from the goethite that was thereafter retained in the soil below the goethite layer ($Retained_{MC}$). In the first depth compartment of the sandy soil, this amounted to 7.9 mg OC, whereas 5.2 mg OC and 7.1 mg OC were calculated for the second and third depth compartments, respectively (eq. 12). In the columns with silty soil, 13.9 mg of the mobilized OC was retained under the goethite layer of the first depth and 11.3 mg OC and 13.0 mg OC were retained in the second and third depths, respectively (Table 3).

Microbial community composition

The microbial communities in the soil and of the goethite in all depth compartments of the sandy Dystric Cambisol were dominated by bacteria with relative proportions of 69-92% (Fig. 9A). Post-experimental absolute abundances of bacteria increased significantly from the first to the second soil depth for both bulk soil and goethite layers, with the highest mean increase in bacterial abundance of 265% in the goethite layer at 30 cm depth compared to the respective layer at the 4 cm depth (depth: $F_{1,18} = 13.29$, $p < 0.01$). Bacterial abundances also tended to differ between sampling points within each depth compartment, with the largest differences between the soil above the goethite layer and the goethite itself (pos: $F_{2,18} = 3.18$, $p < 0.1$). Fungi and archaea showed highest relative proportions in the 4 cm soil columns of up to 13 and 19%, respectively. Archaea exhibited increasing absolute abundances with depth and showed pronounced differences within each depth compartment (Fig. 9A). Greatest changes were found between the goethite layers (lowest abundances) and the soil below (highest abundances, depth: $F_{1,15} = 7.40$, $p < 0.05$; pos: $F_{2,15} = 6.16$, $p < 0.05$).

Taxa-specific assays of the bacterial communities revealed that all soil depth compartments, both above and below the goethite layers, were dominated by *Actinobacteria* (up to 60%) and

Acidobacteria (up to 25%). In contrast, goethite layers showed the highest abundances of *Betaproteobacteria*, with relative proportions ranging between 54 and 66% (Fig. 9B). Three of the six investigated taxa were significantly affected by soil depth or position within the column (above or below the goethite). While *Actinobacteria*, *Verrucomicrobia* and *Firmicutes* did not show any significant effects, the abundances of *Acidobacteria*, *Betaproteobacteria* and the generally less abundant *Gemmatimonadetes* increased with depth (Fig 9B; *Acidobacteria*: $F_{1,15} = 7.52$, $p < 0.05$; *Betaproteobacteria*: $F_{1,15} = 6.89$, $p < 0.05$; *Gemmatimonadetes*: $F_{1,15} = 8.22$, $p < 0.05$). Additionally, *Betaproteobacteria* were more abundant in the goethite layers than in the bulk soil compartments, while *Acidobacteria* and *Gemmatimonadetes* showed the opposite effect (*Betaproteobacteria:* $F_{2,15} = 7.90$, $p < 0.01$*; Acidobacteria*: $F_{2,15} = 10.41$, $p < 0.01$; *Gemmatimonadetes:* $F_{2,15} = 4.49$, $p < 0.05$).

Spatial distribution of OM on goethite surfaces

About 2.7 ± 0.7% of the mineral surfaces of the OM-coated goethite used in the column experiments and analysed by NanoSIMS were covered by OM (Fig. 7, Supplement 7). The mean atom% ^{13}C of the ROIs on all samples was 2.2 ± 0.4 with a minimum of 1.6 ± 0.3 and a maximum of 3.2 ± 0.7. The bulk EA-IRMS measurement was in the same range and translates to 2.5 atom% ^{13}C (Fig. 8A). As only the goethite from the columns taken in the sandy soil was analysed by NanoSIMS, the following results are restricted to this soil type. After the experiment, 3.5 ± 1.0% of the goethite surface from the first depth compartment was covered by OM, while the mean atom% ^{13}C changed to 1.9 ± 0.5. The bulk EA-IRMS measurement was in the same range (1.8 atom% ^{13}C). The samples from the second depth compartment showed slightly smaller mineral surface coverage by OC (2.7 ± 1.4%) and a slightly higher mean atom%^{13}C (2.0 ± 0.5), which mirrored the bulk EA-IRMS measurement (2.3 atom% ^{13}C). The samples from the third depth showed a mineral surface coverage (3.5 ± 2.1%) and atom% ^{13}C results (1.9 ± 0.5) comparable to the first depth samples, but the bulk EA-IRMS result was higher (2.3 atom% ^{13}C, Fig. 8A).

On average, 74.5 ± 33.3% of the ROI area of the OM-coated goethite before the experiment showed intermediately enriched atom% ^{13}C values (1.4-2.4 atom% ^{13}C) whereas the remainder showed high ^{13}C enrichments (>2.4 atom% ^{13}C). The ROI area of the goethite from the first depth compartment

comprised the largest proportion of less enriched OM (<1.4 atom%^{13}C) and the smallest proportion with highest ^{13}C enrichment. The ROI area of the goethite from the second and third depth compartments showed comparable proportions of the low enriched category, which decreased compared to the first depth compartment. For all post-experimental goethite samples, slightly above 50% of the ROI fell into the intermediate enriched category, with the maximum area (66.5 ± 14.3% of ROI) observed for goethite from the second depth compartment (Fig. 8B).

4.5 Discussion

Net OC exchange at goethite surfaces

DOC concentration and DOM composition changed through interaction of soils and goethite with the percolated solutions. In the first depth compartments of all experiments, except for the columns from the basalt site with pure goethite, there was a net release of DOC, and the SUVA increased in the outflow solution relative to the inflow solution (leaf leachate). This indicated a release of plant derived aromatic compounds from the topsoil (McDowell and Likens, 1988), which was assumed to be the initial step of the cascade-like transport of DOM down the soil profile (Kaiser and Kalbitz, 2012). The inflow solutions of the second depth compartments consequently had the highest DOC concentrations in the experiments along with the highest proportion of aromatic moieties. Retention processes in the second and third depth compartments led to a decrease in DOC concentration in the effluents; declining SUVA values indicated the preferential sorption of aromatic compounds. Field experiments on DOC dynamics (Kaiser et al., 2004; Leinemann et al., 2016) found comparable results with respect to the behaviour of aromatic moieties; we conclude, therefore, that the column experiment was suitable for investigation of natural processes. The transport of DOM in the second and third depths of the column experiment can thus be characterised as the competitive retention of aromatic, mostly plant derived compounds with higher sorption affinity versus potentially labile microbially-derived compounds that remain in solution or become desorbed from mineral surfaces (Guo and Chorover, 2003). The smaller inter-depth differences in DOC concentrations and SUVA observed for the silty soil cascade were most likely due to the smaller depth gradient, resulting in smaller differences in C and N content between the samples of the different depth increments (Table 1). The larger quantities

of released DOC in the sandy topsoil than in the silty topsoil led to the conjecture that OM is adsorbed more strongly in the more fine-grained substrate with a higher content of dithionite-extractable Fe (Table 1). This is in accordance with studies of the relationship between OC storage and content of pedogenic Fe (and Al) oxides (Eusterhues et al., 2005; Herold et al., 2014; Mikutta et al., 2006).

Gross OC exchange between goethite and soil solution

The use of goethite coated with ^{13}C-labelled OC enabled us to distinguish between sink and source processes on goethite surfaces. This made it possible to determine whether or not a competitive exchange of OC between the mineral phase and soil solution occurs due to the input of reactive DOM compounds as proposed in the "cascade model". Over the whole cascade, the OM-coated goethite acted as a C source as the δ^{13}C in the columns' output solution increased with every step (Fig. 5A). At the same time the OM-coated goethite also sorbed DOM at all three depths, even though its OC content decreased in the third depth compartment of the sandy soil and the second and third depth compartments of the silty soil (Fig. 6).

The proportion of mobilized OC from the goethite (MC) was relatively constant with depth but was higher in the OM-rich silty soil than in the OM-depleted sandy soil, at least in the first and third depth compartments (Fig. 6). Thus, the mobilization of goethite-associated OM was soil specific. The greater mobilization of OC from the goethite in the third depth of the silty soil can be explained by a higher reactivity of the percolating DOM, as in the second depth the aromaticity of the output solution of the silty soil columns was higher than the aromaticity in the output solution of the sandy soil columns (Fig. 4). The SUVA values also help to explain the comparable OC mobilization in the second depth, but not the differences between the sandy and the silty soil in the first depth, where the aromaticity of the solution percolating through the sandy soil columns was higher.

It was not possible to calculate the proportion of solution-derived OC sorbed to the soil samples because changes in δ^{13}C ratios of the soil (above and below the OM-coated goethite) during the experiment were minor. However, the assessment of changes in ^{13}C of the OM-coated goethite and of the DOM output solution enabled us to precisely calculate the retention of OC mobilized from OM-coated goethite in the subsequent soil depth. Following this approach, the shallow silty soil retained

two times more OC than the sandy soil from the OM-coated goethite (Tab. 3) and was thus identified as the more reactive system. This is in accordance with a 10-fold higher dithionite-extractable Fe content (Table 1). Thus, the greater sorption capacity of the silty soil provides an explanation for the ambiguous results of higher proportions of mobilized OC from the goethite (Fig. 6) and lower proportions of goethite-derived OC in the output solution (Fig. 5) in comparison to the sandy soil columns. The lower sorption capacity of the sandy topsoil, in contrast, resulted in a higher proportion of solution-derived OC in the first two depths and as a consequence, more OC could be additionally sorbed to the goethite layer.

The strong decline in solution-derived OC at the goethite surfaces in the third depth of the sandy soil (Fig. 6) likely resulted from its interaction with less reactive DOM, as according to the "cascade model", high-affinity aromatic compounds were already preferentially adsorbed in the second depth compartment (Fig. 4). The retention of aromatic compounds in the second depth most likely occurred for the most part in the soil core above the goethite, since, compared to the first depth, no stronger mobilization of OC from the goethite was found. This is in accordance with results of Hagedorn et al. (2015) who found a strong retention of percolated DOM in the uppermost 2 cm of soil cores. Mobilisation of less strongly sorbing OM components in the second depth compartment is likewise reasonable. According to adsorption experiments using in situ DOM extracts from different soil depths, the reactivity of subsoil DOM is lower than that of topsoils (Rennert and Mansfeldt 2003). Hence, the comparable proportion of solution-derived OC associated with goethite in the second and third depths of the silty soil (Fig. 6) is in accordance with the minor changes in SUVA of the percolating soil solution in these depth increments (Fig. 4).

The release of ^{13}C from the goethite into the percolation solution at every depth step confirms that the interaction of DOM with mineral-associated OM led to a re-mobilisation of previously bound OM, thus providing strong evidence for the partially stepwise transport of DOM through soil profiles (Kaiser and Kalbitz, 2012). Even though the goethite was not OM-coated to its maximum sorption capacity (Kaiser and Guggenberger, 2007) it did not further sorb OC during the experiment but rather directly participated in the cycling of OM. Despite the low OC loading of the goethite, fostering strong

interactions between the mineral and OM, and careful washing of the OM-goethite associations to remove non-sorbed and easily bound OM, as much as 18 to 31% of the initially sorbed OC took part in the cascade transport. Based on other sorption experiments and using the initial mass isotherm approach, the DOC-induced desorption of OC from 48 different mineral soil samples, including topsoils and subsoils, averaged 3.2% (Moore et al., 1992). This is in accordance with the fraction of desorbable goethite-associated OM (2.7%) after treatment with DOC-free synthetic soil solution (Kaiser and Zech 2000). However, the column experiment clearly highlights that for quantification of the cycling potential of OM bound to soil minerals, *gross exchange processes* need to be considered. Batch desorption studies without extra information derived from the use of stable isotope labelling are not suitable for determination of the potential DOC source of mineral-associated OM. Absent this additional information, the importance of mineral-associated OM for soil C cycling cannot be quantified reliably. It has recently been suggested that such exchange processes occur between litter-derived DOC and organic layers (Müller et al., 2009). Using the column experiment with ^{13}C-labelled goethite-bound OM, we were able to provide evidence that DOM from different soil compartments—including mineral topsoil and subsoil horizons—is able to replace mineral-associated OM and thus the transport of DOC does occur in a cascade-like manner, in constant exchange with mineral bound OC.

Depth and substrate effects on microbial abundance and community composition

Reactive minerals such as goethite are hotspots of biochemical interactions between mineral surfaces, organics, and microbial degraders with high bioactivity (Heckman et al., 2013). Consequently, the increase in bacterial abundance by up to 265% and the altered bacterial community composition in the goethite layers in comparison to the surrounding bulk soil reflect high C processing on mineral surfaces as postulated in the "cascade model" (Fig. 9A and B). DOC transport within the soil profile as well as the pronounced C exchange processes on the goethite surfaces led to large amounts of bio-available OC in the goethite layers (Fig.3). The high availability of labile carbon compounds stimulated the growth of predominantly copiotrophic bacteria such as *Betaproteobacteria* in the goethite layers. This result is in accordance with a study of Eilers et al. (2010) characterising

Betaproteobacteria as an important taxon under conditions of high concentrations of labile carbon. The mean fungal-to-bacteria ratio of 1:14 in the goethite layers in comparison to 1:9 in the bulk soil layers also led to the conclusion that labile carbon mainly stimulated the growth of copiotrophic bacteria in the former (Fig. 9B). In addition, *Betaproteobacteria* may have also benefited from higher pH values in the goethite layer (pH 5.1-6.7) in comparison to the bulk soil (pH 3.2-4.6) (Supplement 2; see also Blagodatskaya and Anderson, 1998). Especially in the two deeper soil horizons with lower OC content (Table 1), actual microbial C availability may have been increased in the goethite layers where OC loading was higher than in the surrounding environment. The higher C availability was reflected by the negative net decrease of OC content on the goethite in the 100 cm depth compartments and increasing ^{13}C content of the solution with every depth step (Fig. 6). This suggests that - despite of the high sorption capacity of goethite - sufficiently large amounts of labile C were available for microbial turnover processes and may indicate an active function of microorganisms in remobilization processes of mineral-bound OM. However, future studies using stable isotope probing need to clarify the re-mobilization potential of microorganisms in bioactive mineral-microbe systems. Nevertheless, the increased microbial access to OC in the goethite layers explains the increase in copiotrophic (r-strategists, fast growth rates) *Betaproteobacteria* and decrease in oligotrophic (K-strategists, low growth rates) *Acidobacteria*, which decreased in relative proportions in the microbial communities under increased OC availability (Fierer et al., 2007). Consequently, *Betaproteobacteria* may be initial colonizers of reactive minerals such as goethite and the relative increase in this taxon could indicate a shift from *K*- to *r*-strategist-dominated microbial communities from bulk soil to goethite layers. The dominance of *Acidobacteria* and *Actinobacteria* in the soil compartments was also found *in situ* at the field site of the Dystric Cambisol (Preusser et al., 2017). The microbiological results of this study highlight the contribution of microbial degraders to the cascade processes of DOC transport within the soil profile as well as the magnitude of C exchange processes on surfaces of reactive minerals such as goethite.

Small-scale variability of OC on mineral surfaces

To track the exchange of OC sorption at the small scale, goethite samples were analysed by NanoSIMS. The data suggested that OM occurred in randomly distributed patches over the goethite surfaces (Fig. 7) with a low maximum coverage of 3.5% of the goethite surfaces as detected by NanoSIMS (Supplement 6). Using comparable NanoSIMS measurements, Vogel et al. (2014) observed a fivefold higher OM coverage (19%) mainly on micro-aggregates composed of clay-sized soil minerals at an OC loading of 1.1 mg m-2, which is roughly five times the OC loading of the OM-coated goethite used in our experiment (Tab. 2). However, Xiao et al. (2016) analysed extracted Fe-bearing soil colloids with C content of 15 to 25 mg C g-1 by NanoSIMS and found C surface coverages of 7 to 10%. The rather small surface coverages found on our samples are thus in a range comparable to other NanoSIMS studies.

In our NanoSIMS study it was possible to additionally distinguish between OC sorbed before and during the experiment based on changes in atom% 13C values in selected ROIs. The approximately 25% of OC on the mineral surface residing in the highly enriched category can be considered as sorbed before the experiment and to have remained unchanged during the experiment. Evidence for this is that the proportion of OC on the goethite samples in the highly enriched category after the experiment declined only relatively in the first and second depth samples as their total carbon content increased over the course of the experiment. In the third depth sample the proportion increased relatively because of the decreasing total OC content (Table 2, Fig.8). Between 15 and 25% of the OM on the surface of the goethite after the experiment was freshly sorbed. In the first and second depths this was less than the proportion of solution-derived OC on the goethite determined by EA-IRMS measurements (Fig. 6), suggesting that the intermediate enriched category was involved in the interactions with the DOM to a great extent. These results provide further evidence for a mobilisation of previously bound OM. It also corroborates the findings of Vogel et al. (2014) who were able to show a rapid accrual of fresh C and N on micro-aggregate surfaces with a specific sorption to inherited OM. Our study highlights the importance of microscale OM patches for the cycling of OC at microscale mineral interfaces as indicated by the dilution of the 13C signals. This interaction of previously sorbed OC and DOC as indicated by declining 13C enrichment at certain spots on the

goethite surface supports the "cascade model" (Kaiser and Kalbitz 2012) and thus the exchange of inherited OM by percolating DOC.

4.6 Conclusions

Undisturbed soil column experiments with ^{13}C-labelled goethite-associated OM were conducted to verify the "cascade model" of DOM transport through soil profiles and to quantify the *net* and *gross* exchange processes on mineral surfaces as well as associated shifts in microbial communities. We found that, during the transport of DOM through soil columns, aromatic DOM moieties were preferentially retained, similar to natural conditions. Variable *gross* OC exchange rates of up to 31% showed that fresh OM inputs can replace a significant fraction of mineral-associated OM. Exchange processes at mineral surfaces due to simultaneous adsorption and desorption of OM thus play a crucial role in DOM transport, as well as in the fate and properties of mineral-associated OM. Comparably high microbial abundances in goethite layers highlight the role of secondary minerals as hotspots for OM transformation and decomposition. The high concentrations of copiotrophic bacteria such as *Betaproteobacteria* in the goethite layers provided evidence that large quantities of labile carbon are processed on the surfaces of reactive minerals. Nevertheless the roles of different microbial taxa and phyla in re-mobilization need further study, for example by using different stable isotope probing techniques. In conclusion, sorbed OM can be mobilized and replaced by DOC over an entire soil profile even at depth, thus confirming the validity of the "cascade model".

Acknowledgements

Funding of the research was provided by the Deutsche Forschungsgemeinschaft DFG within the research unit FOR 1806 ''The Forgotten Part of Carbon Cycling: Organic Matter Storage and Turnover in Subsoils (SUBSOM)''. The funding for NanoSIMS analyses was provided by MU 3021/4-1. We would like to thank Dr. Stefanie Heinze and Prof. Dr. Bernd Marschner for project coordination and Petra Kuner and numerous student helpers for support in the laboratory.

4.7 References

Angst, G., Kögel-Knabner, I., Kirfel, K., Hertel, D., Mueller, C.W., 2016. Spatial distribution and chemical composition of soil organic matter fractions in rhizosphere and non-rhizosphere soil under European beech (*Fagus sylvatica* L.). Geoderma 264, 179-187.

Bates, D., Maechler, M., Bolker, B., Walker, S., 2015. Fitting Linear Mixed-Effects Models Using lme4. Journal of Statistical Software 67(1), 1-48.

Blagodatskaya, E.V., Anderson, T.-H., 1998. Interactive effects of pH and substrate quality on the fungal-to-bacterial ratio and qCO_2 of microbial communities in forest soils. Soil Biology and Biochemistry 30, 1269-1274.

Chorover, J., Amistadi M.K., 2001. Reaction of forest floor organic matter and goethite, birnessite and smectite surfaces. Geochimica et Cosmochimica Acta 65, 95-109.

Coplen, T.B., Brand, W.A., Gehre, M., Groning, M., Meijer, H.A.J., Toman, B., Verkouteren, R.M., 2006. New guidlines for $\delta^{13}C$ measurements. Analytical Chemistry 78, 2439-2441.

Eilers, K.G., Lauber, C.L., Knight, R., Fierer, N., 2010. Shifts in bacterial community structure associated with inputs of low molecular weight carbon compounds to soil. Soil Biology and Biochemistry 42, 896-903.

Eusterhues, K., Rumpel, C., Kögel-Knabner, I., 2005. Organo-mineral associations in sandy acid forest soils: importance of specific surface area, iron oxides and micropores. European Journal of Soil Science 56, 753-763.

Federherr E., Cerli C., Kirkels F.M., Kalbitz K., Kupka H.J., Dunsbach R., Lange L., Schmidt T.C., 2014. A novel high-temperature combustion based system for stable isotope analysis of dissolved organic carbon in aqueous samples. I: development and validation. Rapid Communication in Mass Spectrometry 28, 2559-73.

Fierer, N., Bradford, M.A., Jackson, R.B., 2007. Toward an ecological classification of soil bacteria. Ecology 88, 1354-1364.

Fröberg, M., Jadrin, P.M., Hanson, P.J., Swanston, C.W., Todd, D.E., Tarver, J.R., Garten, C.T. Jr., 2007. Low dissolved organic carbon input from fresh litter to deep mineral soils. Soil Science Society of America Journal 71, 347–354.

Guo, M., Chorover, J., 2003. Transport and fractionation of dissolved organic matter in soil columns. Soil Science 168, 108-118.

Gu, B., Schmitt, J., Chen, Z., Liang, L., McCarthy, J.F., 1994. Adsorption and desorption of natural organic matter on iron oxide: Mechanisms and Models. Environmental Science and Technology 28, 38-46.

Hagedorn, F., Bruderhofer, N., Ferrari, A., Niklaus, P.A., 2015. Tracing litter-derived dissolved organic matter along a soil chronosequence using ^{14}C imaging: Biodegradation, physic-chemical retention or preferential flow? Soil Biology and Biochemistry 88, 333-343.

Hagedorn, F., Saurer, M., Blaser, P., 2004. A ^{13}C tracer study to identify the origin of dissolved organic carbon in forested mineral soils. European Journal of Soil Science 55, 91-100.

Heckman, K., Welty-Bernard, A., Vasquez-Ortega, A., Schwartz, E., Chorover, J., Rasmussen, C., 2013. The influence of goethite and gibbsite on soluble nutrient dynamics and microbial community composition. Biogeochemistry 112, 179-195.

Herold, N., Schöning, I., Michalzik, B., Trumbore, S., Schrumpf, M., 2014. Controls on soil carbon storage and turnover in German landscapes. Biogeochemistry 119, 435-451.

IUSS Working Group WRB, 2014.World Reference Base for Soil Resources 2014. International soil classification system for naming soils and creating legends for soil maps. World Soil Resources Reports No. 106. FAO, Rome.

Kaiser, K., 2003. Sorption of natural organic matter fractions to goethite (α-FeOOH): effect of chemical composition as revealed by liquid-state ^{13}C NMR and wet-chemical analysis. Organic Geochemistry 34, 1569-1579.

Kaiser, K., Guggenberger, G., 2000. The role of DOM sorption to mineral surfaces in the preservation of organic matter in soils. Organic Geochemistry 31, 711-725.

Kaiser, K., Guggenberger, G., 2007. Sorptive stabilization of organic matter by microporous goethite: sorption into small pores vs. surface complexation. European Journal of Soil Science 58, 45-59.

Kaiser, K., Kalbitz, K., 2012. Cycling downwards - dissolved organic matter in soil. Soil Biology and Biochemistry 52, 29-32.

Kaiser, K., Guggenberger, G., Haumaier L., 2004. Changes in dissolved lignin-derived phenols, neutral sugars, uronic acids, and amino sugars with depth in forested Haplic Anenosols and Rendzic Leptosols. Biogeochemistry 70, 135-151.

Kaiser, K., Guggenberger, G., Haumaier, L., Zech, W., 1997. Dissolved organic matter sorption on subsoils and soil minerals studied by ^{13}C NMR and DRIFT spectroscopy. European Journal of Soil Science 48, 301-310.

Kaiser, K., Zech, W., 2000. Sorption of dissolved organic nitrogen by acid subsoil horizons and individual mineral phases. European Journal of Soil Science 51, 403-411.

Kalbitz, K., Kaiser, K., 2008. Contribution of dissolved organic matter to carbon storage in forest mineral soils. Journal of Plant Nutrition and Soil Science 171, 52-60.

Kirkels, F.M.S.A., Cerli, C., Fedeherr, E., Gao, J., Kalbitz, K., 2014. A novel high-temperature combustion based system for stable isotope analysis of dissolved organic carbon in aqueous samples. II: optimization and assessment of analytical performance. Rapid Communications in Mass Spectrometry 28, 2574-2586.

Lenth, R.V., 2016. Least-Squares Means: The R Package lsmeans. Journal of Statistical Software 69, 1-33.

Manerkar, M.A., Seena, S., Bärlocher, F., 2008. Q-RT-PCR for Assessing Archaea, Bacteria, and Fungi during Leaf Decomposition in a Stream. Microbial Ecology 56, 467–473.

McDowell, W.H., Likens, G.E., 1988. Origin, composition, and flux of dissolved organic carbon in the Hubbard Brook valley. Ecological Monograph 58, 177-195

Michalzik, B., Kalbitz, K., Park, J-H., Solinger, S., Matzner, E., 2001. Fluxes and concentrations of dissolved organic carbon and nitrogen – a synthesis for temperate forests. Biogeochemistry 52, 173-205.

Mikutta, R., Kleber, M., Torn, M.S., Jahn, R., 2006. Stabilization of soil organic matter: association with minerals or chemical recalcitrance? Biogeochemistry 77, 25-56.

Mikutta, R., Lorenz, D., Guggenberger, G., Haumeier, L., Freund, A., 2014. Properties and reactivity of Fe-organic matter associations formed by coprecipitation versus adsorption: Clues from arsenate batch adsorption. Geochimica et Cosmochimica Acta 144, 258-276.

Moore, T.R., de Douza, W., Koprivnjak, J-F., 1992. Controls on the sorption of dissolved organic carbon by soils. Soil Science 154, 120-129.

Müller, M., Alewell, C., Hagedorn, F., 2009. Effective retention of litter-derived dissolved organic carbon in organic layers. Soil Biology and Biochemistry 41, 1066-1074.

Saidy, A.R., Smernik, R.J., Baldock, J.A., Kaiser, K., Sanderman, J., 2013. The sorption of organic carbon onto differing clay minerals in the presence and absence of hydrous iron oxide. Geoderma 209-210, 15-21.

Sanderman, J., Baldock, J.F., Amundson, R., 2008. Dissolved organic carbon chemistry and dynamics in contrasting forest and grassland soils. Biogeochemistry 89, 181-191.

Schwertmann, U., Cornell, R.M., 2000. Iron Oxides in the Laboratory: Preparation and Characterization. Second ed. Wiley-VCH. Weinheim. Germany.

Scheel, T., Haumaier, L., Ellerbrock, R.H., Rühlmann, J., Kalbitz, K., 2008. Properties of organic matter precipitated from acidic forest soil solutions. Organic Geochemistry 39, 1439-1453.

Polerecky, L., Adam, B., Milucka, J., Musat, N., Vagner, T., Kuypers, M.M.M., 2012. Look@NanoSIMS – a tool for the analysis of nanoSIMS data in environmental microbiology. Environmental Microbiology 14, 1009–1023.

Preusser, S., Marhan, S., Poll, C., Kandeler, E., 2017. Microbial community response to changes in substrate availability and habitat conditions in a reciprocal subsoil transfer experiment. Soil Biology and Biochemistry 105, 138-152.

R Core Team, 2015. R: A language and environment for statistical computing. R Foundation for Statistical Computing, Vienna, Austria. URL http://www.R-project.org/.

Vogel, C., Müller, C.W., Höschen, C., Buegger, F., Heister, K., Schulz, S., Schloter, M., Kögel-Knabner, I., 2014. Submicron structures provide preferential spots for carbon and nitrogen sequestration in soils. Nature Communications 5, 2947.

4.8 Tables

Table 1: Basic physical and chemical soil properties of the three sampling depths of each of the two soils before the experiment.

Texture	Horizon	Depth (cm)	pH ($CaCl_2$)	C (mg g^{-1})	N (mg g^{-1})	C/N	$\delta^{13}C$ (‰)	Fe_d (mg g^{-1})	Sand (%)	Silt (%)	Clay (%)
Sand	AE	4	3.23	56.31	0.80	27.46	-28.32	2.97	54	41	5
Sand	Bw	30	4.27	5.99	0.32	18.80	-26.62	2.46	56	39	5
Sand	Cw	100	4.28	0.20	0.06	3.63	-26.41	1.38	76	23	1
Silt	A	4	3.85	48.79	3.75	13.02	-26.54	20.85	0	89	11
Silt	Bw	12	3.88	44.80	3.57	12.53	-26.28	21.49	0	87	13
Silt	Bw	26	4.27	30.25	2.77	10.94	-25.96	22.4	1	89	11

Table 2: Specific surface area (SSA), carbon (C) and nitrogen (N) contents, C/N ratio, change of carbon concentration over the course of the experiment (ΔC), $\delta^{13}C$, proportion of carbon sorbed to the goethite derived from before the experiment (GDC), proportion of solution-derived carbon associated with goethite after the experiment (SDC), and previously bound carbon that got either removed or replaced over the course of the experiment (MC). Results are shown of the uncoated goethite before the experiment (Gp), and the samples from the respective three depth columns with sandy soil (GpSa1, GpSa2 GpSa3) and silty soil (GpSi1, GpSi2, GpSi3) and the OM-coated goethite before the experiment (G0) and the respective three depth columns with sandy soil (G0Sa1, G0Sa2, G0Sa3) and with silty soil (G0Si1, G0Si2, G0Si3).

Sample	SSA ($m^2\ g^{-1}$)	C ($mg\ m^{-2}$)	C ($mg\ g^{-1}$)	N ($mg\ m^{-2}$)	N ($mg\ g^{-1}$)	C/N	ΔC (%)	$\delta^{13}C$ (‰)	GDC (%)	SDC (%)	MC (%)
Gp	102.80	0.02	2.36	0.00	0.50	4.68	-	-20.58	-	-	-
G0	79.50	0.19	19.44	0.02	1.72	11.32	-	1298.92	100	0	-
G0Sa1	82.29	0.30	31.04	0.03	2.13	14.58	37.31 ± 2.31	631.43 ± 29.05	48.96 ± 3.44	51.04 ± 3.44	21.93 ± 3.89
G0Sa2	85.97	0.23	23.93	0.02	1.70	13.94	14.72 ± 21.15	893.84 ± 226.05	68.57 ± 17.20	31.43 ± 17.20	19.62 ± 2.27
G0Sa3	86.49	0.18	18.28	0.02	1.57	11.61	-6.77 ± 7.66	1146.55 ± 74.09	87.89 ± 6.13	12.11 ± 6.13	17.65 ± 2.25
G0Si1	84.91	0.24	24.51	0.02	1.43	13.05	20.71 ± 0.86	699.46 ± 19.83	54.35 ± 0.78	45.65 ± 0.78	31.46 ± 0.24
G0Si2	80.91	0.19	19.09	0.02	1.44	11.6	-1.82 ± 0.46	1029.33 ± 37.50	78.94 ± 1.64	21.06 ± 1.64	22.47 ± 1.96
G0Si3	84.80	0.18	18.04	0.02	1.42	12.62	-7.77 ± 1.55	1046.11 ± 36.31	80.37 ± 2.70	19.63 ± 2.70	25.44 ± 1.57

Table 3: Mean mobilized OC from the OM-coated goethite (MC), mean goethite-derived OC (GDC) in the solution and mean $Retained_{MC}$ (eq. 12), and the proportion of $retained_{MC}$ relative to the total amount of mobilized OC from the respective goethite sample (± standard deviation) in the three depths of the columns with sandy and silty soils. $Retained_{MC}$ represents the fraction of OC mobilized from the OM-coated goethite but retained in the soil core below the goethite and thus not transported out of the column.

Texture	Depth (cm)	MC from OM-coated goethite (mg)	GDC in solution (mg)	$Retained_{MC}$ (mg)	$Retained_{MC}$ (% of MC)
Sand	4	11.94 ± 2.10	4.11 ± 0.54	7.83 ± 2.17	64.88 ± 6.86
Sand	30	10.68 ± 1.23	5.02 ± 1.20	5.66 ± 1.22	53.11 ± 9.63
Sand	100	9.61 ± 1.22	2.79 ± 0.65	6.81 ± 1.76	70.05 ± 9.47
Silt	4	17.12 ± 0.09	3.29 ± 0.78	13.83 ± 0.87	80.74 ± 4.68
Silt	12	12.23 ± 0.75	0.86 ± 0.99	11.37 ± 1.21	92.98 ± 8.09
Silt	26	13.85 ± 0.85	0.77 ± 0.14	13.08 ± 0.96	94.39 ± 1.26

4.9 Figures

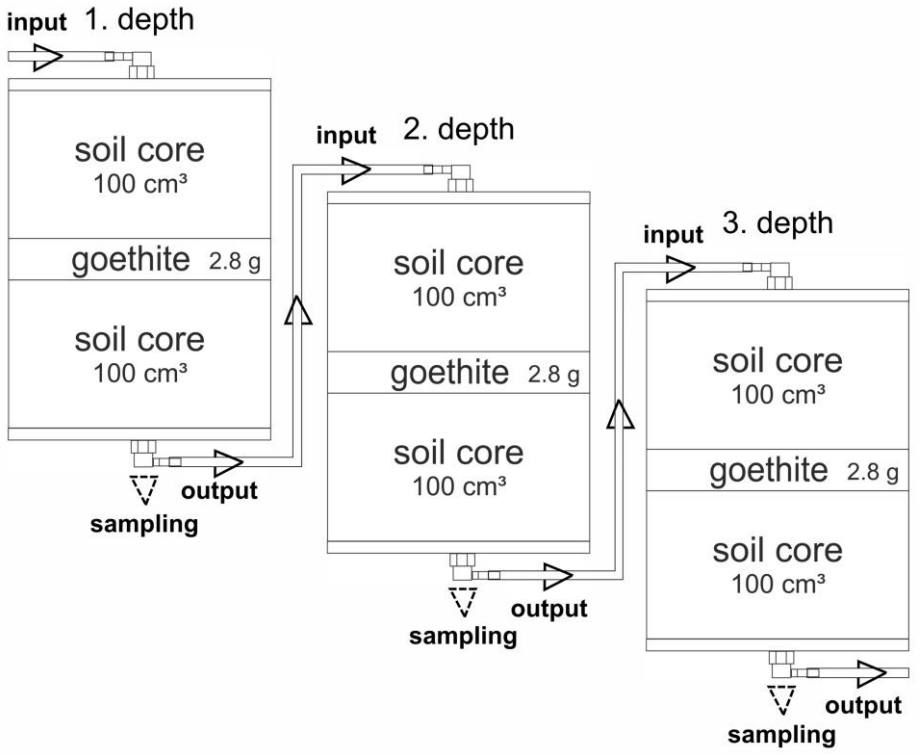

Figure 1: Experimental setup of the column experiment. The arrows represent the direction of water flow. The dotted arrows represent sampling ports.

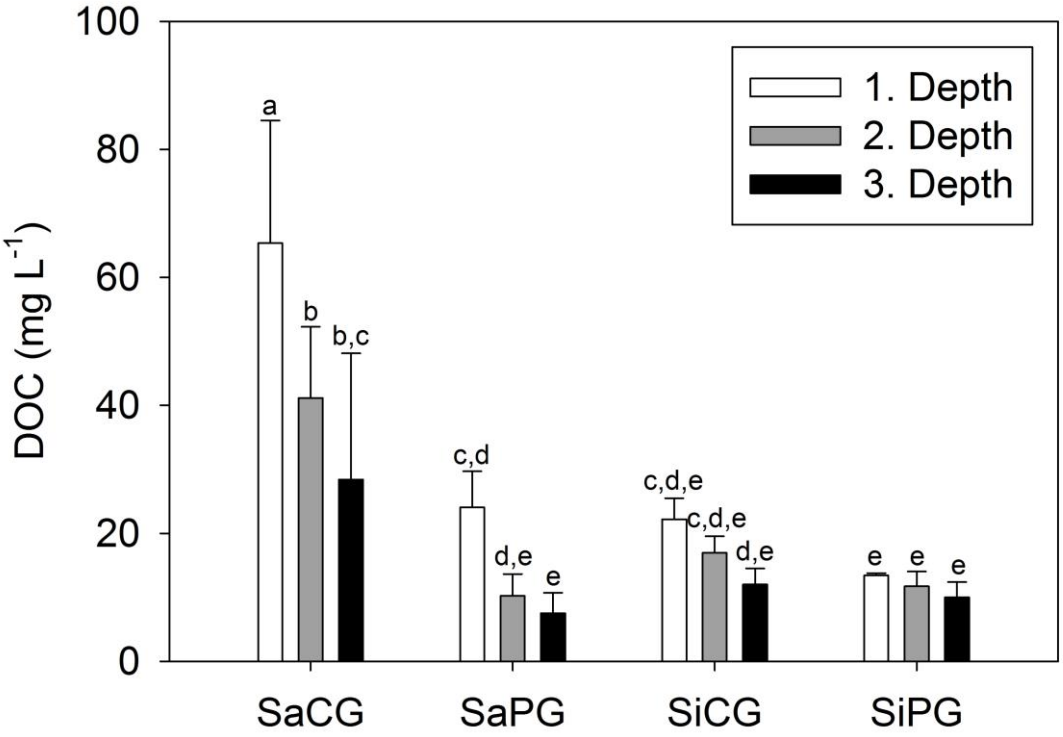

Figure 2: Mean DOC concentrations (mg L^{-1}) and standard deviations of the outflow solution per treatment and depth (4, 30, and 100 cm for the columns with sandy soil and 4, 12, and 26 cm for the columns with silty soil). Abbreviations: SaCG = sandy soil and OM-coated goethite, SaPG = sandy soil and pure goethite, SiCG = silty soil and OM-coated goethite, SiPG = silty soil and pure goethite. Different letters above the error bars indicate significant differences with p-values <0.05.

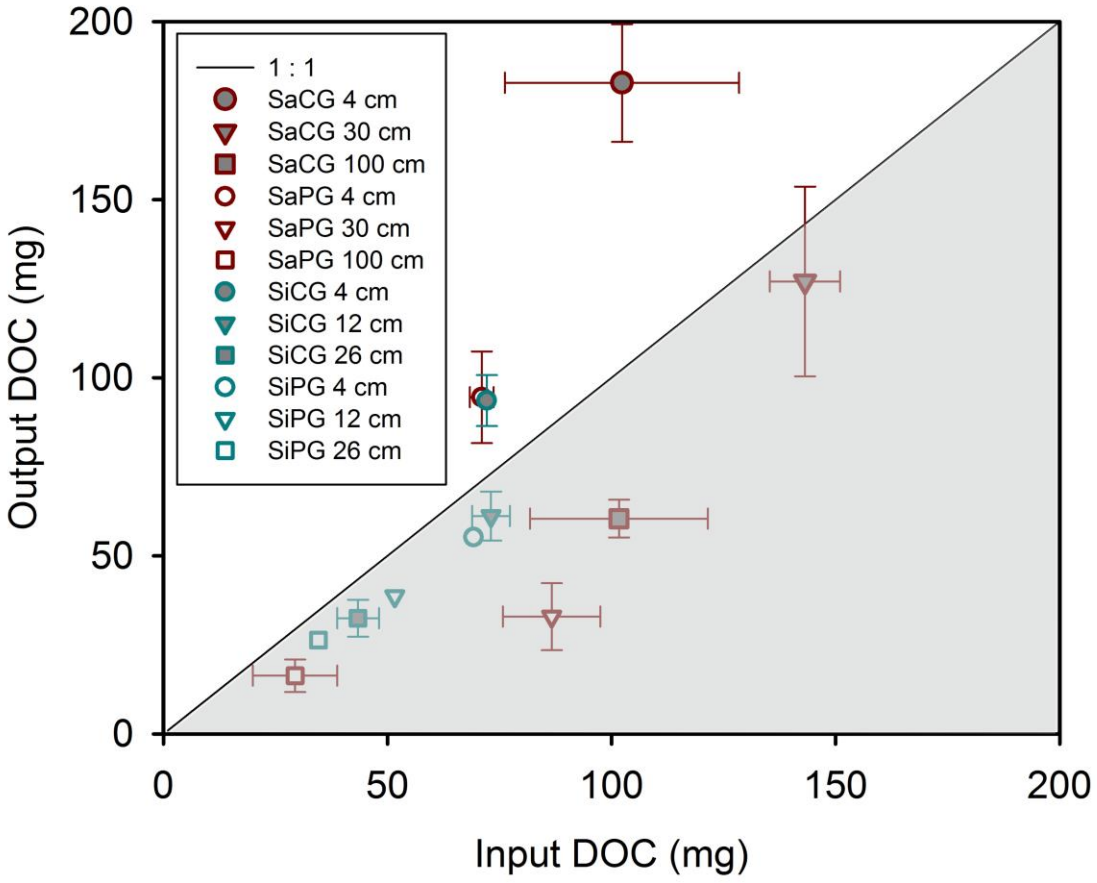

Figure 3: Total output DOC (mg) vs. total input DOC (mg) of all experimental treatments. Abbreviations: SaCG = sand and OM-coated goethite, SaPG = sand and pure goethite, SiCG = silt and OM-coated goethite, SiPG = silt and pure goethite. Values above the 1:1 line represent net leaching, whereas values below the 1:1 line represent net retention. Error bars indicate the standard deviation. Filled symbols represent columns with OM-coated goethite whereas empty symbols represent columns with pure goethite.

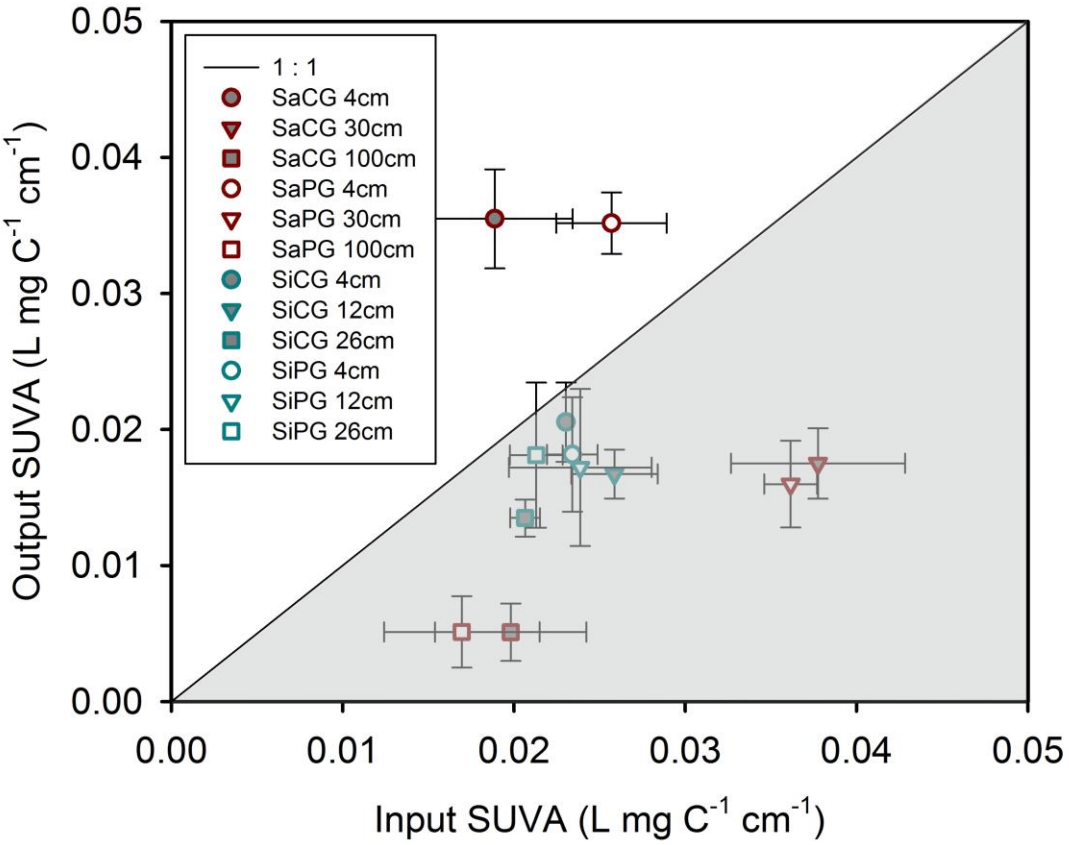

Figure 4: Mean values of output specific UV-Vis absorbance (SUVA) at 280 nm (L mg C^{-1} cm^{-1}) vs. input SUVA at 280 nm of all experimental variations. Abbreviations: SaCG = sand and OM-coated goethite, SaPG = sand and pure goethite, SiCG = silt and OM-coated goethite, SiPG = silt and pure goethite. Values above the 1:1 line represent increasing SUVA values as a result of sorption / desorption processes, whereas values below the 1:1 line represent decreasing SUVA values. Error bars indicate the standard deviation.

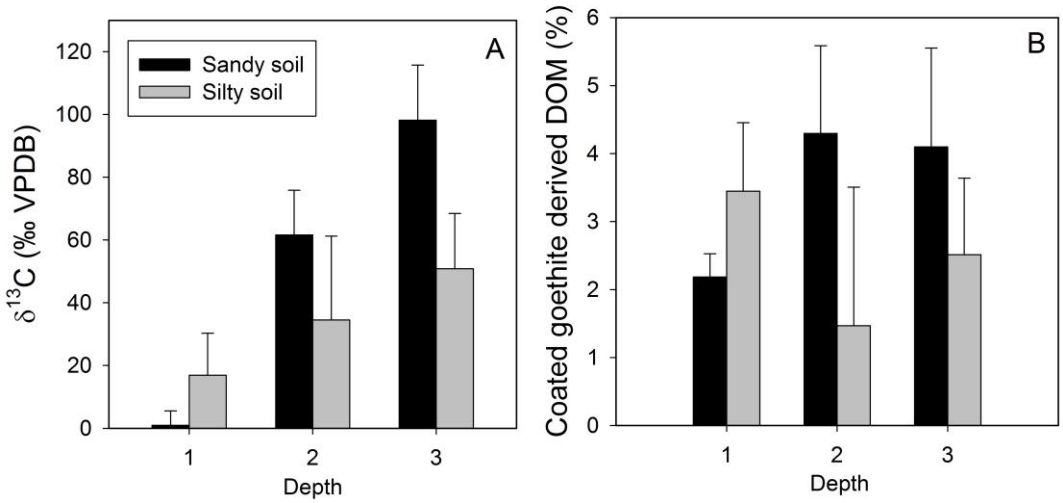

Figure 5: (A) $\delta^{13}C$ value of the outflow solution of the three cascade depths of the columns from both soils. (B) Mean proportion of OM derived from the coated goethite in the outflow solution of the three cascade depths of the columns from the sandy and the silty soils. Error bars indicate the standard deviation. Different letters above the error bars indicate significant differences ($p < 0.05$).

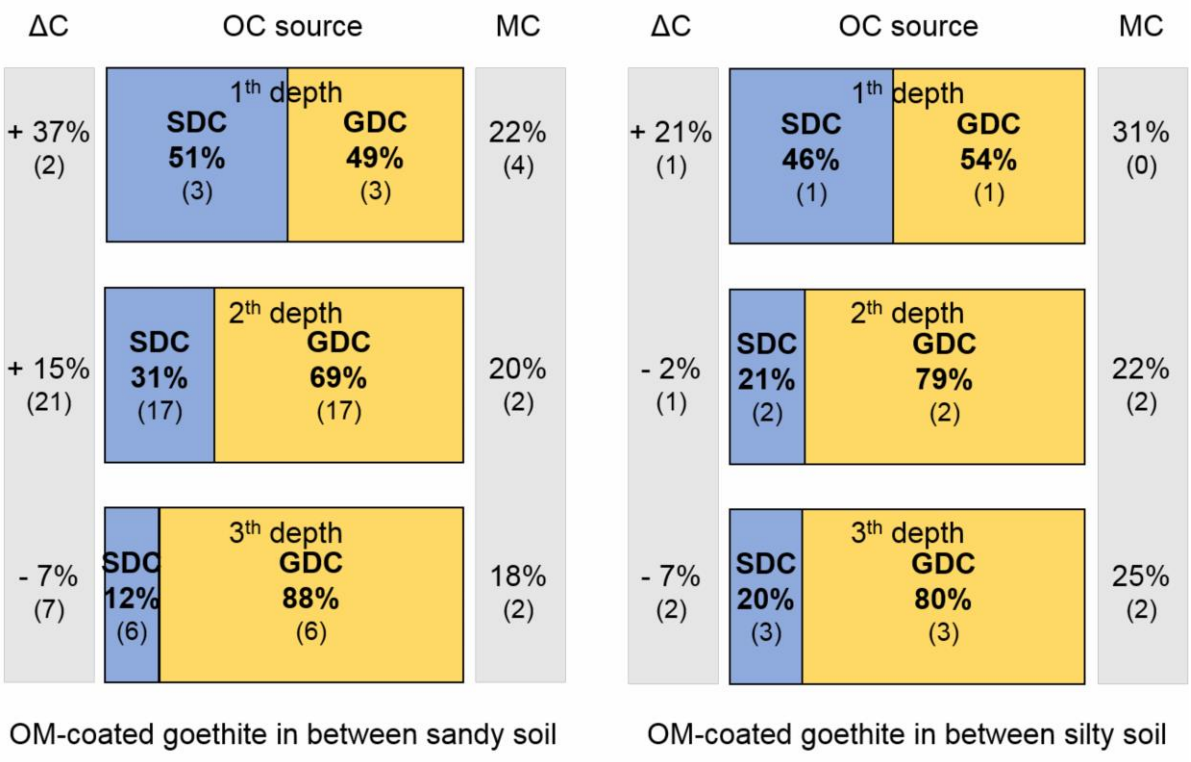

Figure 6: Mean fraction of the newly sorbed solution-derived carbon (SDC; eq. 9) versus the remaining carbon of the initial carbon coating (GDC; eq. 8) on the goethite samples after the column experiment for the sandy soil (4, 30, and 100 cm) and the silty soil (4, 12, and 26 cm) and the net carbon exchange (ΔC; eq. 10) and the mobilized carbon (MC; eq. 11) of the respective samples. Standard deviations are given in brackets.

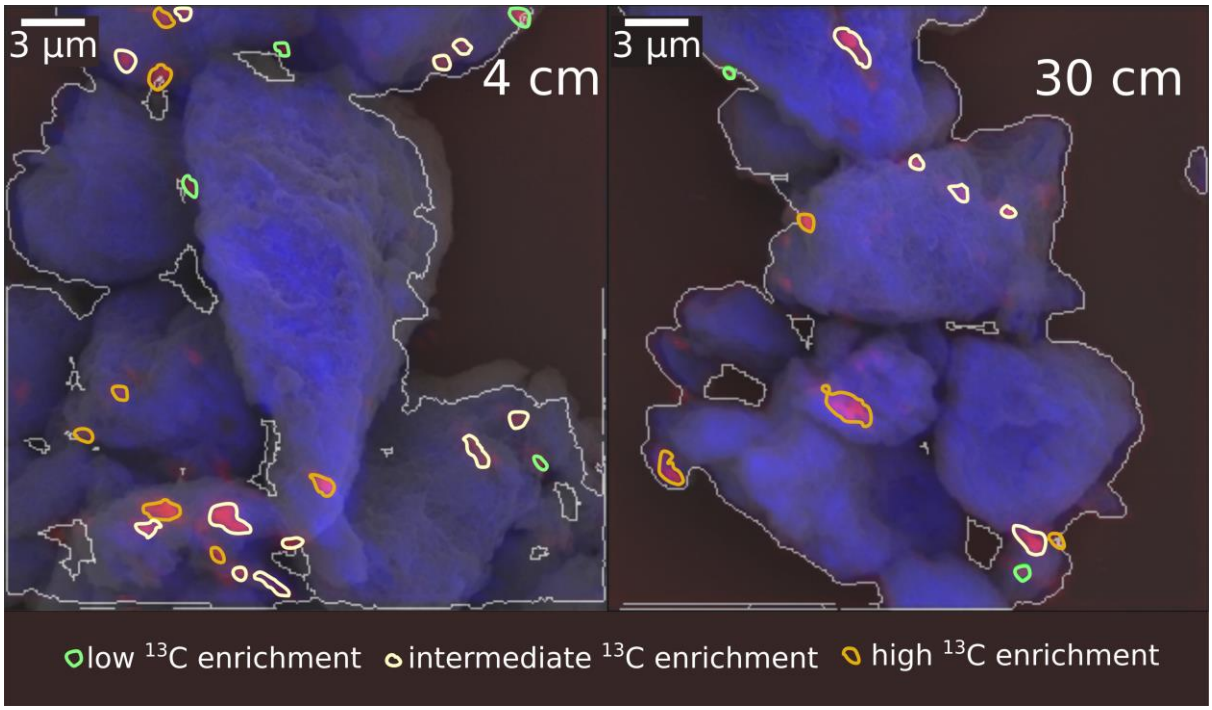

Figure 7: SEM image of goethite superposing the NanoSIMS image of $^{12}C^-$ in red and $^{56}Fe^{16}O^-$ in blue. A) Sample from the 4-cm depth column with sandy soil; B) Sample from 30-cm depth column with sandy soil. Regions of carbon accumulation on the goethite surface identified as regions of interest (ROI) are encircled. The color represents the range of the atom% ^{13}C for the respective ROI: green marks OM with <1.4 atom% ^{13}C (high abundance of newly adsorbed organic matter; low ^{13}C enrichment), white marks OM with 1.4-2.4 atom% ^{13}C (intermediate abundance of newly adsorbed organic matter, intermediate ^{13}C enrichment), and brown marks OM with >2.4 atom% ^{13}C (low abundance of newly adsorbed organic matter, high ^{13}C enrichment). The white line surrounds the mineral surface.

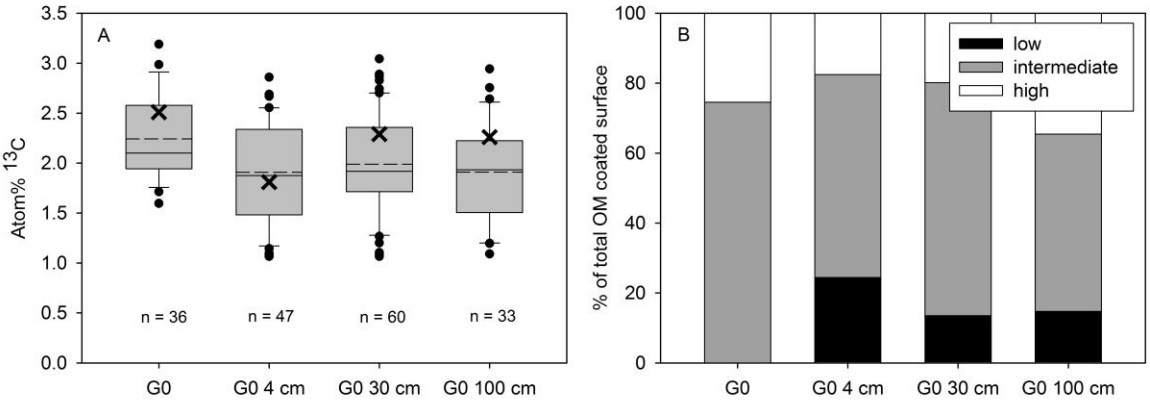

Figure 8: Results from NanoSIMS measurements of the OM-coated goethite samples from the columns with sandy soil. A) Atom% ^{13}C of the ROIs of the OM-coated goethite before the experiment (G0) and from the three depth columns with sandy soil after the experiment, as reveled by NanoSIMS. For Comparison the respective bulk atom% ^{13}C value as calculated from the IRMS measurements is shown as a black cross. The number of ROIs is given for each boxplot (n). B) Area of high (atom% $^{13}C > 2.4$), intermediate (atom% ^{13}C 1.4-2.4) and low (atom% $^{13}C < 1.4$) ^{13}C enrichment, relative to the total OM covered surface, as determined by NanoSIMS.

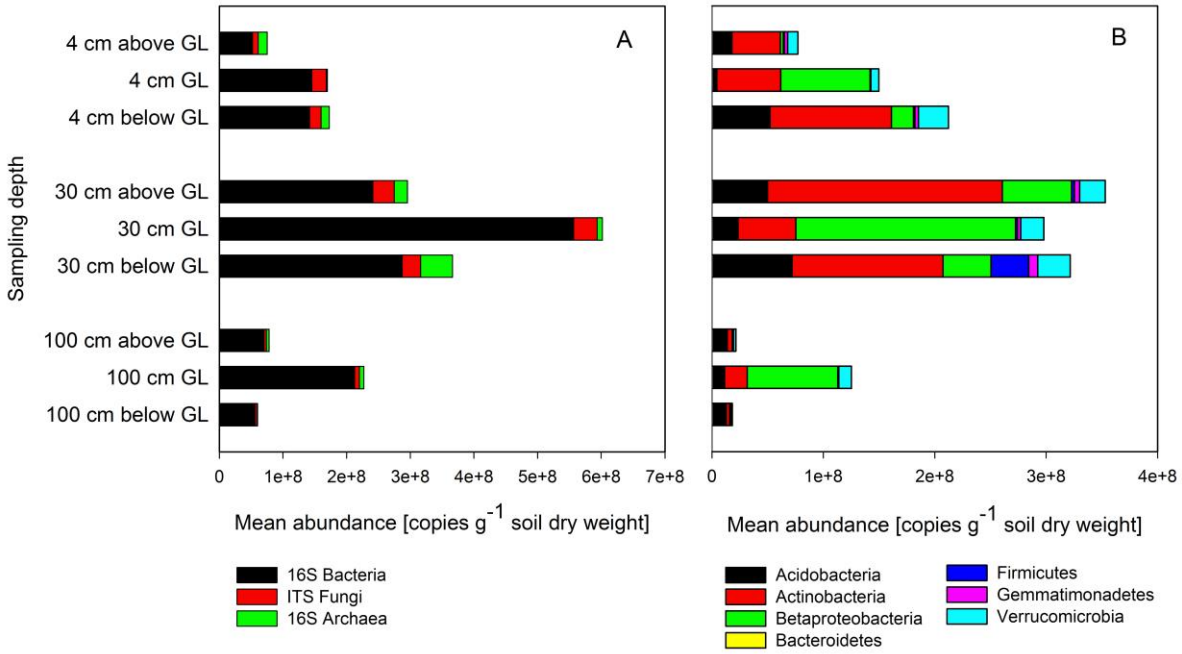

Figure 9: Microbial abundances of the sandy soil above and below the goethite layer (GL) as well as in the goethite itself sampled from the 4 cm, 30 cm, and 100 cm depth increments. A) Mean abundances of bacteria, fungi and archaea; B) Mean abundances of the bacterial taxa *Acidobacteria*, *Actinobacteria*, *Betaproteobacteria*, *Bacteroidetes*, *Firmicutes*, *Gemmatimonadetes*, and *Verrucomicrobia*.

4.10 Supplement

Supplement 1: qPCR primers and conditions.

Gene	Primer*	Thermal profile**	No. of Cycles	Efficiency mean (%)	Reference
16S rRNA genes	341F 515R	95°C – 10 m, 95°C – 15 s, 60°C – 30 s, 72°C – 30 s, 75°C – 30 s	1 35	99%	(Lopez-Gutierrez et al., 2004)
Fungal ITS fragment	ITS3F ITS4R	95°C – 10 m95°C – 15 s, 55°C – 30 s, 72°C – 30 s, 76°C – 30 s	1 35	93%	(White et al., 1990; Manerkar et al.,2008)
16S Archaea	Ar912R Ar109F	95°C – 10 m, 95°C – 30 s, 52°C – 60 s, 72°C – 60 s, 75°C – 30 s	1 40	92%	(Lueders and Friedrich, 2000)
Acidobacteria	Acid31 Eub518	95°C – 10 m, 95°C – 15 s, 55°C – 30 s, 72°C – 30 s, 81°C – 30 s	1 35	92%	(Fierer et al., 2005)
Actinobacteria	Act920F3 Act1200R	95°C – 10 m, 95°C – 15 s, 61.5°C – 30 s, 72°C – 30 s, 78°C – 30 s	1 35	92%	(Bacchetti De Gregoris et al., 2011)
β-Proteobacteria	Eub338 Bet680	95°C – 10 m, 95°C – 15 s, 55°C – 30 s, 72°C – 30 s, 80°C – 30 s	1 35	92%	(Fierer et al., 2005)
Firmicutes	Lgc353 Eub518	95°C – 10 m, 95°C – 15 s, 60°C – 30 s, 72°C – 30 s, 79°C – 30 s	1 35	97%	(Fierer et al., 2005)
Verrucomicrobia	Verr 349 Eub 518	95°C – 10 m 95°C – 15 s, 60°C – 30 s, 72°C – 30 s, 77°C – 30 s	1 35	90%	(Philippot et al., 2009)
Gemmatimonadetes	Gem440 Eub518	95°C – 10 m, 95°C – 15 s, 58°C – 30 s, 72°C – 30 s, 78°C – 30 s	1 35	95%	(Philippot et al., 2009)
Bacteroidetes	Cfb798F Cfb967R	95°C – 10 m, 95°C – 15 s, 61.5°C – 30 s, 72°C – 30 s, 75°C – 30 s	1 35	96%	(Bacchetti De Gregoris et al., 2011)

*Primer concentration was 10 pmol μl^{-1}

**Additionally, a 60°C to 95°C step was added to each run to obtain the denaturation curve specific for each amplified sequence.

Supplement 2: Selected soil and goethite parameters of the samples from the experimental run with pure goethite used for the qPCR analyses.

Depth column	Sample type	pH ($CaCl_2$)	C (mg g^{-1})	N (mg g^{-1})	C/N	Sand (%)	Silt (%)	Clay (%)
4	Soil	3.2	58.22	2.42	24	54	41	5
4	Goethite	5.1	15.54	1.13	14	-	-	-
30	Soil	4.1	8.72	0.37	23	56	39	5
30	Goethite	6.3	4.96	0.66	8	-	-	-
100	Soil	4.6	1.00	0.19	5	76	23	1
100	Goethite	6.7	1.94	0.57	3	-	-	-

Supplement 3: Mean DOC concentrations (mg L^{-1}) of the outflow solutions of all experimental variations at the three respective depths (cm).

Depth (cm)	4	30	100
Sandy soil OM-coated goethite	65.35 ± 19.17	41.17 ± 11.11	28.41 ± 19.73
Sandy soil pure goethite	24.07 ± 5.64	10.22 ± 3.42	7.53 ± 3.17
Depth (cm)	4	12	26
Silty soil OM-coated goethite	22.21 ± 3.28	16.95 ± 2.60	12.01 ± 2.52
Silty soil pure goethite	13.42 ± 0.36	11.73 ± 2.32	10.00 ± 2.39

Supplement 4: Cumulative mean DOC inflow (mg), and outflow (mg) as well as the gross balance of both (± standard deviation). Negative values represent adsorption processes from the solution, whereas positive values represent desorption processes into the solution. The balance in percent is calculated relative to the inflow solution.

Sandy soil and OM-coated goethite*			
Depth (cm)	4	30	100
DOC in	102.34 ± 26.13	143.77 ± 7.85	101.64 ± 19.84
DOC out	182.79 ± 16.53	127.04 ± 26.62	60.44 ± 5.26
Balance	80.45 ± 12.40	-16.73 ± 18.86	-41.19 ± 20.08
Balance (%)	85.04 ± 38.18	-11.24 ± 12.51	-38.99 ± 12.44
Sandy soil and pure goethite*			
Depth (cm)	4	30	100
DOC in	71.04 ± 2.63	86.62 ± 10.87	29.40 ± 9.40
DOC out	94.51 ± 12.88	32.92 ± 9.40	16.37 ± 4.57
Balance	23.47 ± 10.25	-53.71 ± 20.28	-13.03 ± 13.97
Balance (%)	32.80 ± 13.21	-61.01 ± 15.75	-38.70 ± 35.15
Silty soil and OM-coated goethite*			
Depth (cm)	4	12	26
DOC in	72.17 ± 0.00	73.10 ± 4.21	43.43 ± 4.64
DOC out	93.62 ± 7.16	61.17 ± 6.89	32.49 ± 5.19
Balance	21.45 ± 7.16	-11.92 ± 5.30	-10.95 ± 3.40
Balance (%)	29.73 ± 9.92	-16.36 ± 7.51	-25.31 ± 7.49
Silty soil and pure goethite*			
Depth (cm)	4	12	26
DOC in	69.18	51.64	34.60
DOC out	55.24	38.61	26.35
Balance	-13.94	-13.03	-8.25
Balance (%)	-20.15	-25.23	-23.86

* Differences in output concentration and the consecutive input concentration of the next depth column are caused by the delayed start of the next column leaching as some solution was used for sampling.

Supplement 5: Mean values of total specific UV absorbance (SUVA) at 280 nm (L mg C^{-1} cm^{-1}) of DOM in the inflow and in the outflow as well as the balance of both (± standard deviation). Negative values represent decreasing SUVA in the outflow whereas positive values represent increasing SUVA in the outflow. The balance in percent is calculated relative to the inflow solution.

Sandy soil and OM-coated goethite*			
depth (cm)	4	30	100
SUVA in	0.019 ± 0.005	0.038 ± 0.005	0.020 ± 0.004
SUVA out	0.035 ± 0.004	0.018 ± 0.003	0.005 ± 0.002
Balance	0.017 ± 0.006	-0.020 ± 0.005	-0.015 ± 0.004
Balance (%)	97.63 ± 53.94	-53.3 ± 8.14	-73.53 ± 11.05
Sandy soil and pure goethite*			
depth (cm)	4	30	100
SUVA in	0.026 ± 0.003	0.036 ± 0.002	0.017 ± 0.005
SUVA out	0.035 ± 0.002	0.016 ± 0.003	0.005 ± 0.003
Balance	0.009 ± 0.001	-0.020 ± 0.005	-0.012 ± 0.007
Balance (%)	37.40 ± 8.46	-55.56 ± 10.72	-66.56 ± 24.43
Silty soil and OM-coated goethite*			
depth (cm)	4	12	26
SUVA in	0.023 ± 0.000	0.026 ± 0.003	0.021 ±0.001
SUVA out	0.021 ± 0.003	0.017 ± 0.002	0.014 ± 0.001
Balance	-0.002 ± 0.003	-0.009 ± 0.004	-0.007 ± 0.002
Balance (%)	-10.85 ± 12.67	-34.47 ± 13.29	-34.45 ± 9.07
Silty soil and pure goethite*			
depth (cm)	4	12	26
SUVA in	0.023 ± 0.001	0.024 ± 0.004	0.021 ± 0.002
SUVA out	0.018 ± 0.004	0.017 ± 0.006	0.018 ± 0.005
Balance	-0.005 ± 0.006	-0.005 ± 0.004	-0.002 ± 0.003
Balance (%)	-19.65 ± 25.77	-25.22 ± 20.32	-9.03 ± 15.66

* Differences in the output SUVA and the consecutive input SUVA of the next depth column are caused by the delayed start of the next column leaching as some solution was used for sampling.

Supplement 6: Mean OC concentration and $\delta^{13}C$ ratio of the soil samples before and after the experiment and the respective change of both, per depth increment and used soil, on basis of bulk EA-IRMS measurements.

Texture	Depth	Position*	OC after the experiment (mg g^{-1})	OC before the experiment (mg g^{-1})	C change (mg g^{-1})	$\delta^{13}C_{AE}$ (‰)	$\delta^{13}C_{BE}$ (‰)	$\delta^{13}C_{change}$ (‰)
sand	4	above	83.21 ± 30.05	56.31	26.90 ± 30.04	-28.53 ± 0.13	-28.32	-0.21 ± 0.13
sand	4	below	109.38 ± 8.01	56.31	53.07 ± 8.01	-28.34 ± 0.33	-28.32	-0.25 ± 0.33
sand	30	above	10.36 ± 1.63	5.99	4.37 ± 1.63	-27.12 ± 0.17	-26.62	-0.50 ± 0.17
sand	30	below	10.60 ± 1.62	5.99	4.60 ± 1.62	-26.28 ± 0.04	-26.62	0.34 ± 0.04
sand	100	above	1.17 ± 0.04	0.20	0.97 ± 0.04	-16.06 ± 4.83	-26.41	10.35 ± 4.83
sand	100	below	0.95 ± 0.35	0.20	0.75 ± 0.34	-14.71 ± 1.00	-26.41	11.70 ± 1.00
silt	4	above	47.29 ± 5.36	48.79	-1.50 ± 5.36	-26.31 ± 0.36	-26.54	-0.23 ± 0.36
silt	4	below	47.94 ± 8.27	48.79	-0.85 ± 8.27	-26.97 ± 0.59	-26.54	-0.43 ± 0.59
silt	12	above	45.16 ± 5.93	44.80	0.36 ± 5.93	-26.33 ± 0.26	-26.28	-0.05 ± 0.26
silt	12	below	44.45 ± 6.82	44.80	-0.35 ± 6.82	-26.29 ± 0.42	-26.28	-0.01 ± 0.42
silt	26	above	32.47 ± 4.59	30.25	2.22 ± 4.59	-25.52 ± 0.14	-25.96	0.44 ± 0.14
silt	26	below	33.59 ± 3.97	30.25	3.34 ± 3.97	-25.89 ± 1.34	-25.96	0.07 ± 1.34

* Above and below the goethite layer.

Supplement 7: Surface coverage and isotopic data based on NanoSIMS images of OM-coated goethite before (G0) and after the experiment (G0 4 cm, G0 30 cm, G0 100 cm). We report mean atom% ^{13}C values of regions of interest (ROIs) that represented regions with OM coating and the respective bulk IRMS measurements for the whole sample. The ROIs with an atom% ^{13}C of <1.40 were considered to be related to newly sorbed OC (low ^{13}C enrichment), the ROIs with an atom% ^{13}C of >1.40 and <2.40 were considered to consist of a mixture of old and new sorbed OC (intermediate ^{13}C enrichment), and ROIs with an atom% ^{13}C of >2.40 were assumed to consist of mainly old OC (high ^{13}C enrichment). The table shows the relative proportion of the surface covered by OC of each category and the number of ROIs (n) in each category.

Sample	Surface covered by OM (% ± SD)	Mean atom% ^{13}C of ROI (± SD)	Bulk IRMS (atom% ^{13}C)	low ^{13}C (% of total OC ± SD)	n	intermediate ^{13}C (% of total OC ± SD)	n	high ^{13}C (% of total OC ± SD)	n
G0	2.68 ± 0.71	2.24 ± 0.41	2.51	0.00 ± 0.00	0	74.55 ± 33.26	18	25.45 ± 33.26	8
G0 4 cm	3.45 ± 0.99	1.91 ± 0.50	1.81	24.54 ± 19.36	11	57.96 ± 22.33	25	17.51 ± 12.26	11
G0 30 cm	2.72 ± 1.43	1.99 ± 0.49	2.29	13.65 ± 10.95	7	66.50 ± 14.32	42	19.85 ± 19.05	11
G0 100 cm	3.52 ± 2.09	1.91 ± 0.50	2.26	14.87 ± 29.74	6	50.56 ± 19.58	21	34.57 ± 29.49	6

5. Discussion

5.1 Transport of dissolved organic carbon

DOC is present in all ecosystems and as the most mobile form of C in soil it connects organic horizons with mineral soils and mineral soils with groundwater and streams. To evaluate the quantity and quality of DOM fluxes thus is of high importance to understand the processes controlling the terrestrial carbon cycle (Deb and Shukla 2011). The DOC fluxes ascertained in *study I* of this thesis were in the upper range compared to other studies covering sandy soils in temperate ecosystems, as summarized in Table 1. The main difference of *study I* from the other studies was the use of segmented plate lysimeters. They were used to challenge the first hypothesis, as small scale spatial variabilities can be recognized with this sampling technique, which are possibly overlooked by using suction cups. For every lysimeter segment an individual water flux was calculated and the determination of DOC fluxes was not limited to hydrological modelling results. It was thus possible to investigate the differences between matrix flux and preferential flux, addressed in the second and third hypothesis.

5.2 Transformation of dissolved organic matter during the transport to the subsoil

The DOC concentrations and fluxes strongly decline with depth due to sorption to reactive minerals and the formation of mineral-organic complexes (Feng et al. 2014). This process leads to a selective retention of aromatic compounds and thus a relative increase of aliphatic compounds in DOM with depth (Kaiser et al. 2002, Sandermann et al. 2008). Microbial consumption and loss via CO_2 are of minor importance for the reduction of DOC concentrations with depth as microbial metabolism processes preferentially alter non aromatic compounds (Kalbitz et al. 2003). Thus we hypothesized that at moderate flow rates sorption of DOM compounds to minerals leads to strongly decreasing DOC concentrations and changing DOM compositions from topsoil to subsoil.

The monitoring results from *study I* confirmed this hypothesis as the DOC concentration declined with depth (table. 1) and the DOM components were reduced in aromaticity in the subsoil according to specific UV absorbance (SUVA) at 280 nm. A change of DOM composition with depth was also recorded in a

subset of the monitoring data, analyzed for the concentration of hexoses, pentoses, amino acids, proteins and phenols. The concentrations of nearly all measured compounds decreased with depth. An increase in the amino acid to phenol ratio with depth indicates that the DOM in the subsoil is rather derived from highly degraded compounds than DOM in the topsoil (*study II*).

Table 1: Concentration and fluxes of dissolved organic carbon from different studies covering sandy soils in temperate ecosystems.

Depth (cm)	DOC (mg L^{-1})	DOC flux (g m^{-2} $year^{-1}$)	Reference
10	59.2 ± 21.2	18.5 ± 4.1	This theses, *study I*
50	18.9 ± 20.1	1.9 ± 1.6	This theses, *study I*
150	7.5 ± 6.7	1.2 ± 1.3	This theses, *study I*
9 - 15	28.5	20.7	Mc Dowell and Likens 1988
18	5.9	4.3	Mc Dowell and Likens 1988
30	3	1.7	Mc Dowell and Likens 1988
10	25.5 ± 7.1	12.8	Dosskey and Bertsch 1997
30	13.7 ± 6.1	5.5	Dosskey and Bertsch 1997
76 - 99	1.8 ± 0.3	0.6	Dosskey and Bertsch 1997
0	49.3	26.3	Fröberg et al., 2006
40 - 50	5.9	1.3	Fröberg et al., 2006
40	30.2	5.3 ± 1.6	Rieckh et al., 2014
70	10.8	1.4 ± 0.7	Rieckh et al., 2014
160	5.7	0.8 ± 0.4	Rieckh et al., 2014

Corresponding to the reduction in SUVA and the change in DOM composition the proportion of litter derived C in DOC strongly declines with depth as observed in the labelling experiment described in *study II*, confirming this part of the second hypothesis. The DOC in the mineral soil is to a great extent derived from older OM. DOM mobilized from fresh litter was otherwise retained in the first centimeters of the mineral soil, as only small amounts were transported to the subsoil. Other studies using labelled litter were limited to processes in the organic layer (Fröberg et al. 2007) or the first 10 to 15 cm of the mineral soil (Egli et al. 2016, Guelland et al. 2013), due to lower enrichments of the used labelled substances. With the

high ^{13}C enrichment used in *study II* it was possible to detect even the small amounts of litter derived C in the deep subsoil (150cm).

5.3 Variability of water and dissolved organic carbon fluxes

A seasonal variation of the DOC concentrations was recognized in 10 cm depth with the largest values during the late summer and beginning autumn, most likely due to a greater microbial activity and higher DOC production at higher temperatures (Anderson and Ingvar Nilsson 2001). In 50 and 150 cm depth seasonal trends were absent, as in some weeks in the summer of both displayed years no sampling was possible due to dry conditions (Fig. 1). However, the variability of the water flux was highest between the individual segments and the left seasonal fluctuations were less important. In the subsoil this became apparent by comparable minimum and maximum values at nearly all sampling dates (Fig. 1). This partly confirms the first hypothesis, as the small scale spatial variability of DOC concentrations was only dominant in the subsoil with increasing importance in the deep subsoil (150 cm) but not in the topsoil.

As the DOC flux was calculated as the product of water flux and DOC concentration the seasonal variability in 10 cm depth was less apparent than with the DOC concentration. This leads to the assumption that the hydrology rather than the production rate of DOC are important for the DOC transport (Fig. 2). In *study I* the relative importance of the "temporal heterogeneity" (differences between sampling dates) and the "small scale spatial heterogeneity" (differences between the individual lysimeter segments) were assessed by the calculation of intra-class correlations (Johnson and Koch 2011). The described trends (Fig.1, Fig.2) were supported by these analyses, which revealed an increasing importance of the spatial heterogeneity in the subsoil. The three observatories were not significantly different from each other, leading to the assumption that the variability of the soil solution on the centimeter scale is at least of the same extent than the variability between the observatories.

Comparable investigations of soil solution on the centimeter scale are very rare. Göttlein and Stanjek (1996) found high variations in soil solution chemistry using micro suction cups. The variability of the assessed DOM parameters was significantly different between different soil horizons, but did not always

increase with depth. That was most probably induced by the smaller depth gradient (15 cm between the highest and the deepest suction cup) compared to the experiments described in this thesis.

5.4 Relevance of variable water fluxes for the dissolved organic carbon concentration and dissolved organic matter composition

With increasing water fluxes the DOC concentrations decreased, hence high water fluxes lead to a dilution rather than an increase of DOC concentrations (*study I*) and thus the third hypothesis is partly incorrect. However, the results are confirmed by a study from Mertens et al. (2007) how found comparable dilution processes using plate lysimeters. Contrastingly, Sandermann et al. (2008) found higher DOC concentrations in soil water sampled after storm events with zero tension lysimeters. This contradicting results might be induced by the different sampling approaches, as zero tension lysimeters only sample at extreme water fluxes and cannot be used to evaluate the variability of average water fluxes. The maybe even more important difference between the studies is, that the soils investigated by Sandermann et al. (2008) were fine textured and exhibited up to 100 times higher OC contents in the subsoil compared to the sandy soils at the Grinderwald study site. Thus a greater pool of OC was available for the mobilization by rapidly percolating water. This indicates that in future studies a sampling with segmented plate lysimeters should be carried out over a range of soil types to evaluate the validity of the gained results for other than sandy soils.

Contrary to the DOC concentration the DOC flux correlated positively with the water flux. With regard to the decreased DOC concentrations with increased water fluxes it shows, that at given depth the velocity of water flux is most important for the magnitude of the DOC transport. Thus, the third hypothesis is at least partly confirmed, as the total DOC transport is strongly affected by the water flux, even though the DOC concentrations rather decline at high water fluxes.

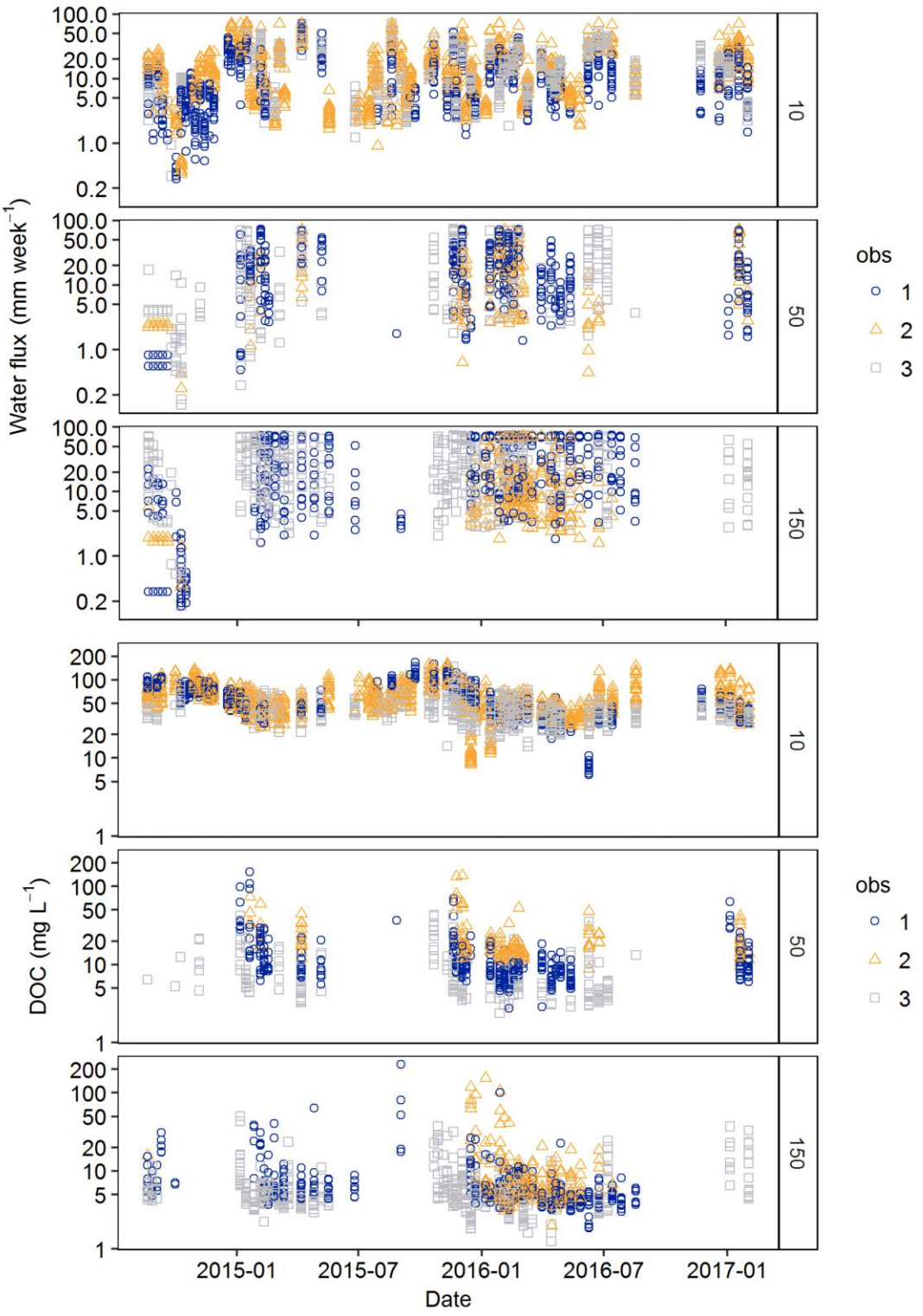

Figure 1: Water flux and DOC concentration of the individual segments of each plate lysimeter per observatory (obs) and depth (cm) from the 21.08.2014 until the 02.02.2017.

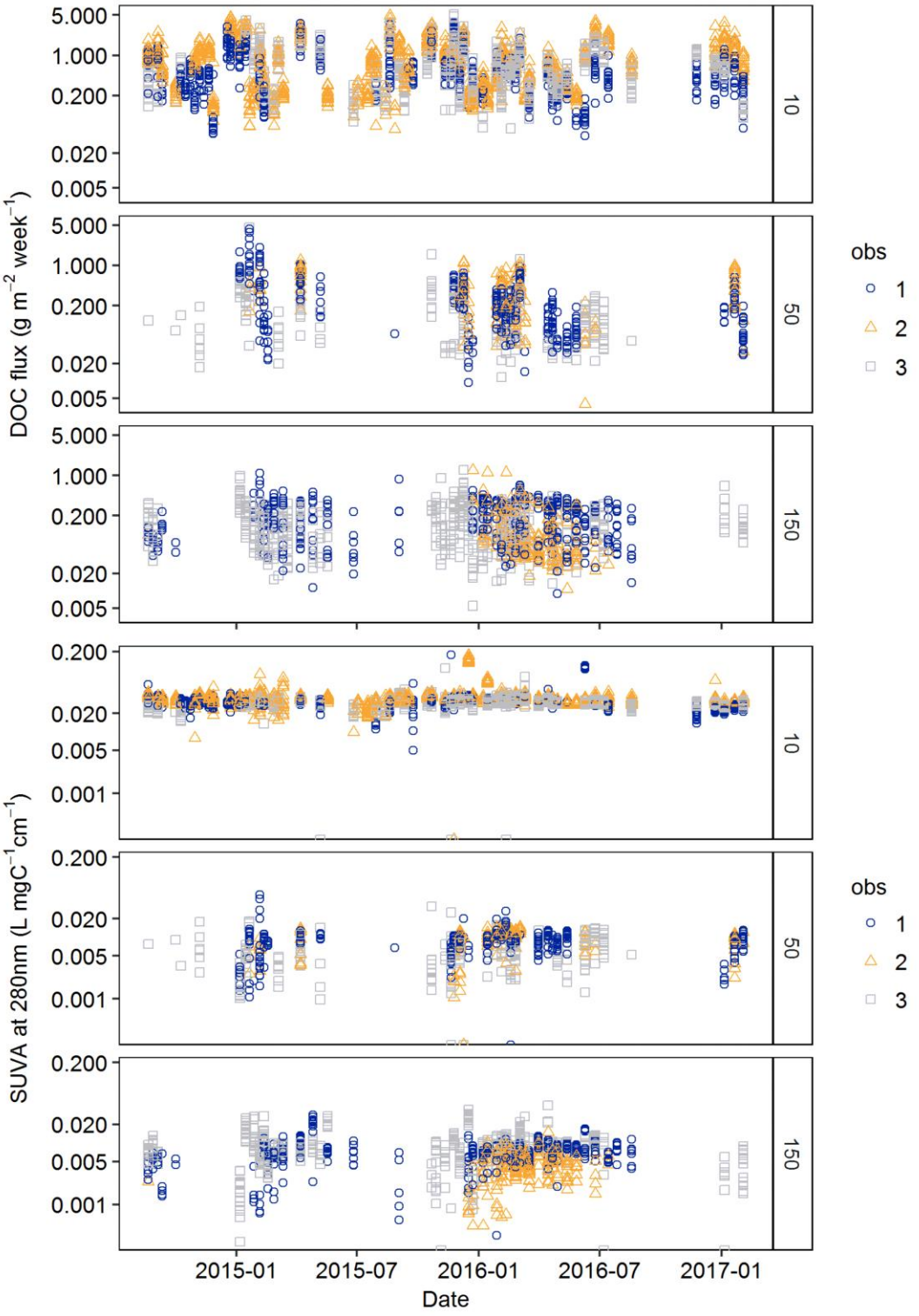

Figure 2: DOC flux and SUVA at 280 nm of the individual segments of each plate lysimeter per observatory (obs) and depth (cm) from the 21.08.2014 until the 02.02.2017.

The DOM composition is affected by the water flux, as in *study I* a positive correlation of SUVA at 280 nm and water flux in the subsoil was detected. This gives evidence for DOM bypassing sorption sites at higher water fluxes, as less aromatic moieties were retained. This finding is in accordance with studies analysing the influence of storm events on the soil solution chemistry in structured clay rich soils (Kaiser and Guggenberger 2005, Sandermann et al. 2008), which are known to be more prone to preferential flow as reviewed by Jarvis (2007). *Study I* gives evidence for such bypassing processes at moderate flow velocities in sandy, poorly structured soils as well, confirming this part of hypothesis three.

In accordance with the positive relationship between water flux and aromaticity, a positive correlation of water flux and labelled litter derived C in DOC in 10 and 150 cm depth was found in *study II*. In 10 cm depth this is probably induced by a higher release and transport of $DO^{13}C$ form the added litter at higher water fluxes and a reduced sorption in the first centimeters of the mineral soil. In 150 cm depth the relationship between %-labelled C in DOC and water flux was more pronounced, which could be induced by longer flow paths and a thus increasing heterogeneity in flow patterns as already observed in *study I.* The increased transport of litter derived DOC in macropores was also shown for topsoils by a labelled column experiment, using ^{14}C imaging (Hagedorn et al. 2015). The high difference of flow regimes on the centimeter scale and their persistence was evident, as one year after the label addition still some segments of the plate lysimeters in 150 cm depth showed no ^{13}C enrichment in the sampled DOM. The recorded absence of a relationship between leaf litter derived C in DOC and water flux in the relatively Fe-oxide rich B*w*-horizon (above 50 cm) leads to the assumption that in soils with high concentrations of reactive minerals the described mechanisms are less important. To verify this assumption a labelling experiment using segmented plate lysimeters to sample soil solution should be conducted in a Fe-oxide rich soil perhaps developed from loess.

5.4 Exchange processes between DOC and mineral-organic complexes

The sorption of DOC to reactive minerals is the dominating mechanism controlling the reduction of DOC concentration with depth (McDowell and Likens 1988) and the formation of mineral-organic complexes is

important for the protection of OC from microbial degradation (Kaiser and Guggenberger 2000) and is thus the major stabilization mechanism for OC in the mineral soil (Eusterhues et al. 2003, Mikutta et al. 2006). The sorption of OC to reactive minerals like goethite was considered to be an intimate interaction and the remobilization to soil solution of such stabilized OC was considered of minor importance (Moore et al. 1992, Kaiser and Zech 2000).

In *study III* we were able to quantify net and gross OC exchange processes using ^{13}C labelled OM-coated goethite in undisturbed soil columns. Here exchange processes between soil solution and soil minerals were found to be of high importance, as a significant proportion of 18 to 31% OC sorbed to goethite before the experiment was mobilized and exchanged by DOC from the percolate. Confirming the fourth hypothesis, the input of DOC with the soil solution was identified to be important for the cycling of OC involved in interactions with the mineral phase. In a recent study the quality of dynamic OC exchange processes was determined, as the input of highly sorptive hydrophobic compounds led to the release of previously bound weaker binding hydrophilic compounds (Scott and Rothstein 2014). With the labelling approach used in *study III* it was possible to quantify this exchange processes by calculating gross OC exchange by the change in ^{13}C enrichment on the used OM-coated goethite and in the soil solution, which were overlooked by approaches limited on net changes in OC concentrations. This confirms the relevance of mineral-organic complexes in general and OC-coated goethite in particular for the cycling of OC down the soil profile, as assumed in hypothesis five. Thus, the results from *study III* highlight the importance of a cascade like transport of DOC featuring sorption of reactive DOC compounds to the soil matrix and a competitive remobilization of less binding affine, rather degraded OM in numerous cascade steps down the soil profile (Kaiser and Kalbitz et al. 2012).

The field labeling experiment described in *study II* confirms this findings as the transport of litter derived carbon with DOC in the soil profile was found to be a slow process. Despite the low mean ^{13}C enrichment (<3%) in 10 cm depth, 1 to 2 month after the addition of labelled litter all samples were measurably enriched in ^{13}C and the mean %-labelled C in DOC showed only minor significant differences between the

sampling dates. In the subsoil the mean values of litter derived C in DOC were at least ten times lower, than in the topsoil, but increased significantly as recent as one year after the label addition. This again is an indication for a slow stepwise transport of DOC down the soil profile.

6. Conclusion and outlook

Understanding the processes controlling the transport of DOC is important to assess the dynamic of the largest terrestrial carbon pool, which is in constant exchange with the carbon pools in the biosphere, hydrosphere and atmosphere.

The availability of water is of utmost importance for any ecosystem development. As water is the major requirement for the development of life, it also is essential for the processing of dead OM and likewise important for the formation and transport of DOC. To assess the characteristics of DOC concentration and DOM composition in the subsoil a high intensity soil solution monitoring was conducted in a Dystric Cambisol under European beech (*Fagus sylvatica L.)*, located in the Grinderwald 40 km NW of Hannover. The use of segmented plate lysimeters in three replicates down to 150 cm depth enabled to determine the variability of water flux, DOC concentration and DOM composition on the centimetre scale.

The determined mean DOC concentrations were in the upper range of other studies in comparable ecosystems and confirmed the universal assumption of strong declining DOC concentrations with depth. The DOM composition changed from topsoil to subsoil with decreasing aromaticity indicating a strong influence of mineral sorption on the DOM transport in the mineral soil. Unique to this monitoring was the high spatial resolution of the sampling. Consequently a high variability of all collected data was apparent. The statistical analysis of the heterogeneity patterns confirmed a high importance of seasonal variations in 10 cm depth and an increasing importance of small scale spatial heterogeneities in the subsoil.

The importance of the water flux for the fate of DOM in the subsoil became apparent as a strong positive correlation between water flux and DOC flux was found, which outmatches the also apparent dilution effects of higher water fluxes on DOC concentrations. In the subsoil a positive correlation of water flux and aromaticity of DOM was recorded, showing that also the DOM composition is affected by differences in flow velocity. This finding suggest that hydrological rather than physicochemical processes affect the sorption behaviour of DOM, even in poorly structured sandy soils.

The origin of DOC in the topsoil and the subsoil was investigated by a field labelling approach using ^{13}C labelled leaf litter at the Grinderwald monitoring site. As expected the mean contribution of litter derived C to DOC was minor with only <3% in 10 cm depth and was mostly constant over the 18 month observation period. Thus the majority of litter derived OC is either lost as CO_2 to the atmosphere or adsorbed in the organic layer and the first centimetres of the mineral soil. In the subsoil the contribution of litter derived C to DOC was ten times smaller and was only detectable due to the high ^{13}C enrichment of the used litter material. Despite the low mean values of litter derived C in DOC over the whole soil profile the sampling with segmented plate lysimeters revealed a high variability on the centimetre scale, with zero enrichment in some samples of 150 cm depth over the whole 18 month sampling. A closer connection of some parts of the subsoil with the topsoil was evident, as more litter derived DOC was transported at certain segments. The analyses of the relationship between water flux and %-labelled C in DOC gave evidence for an intensified transport of litter derived C at high water flux.

The high retention of litter derived DOC in the topsoil and the reduction in aromaticity with depth indicates that DOC is in intimate interaction with the soil matrix. In the column experiment using ^{13}C labelled OM-coated goethite it was possible to give evidence for remobilisation processes of OC bound to highly reactive mineral surfaces by the input of DOC from the solution. This proves the importance of a cascade like transport of DOC leading to a preferential translocation of degraded, less binding affine moieties to the subsoil.

For the determination of DOC transport and cycling of OC in soil it is thus important to evaluate hydrological circumstances on the centimetre scale, or at least include the possibility of a larger DOC transport at higher water fluxes. Furthermore OC pools should not be considered as distinct, as exchange between sorbed and dissolved organic matter is evident, even without minerals reaching their sorption maximum. It is supposable that the litter derived C that sorbed to the mineral soil and was not transferred to CO_2 gets remobilized by the next input of fresh litter derived DOC.

Thus, the monitoring of the label experiment should be continued to investigate, if the litter derived carbon will reach the subsoil to a greater proportion after several years. It is possible that the peak concentration in the subsoil is not yet reached and the monitoring should be continued until the signal is diluted too much to be recovered. The analyses of the gas phase for the production of CO_2 from the labelled litter and investigations on the sorbed OC from the labelling experiment in the mineral soil will complement the findings of this thesis.

The monitoring of soil solution with segmented plate lysimeters should be conducted in other ecosystems and soil types to evaluate the accuracy of the results gained in this thesis in fine grained structured soils that are known to be rather prone for the occurrence of preferential flux.

7. References

Ahrens, B., Braakhekke, M., C., Guggenberger, G., Schrumpf, M., Reichstein, M., 2015. Contribution of sorption, DOC trasnport and microbial interactions to the 14C age of a soil organic carbon profile: Insights from a calibrated process model. Soil Biology & Biochemistry 88, 390-402.

Anderson, J., M., The Breakdown and Decomposition of Sweet Chestnut (Castanea sativa Mill.) and Beech (Fagus sylvatica L.) in Two Deciduous Woodland Soils. Oecologia 12, 251-274.

Blume, E., Bischoff, M., Reichert. J., M., Moorman, T., Konopka, A., Turco, R., F., 2002. Surface and subsurface microbial biomass, community structure and metabolic activity as a function of soil depth and season. Applied Soil Ecology 20, 171-181.

Bogner, C., Borken, W., Huwe, B. 2012. Impact of preferential flow on soil chemistry of a podzol. Geoderma 175-176, 37-46.

Brunn,, M., Spielvogel, S., Sauer, T., Oelmann, Y., 2014. Temperature and Precipitation effects on δ13C depth profiles in SOM under temperate beech forests. Geoderma 235-236, 146-153.

Coleman, D., C., Crossley, Jr., D., A., Hendrix, P., F., 2004. Fundamentals of Soil Ecology. 2nd ed. Elsevier Academic Press.

Don, A., Kalbitz, K., 2005. Amounts and degradability of dissolved organic carbon from foliar litter at different decomposition stages. Soil Biology & Biochemistry 37 2171-2179.

Don, A., Steinberger, B., Schöning, I., Pritsch, K., Joschko, M., Gleixner, G., Schulze, E-D., 2008. Organic carbon sequestration in earthworm burrows. Soil Biology & Biochemistry 40, 1803-1812.

Dungait, J., A., J., Hopkins, D., W., Gregory, A., S., Whitmore, A., P., 2012. Soil organic matter turnover is governed by accessibility not recalcitrance. Global Change Biology 18, 1781-1796.

Eusterhues, K., Rennert, T., Knicker, H., Kögel-Knabner, I., Totsche, K., U., Schwertmann, U., 2011. Fractionation of Organic Matter Due to Reaction with Ferrihydrite: Coprecipitation versus Adsorption. Environmental Science & Technology 45, 527-533.

Eusterhues, K., Rumpel, C., Kögel-Knabner, I., 2005. Organo-mineral associations in sandy acid forest soils: importance of specific surface area, iron oxides and micropores. European Journal of Soil Science 56, 753-763.

Finzi, A., C., Abramoff, R., Z., Spiller, K., S., Brzostek, E., R., Darby, B., A., Kramer, M., A., Phillips, R., P., 2015. Rhizosphere processes are quantitatively important components of terrestrial carbon and nutrient cycles. Global Change Biology 21, 2082-2094.

Fröberg, M., Kleja, B., D., Hagedorn, F., 2007. The contribution of fresh litter to dissolved organic carbon leached from a coniferous forest floor. European Journal of Soil Science 58, 108-114.

Frouz, J., Pižl, V., Cienciala E., 2009. Carbon storage in post-mining forest soil, the role of tree biomass and soil bioturbation. Biogeochemistry 94, 111-121.

Göttlein, A., Stanjek, H., 1996. Mico-scale variation of solid-phase properties and soil solution chemistry in a forest podzol and its relation to soil horizons. European Journal of Soil Science 47, 627-636.

Grüneberg, E., Riek, W., Schöning, I., Evers, J., Hartmann, P., Ziche, D.., 2017. Das Kohlenstoffspeichervermögen von Waldböden. AFZ Wald 72, 23-25

Hagedorn, F., Bundt, M., 2002. The age of preferential flow paths. Geoderma 108 119-132.

Hendrickx, J., Flury, M., 2001. Uniform and preferential flow mechanisms in the vadose zone. In: Council N R (ed) Conceptual Models of Flow and Transport in the Fractured Vadose Zone, National Academy Press, Washington, DC, pp 149-187

Herold, N., Schöning, I., Berner, D., Haslwimmer, H., Kandeler, E., Michalzik, B., Schrumpf, M., 2014. Vertical gradients of potential enzyme activities in soil profiles of European Beech, Norway spruce and Scots pine dominated forest sites. Pedobiologia 57, 181-189.

Jarvis, N., J., 2007. A review of non-equilibrium water flow and solute transport in soil macropores: principles, controlling factors and consequences for water quality. European Journal of Soil Science 58 523-546.

Jobbágy, E., G., Jackson, R., B., 2000. The vertical distribution of soil organic carbon and its relation to climate and vegetation. Ecological Applications 10, 423-436.

Kaiser, K., Guggenberger, G., 2003. Mineral Surfaces and soil organic matter. European Journal of Soil Science 54, 219-236.

Kaiser, K., Guggenberger, G., 2005. Storm flow flushing in a structured soil changes the composition of dissolved organic matter leached into the subsoil. Geoderma 127, 177-187.

Kaiser, K., Guggenberger, G., Haumaier, L., 2004. Changes in dissolved lignin-derived phenols, neutral sugars, uronic acids, and amino sugars with depth in forest Haplic Arenosols and Rendzic Leptosols. Biogeochemistry 70, 135-151.

Kaiser, K., Guggenberger, G., Haumaier, L., Zech, W., 2002. The composition of dissolved organic matter in forest soil solution: changes induced by seasons and passage through the mineral soil. Organic Geochemistry 33, 307-318.

Kaiser, K., Kalbitz, K. 2012. Cycling downwards – dissolved organic matter in soils. Soil Biology and Biochemistry 52, 29-32.

Kalbitz, K., Schwesig, D., Rethemeyer, J., Matzner, E., 2005. Stabilization of dissolved organic matter by sorption to the mineral soil. Soil Biology & Biochemistry 37 1319-1331.

Kalbitz, K., Schwesig, D., Schmerwitz, J., Keiser, K., Haumaier, L., Galser, B., Ellerbrock, R., Leineweber, P., 2003. Changes in properties of soil-derived dissolved organic matter induced by biodegradation. Soil Biology & Biochemistry 35 1129-1142.

Kammer, A., Hagedorm, F., 2011. Mineralisation, leaching and stabilization of 13C-labelled leaf and twig litter in a beech forest soil. Biogeosciences 8, 2195-2208.

Kleja, D., B., Svensson, M., Majdi, H., Jansson, P-E., Langvall, O., Bergkvist, B., Johansson, M-B., Weslien, P., Truusb, L., Lindroth, A., Ågren, G., I., 2008. Pools and fluxes of carbon in three Norway spruce ecosystems along a climatic gradient in Sweden. Biogeochemistry 89, 7-25.

Köhler, S., J., Buffam, I., Laudon, H., Bishop, K.,H., 2008. Climate's control of intra-annual and interannual variability of total organic carbon concentration and flux in two contrasting boreal landscape elements. Journal of Geophysical Research 113, G03012.

Kothawala, D., N., Moore, T., R., Hendershot, W., H., 2009. Soil Properties Controlling the Adsorption of Dissolved Organic Carbon to Mineral Soils. Soil Science Society of America Journal 73, 1831-1842.

Kuzyakov, Y., Blagodatskaya, E., 2015. Microbial hotspots and hot moments in soil: Concept & review. Soil Biology & Biochemistry 83, 184-199.

Lal, R., 2004. Soil Carbon Sequestration Impacts on Global Climate Change and Food Security. Science 304, 1623-1627

Lal, R., 2013. Soil carbon management and climate change. Carbon Management 4, 439-462.

Lavelle, P., Gignell, D., Lapage, M., Wolters, V., Roger, P., Ineson, P., Heal, O., W., Dhillion, S., 1997. Soil function in a changing world: the role of invertebrate ecosystem engineers. European Journal of Soil Biology 33, 159-193.

Lehmann, J., Kleber, M., 2015. The contentious nature of soil organic matter. Nature 528, 60-68.

Lerch, T., Z., Nunan, N., Dignac, M.-F., Chneu, C., Mariotti, A., 2011. Variations on microbial isotopic fractionation during soil organic matter decomposition. Biogeochmistry 106, 5-21.

Lynch J., M., Whipps J., M., 1990. Substrate flow in the rhizosphere. Plant and Soil 129, 1-10.

McCharty, J., F., Gu, B., Liang, L., Mas-Pla, J., Williams, T., M., Yeh, T.-C., J., 1996. Field tracer tests on the mobility of natural organic matter in a sandy aquifer. Water Resources Research 32, 1223-1238.

Mertens, J., Vanderborght, J., Kasteel, R., Pütz, T., Merckx, R., Feyen, J., Smolders, E., 2007. Dissolved Organic Carbon Fluxes under Bare Soil. Journal of Environmental Quality 36, 597-606.

Michalzik, B., Kalbitz, K., Park, J.-H., Solinger , S., Matzner, E., 2001. Fluxes and concentrations of dissolved organic carbon and nitrogen – a synthesis for temperate forests. Biogeochemistry 52, 173-205.

Mikutta, R., Kleber, M., Torn, M., S., Jahn, R., 2006. Stabilization of soil organic matter: association with minerals or chemical recalcitrance? Biogeochemistry 77, 25-56.

Mikutta, R., Lorenz, D., Guggenberger, G., Haumaier, L., Freund, A., 2014. Properties and reactivity of Fe-organic matter associations formed by coprecipitation versus adsorption: Clues from arsenate batch adsorption. Geochimica et Cosmochimica Acta 144 258-276.

Mikutta, R., Mikutta, C., Kalbitz, K., Scheel, T., Kaiser, K., Jahn, R., 2007. Biodegradation of forest floor organic matter bound to minerals via different binding mechanisms. Geochimica et Cosmochimica Acta 71 2569-2590.

Neff, J., C., Asner, G., P., 2001. Dissolved Organic Carbon in Terrestrial Ecosystems: Synthesis and a Model. Ecosystems 4, 29-48.

Osman, K., T., 2013. Soils. Springer Science+Business Media Dordrecht.

Poeplau, C., Vos, C., Don, A., 2017. Soil organic carbon stocks are systematically overestimated by misuse of the parameters bulk density and rock fragment content. SOIL 3, 61-66.

Rasse, D., P., Rumpel, C., Diganc, M-F., 2005. Is soil carbon mostly root carbon? Mechanisms for a specific stabilization. Plant and Soil 269, 341-356.

Rumpel, C., Chabbi, A., Marschner, B., 2012. Carbon Storage and Sequestration in Subsoil Horizons: Knowledge, Gabs and Potentials. In: Lal, R., Hüttel, K., Schneider, B., U., von Braun, J., 2012. Recarbonization of the Biosphere. Ecosystems and the Global Carbon Cycle. Springer, Heidelberg, New York, pp. 445-464.

Rumpel, C., Kögel-Knabner, I., 2011 Depp soil organic matter – a key but poorly understood component of terrestrial C cycle. Plant Soil 338, 143-158.

Rumpel, C., Rodríguez-Rodríguez, A., González-Pérez, J., A., Arbelo, C., Chabbi, A., Nunan, N., González-Vila, F., J., 2012a. Contrasting composition of free and mineral-bound organic matter in top- and subsoil horizons of Andosols. Biology and Fertility of Soils 48, 401-411.

Sandermann, J., Baldock, J., A., Amundson, R., 2008. Dissolved organic carbon chemistry and dynamics in contrasting forest and grassland soils. Biogeochemistry 89, 181-198.

Scharlemann, J., P., W., Tanner, E., Vj., Hiederer, R., Kapos, V., 2014. Global soil carbon: understanding and managing the largest terrestrial carbon pool. Carbon Management 5, 81-91.

Scott, E., E., Rothstein, D., E., 2014. The dynamic exchange of dissolved organic matter percolating through six diverse soils. Soil Biology & Biochemistry 69, 83-92.

Tarnocai, C., Canadell, J., G., Schuur, E., A., G., Kuhry, P., Mazhitova, G., 2009. Soil organic carbon pools in the northern circumpolar permafrost region. Global Biogeochemical Cycles 23, GB2023.

Tefs, C., Gleixner, G., 2012. Importance of root derived carbon for soil organic matter storage in a temperate old-growth beech forest – Evidence from C, N and 14C content. Forest Ecology and Management 263, 131-137.

Trumbore, S., 2009. Radiocarbon and Soil Carbon Dynamics. Annual Review of Earth and Planetary Sciences 37, 47-66.

van Veen, J., A., Kuikman, P., J., 1990. Soil structural asspects of decomposition of organic matter by micro-organisms. Biogeochemistry 11 213-233.

von Lützow, M., Kögel-Knabner, I., Eckschmitt, K., Matzner, E., Guggenberger, G., Marschner, B., Flessa, H., 2006. Stabilization of organic matter in temperate soils: mechanisms and their relevance under different soil conditions – a review. European Journal of Soil Science 57, 426-445.

Wagai, R., Mayer, L., M., Kitayama, K., 2009. Nature of the "occluded" low-density fraction on soil organic matter studies: A critical review. Soil Science and Plant Nutrition 55, 13-25.

Werth, M., Kuzyakov, Y., 2010. 13C fractionation at root-microorganisms-soil interface: A review and outlook for partitioning studies. Soil Biology & Biochemistry 42, 1372-1384.

Acknowledgements

I like to thank Georg Guggenberger, Robert Mikutta and Karsten Kalbitz, as they gave me the chance to work on this interesting topic. They supported me scientifically, in organizing the experiments and helped me learning how to write manuscripts. Furthermore I like to thank Stefanie Heinze and all the others from the SUBSOM Project for the good collaboration.

In the laboratory I got a whole lot of help with the thousands of samples, especially from Heike Steffen, Anne Katrin Herwig and at least six student helpers spread over the three years. Without this help the project would not have been realizable. Technical and psychological support from the whole other institute members was always available when needed. I like to thank everyone for the support and the good times.

For the $DO^{13}C$ measurements I have to thank Chiara Cerli and Jorien Schoorl in Amsterdam, for working your way through the giant, sometime chaotic cohort of samples, reaching your laboratory and the technical stuff in Dresden for the instant and well organized help at a time when it was really needed.

I also like to thank Jiem, Susanne, Florian, Hanna, Mark, Martin and Jörg Bachmann from the soil physics team for all the help and the good times between the offices. I especially like to thank Jiem for the support with some sampling campaigns and even more for the mental support and the very good atmosphere.

I have to thank Sebastian Preußer for the good collaboration and fruitful discussions about the manuscript and I like to thank Stefan Dulz for spontaneously proofreading and improving a whole manuscript.

Finally I like to thank my friends and family for the support, the patience and the distraction. Especially my wife Juliane was an incredible support all the time. Without you I would not be able to finish this work in any way.

Publikationen

Leinemann, T., Mikutta, R., Kalbitz, K., Schaarschmidt, F., Guggenberger, G. 2016. Small scale variability of vertical water and dissolved organic matter fluxes in sandy Cambisol subsoil as revealed by segmented suction plates. Biogeochemistry 131:1-15.

Leinemann, T., Preusser, S., Mukutta, R., Kalbitz, K., Höschen, C., Mueller, C., W., Kandeler, E., Cerli, C., Guggenberger, G., 2017. Multiple exchange processes on mineral surfaces control the tranport of dissolved organic matter through soil profiles. Under Review in Soil Biology & Biochemistry, Manuscript number: SBB12721

Heize, S., Ludwig, B., Piepo, H.-P., Mikutta, R., Don, A., Wordell-Dietrich, P., Helfrich, M., Hertel, D., Leuschner, C., Kirfel, K., Kandeler, E., Preusser, S., Guggenberger, G., Leinemann, T., Marschner, B., 2017. Factors controlling the variability of organic matter in the top- and subsoil of a sandy Dystric Cambisol under beech forest. Geoderma 311, 37-44.